UNIVERSITAT DE BARCELONA

# Molecular basis of p38α MAPK signaling

Núria Gutierrez Prat

# Molecular basis of p38α MAPK signaling

Núria Gutierrez Prat

Cover design and illustration: Ander Soto
Layout: Nuria Gutierrez

Printing: laimprenta CG- laimprenta@laimprentacg.com, partially funded by the Institute for Research in Biomedicine (IRB).

The research described in this thesis was performed from October 2013 until June 2018 at the IRB Barcelona, and was supported by grants from the European Research Council, the Spanish MINECO and AGAUR.

UNIVERSITAT DE BARCELONA

Facultat de Farmàcia i Ciències de l'Alimentació

Programa de doctorat en Biomedicina

# Molecular basis of p38α MAPK signaling

Memòria presentada per Núria Gutierrez Prat per optar al títol de doctor per la Universitat de Barcelona

Aquesta tesis s'ha realitzat a l'Institut de Recerca Biomèdica de Barcelona (IRB Barcelona)

| DIRECTOR | DOCTORANDA | TUTOR |
|---|---|---|
| Dr. Angel Rodríguez Nebreda | Núria Gutierrez Prat | Dr.Albert Tauler Girona |

A la iaia i al Lluís,

*(...) La teva llar és un refugi, però no et tanquis mai rere la seva porta.*
*L'única persona que t'acompanya tota la vida ets tu mateix.*
*Aguanta't viu en tot el que facis.*
*Encomana l'alegria al teu entorn i no et recloguis dins les teves fronteres.*
*Obre els sentits, no et perdis les coses boniques que tens al teu voltant.*
*Apaga els grisos de la teva vida i encén els colors.*
*Gira l'esquena a la rutina i mira la vida amb el front alt, i quan arribin les llàgrimes sent, pensa i ...camina endevant.*
*Estima la terra i retorna-li les fulles que amb el temps li hauràs près (...)*

A. Alsina

# Acknowledgements

Amb la motxilla una mica més plena, acabo l'etapa del doctorat.

De lluny, el camí semblava fàcil i planer, però a mesura que avançava s'anava complicant. Ara, un cop he arribat al cim, obro la motxilla i me n'adono de tot el que he anat recollint: perseverança, paciència, enginy, amistat i força. Un balanç, sens dubte, molt positiu. Sóc molt conscient de que tot això jo sola no ho hagués aconseguit i voldria agrair de tot cor a totes aquelles persones que m'han ensenyat a fer drecera i han fet que les passes fossin més lleugeres.

Para empezar, me gustaría darte las gracias Angel, por confiar en mí desde el principio, con o sin beca, con o sin inglés, con o sin nota. Me has demostrado que lo importante en ciencia es la motivación y lo demás se aprende con el tiempo. Gracias por haberme dado la oportunidad de emprender este camino y de crecer científicamente en tu grupo. Estoy muy agradecida de haberte tenido como mentor. Gracias por haber hecho de mí una persona más independiente y crítica.

También me gustaría retroceder un poco en el tiempo y agradecer a Pilar y a Neus por darme mi primer empujón en este camino y por hacerme creer que querer es poder.

Je voudrais remercier à Hugo d'avoir ouvert la porte à la science et de me la présenter.

I would also like to thank the members of my thesis advisory committee: Travis Stracker, Joan Roig and Albert Tauler, thanks for following up the developments of my research, your comments and feedback. Thanks to my thesis defense committee: Rosa Aligué, Bernat Crosas, José Miguel Lizcano, Maria Macías and Eulalia de Nadal, for your time and for having been part of this last stage of my PhD.

I would like to express my gratitude to Antonija, Laura and Richa for their nice help and contribution of this work.

Agradecer también a todo el "Nebreda's lab". Vuestro día a día desde el principio. Empezando por la gente que ha dejado huella y que, aunque no estén físicamente, fueron y son parte de su esencia. Iván, gracias por tu implicación, por tus consejos sabios y tus ánimos para seguir adelante. Jalaj, thank you for teaching me during my firsts steps in the lab. Ana, gràcies pel tot el teu suport amb experiments i ratolins. Eli y Sebas, mil gracias por vuestro carisma argentino en los momentos de frustración. Nati, Sandra, Emma, Petra, Michi, Natalia Dave, Mauri, Joanjo, Eva, Mercè, Catrin y Kostia, gracias por vuestro apoyo científico y por los mil momentos compartidos. A mi compañera de

bench/ habitación/ autocar/ birras…, Jessi. Gracias por todo lo que me has ayudado en este PhD, no solo por compartir ideas y discusiones científicas sino por tu apoyo moral en todo momento y creer en mí.
Moltes gràcies a la gent que m'ha acompanyat fins ara i que segueixen al peu del canó. Eli, Raquel, Marc i Lorena, gràcies per la vostra orientació científica i per les tertúlies i xarreres entre Western i Western. Nevenka, Dan, thank you for bringing back the "fresh" energy and enthusiasm. Bego, gracias por tus constantes *besis de fresi,* por ser mi oráculo y resolver mis mil millones de dudas. Mónica, mil gracias por tu "mentoring", por tu paciencia y dulzura, y por haber cogido las riendas del lab. Un gràcies ben especial a la Laura. La meva mitja taronja científica. Amb qui he pogut ser jo en tota la meva essència. Una Núria tossuda, germana gran i perepunyetes. Sense tu, el camí hagués sigut molt més carregós, gràcies.
A la gent de l'IRB, que ha fet que la joventut s'allargués una mica més a la meva vida. L'espontaneïtat i les ganes boges de fer coses i més coses han omplert els dies monòtons amb moments inoblidables. Gràcies Irene, Sandra, Rosa, Victor, Henry, Ivan, Artur, Marc H, Marc G i a tots els PhDs que omplen les Cool-offs i les Welcome parties.
Gràcies "Ladies", per deixar-me sempre la porta oberta i estar allà en tot moment. Anna, per fer que els dies "Moooc" es transformessin en dies plens de riures. Pels "Canet", pels balls de reggaeton, per "la farola, la farola!" i per les mil anècdotes que guardo per que se m'escapi el riure de tant en tant. Berta, gràcies per ser un referent, per transmetre tanta vitalitat i per ser el meu punt en comú en tants escenaris diferents de la meva vida. Morral, gràcies per complementar-me, per ser exigent en la mesura perfecte i per demostrar una passió extraordinària amb allò que sents teu. Suñer, gràcies pel teu optimisme, pel teu bon humor, per animar-me a que confiï en mi mateixa i per creure que tot es possible.
Voldria agrair a les que em vàreu acompanyar abans de creure que hi hauria un camí per fer. Amb qui vaig començar a conèixer ben bé el què era el món de la biologia. A la Pei, l'Ari, la Tere, la Paula, la Lau i la Ifi. Gràcies per ser l'inici de la meva "flor al cul".
Gràcies Laura (Marshall) per haver-me fet costat en aquest i en molts d'altres camins.
Gràcies als "Vividors", per fer que pugui evadir-me i desconnectar de tant en tant en un món lluny de la ciència. Gràcies Ander, per dir que sí sense condicions. Per compartir amb mi els teus dots de dissenyador i per posar el teu granet de sorra en aquesta tesi.
Gràcies "titis" per ser el meu punt "d'escape" preferit. Marta, gràcies pel teu riure que s'encomana i pel teu esperit acollidor. Per haver creat el refugi del Celler, el punt de trobada tant necessari per a tots. Chopo, gràcies per ser confident, per donar-me motivació i energia, per calçar-te unes bambes faci sol o núvol i ajudar-me a despendre'm de l'estrès. Carla, gràcies per ser flexible, tolerant i transmetre'm un amor gegant. Gràcies per ser entusiasta i per mostrar un constant interès en aquest petit projecte. Laia, gràcies per haver compartit amb mi les primeres passes del camí des del carrer Roger de Flor i per ensenyar-me que s'ha de lluitar per aconseguir el que es vol. Joana, per a mi ets un exemple d'evolució personal i superació. Gràcies, per fer que les llàgrimes siguin blocs de ciment que t'ajuden a construir i no a destruir. Per fer que guanyi l'alegria envers el dolor.

Gràcies als Prat Alsina, i als Gutiérrez Jordán, per ensenyar-me els valors de pertànyer i ser-hi sempre.

A en Ricard, Virgi, Richi, Gerard, Lara, iaia Rosa i iaia Ali, gràcies pel vostre suport i ànims durant tants sobretaules.

Marc,
Has fet que la càrrega no pesés mai, que el camí no tingués dificultat, que no hi hagués mai tempesta. M'has donat el més necessari per avançar i poder fer cim. Per poder ser jo sempre, per les ales que em dones i per sentir-me. Per fer que la nena petita que viu amb mi, hi visqui eternament. Gràcies.

Gràcies als més incondicionals, als meus punts cardinals, als que m'indiquen sempre on està el nord perquè no em perdi mai en cap camí de la vida.
Mire i Laia, gràcies per ser part de mi. Per no deixar-me mai sola. Per ser sempre **tres**. Per admirar-me sense motiu i per fer de mi una Núria amb menys defectes.
Papa i Mama, gràcies per ser qui em dona la mà en tot moment, per estar pendents a que no m'entrebanqui ni caigui. Per fer-ho de forma subtil i fer-me creure que puc jo tota sola. Gràcies per ensenyar-me a prendre decisions en moments difícils, gràcies per ensenyar-me a ser feliç.

# Contents

Molecular basis of p38α MAPK signaling

# Abbreviations

| | |
|---|---|
| 4-OHT | 4-hydoxitamoxifen |

## A

| | |
|---|---|
| AAA-ATPase | ATPases associated with diverse cellular activities |
| A-loop | Activation loop |
| ADP | Adenosine diphosphate |
| Ambra1 | Activating molecule in BECN1-regulated autophagy protein 1 |
| Amp | Ampicillin |
| AP | b-AP15 |
| APS | Ammonium persulfate |
| ARE | AU-rich elements |
| Arg | Arginine |
| ASK1 | Apoptosis signal-regulating kinase 1 |
| Asp | Aspartate |
| ATF2 | Activating transcription factor 2 |
| Atg | Autophagy- related protein |
| ATP | Adenosine triphosphate |

## B

| | |
|---|---|
| Bccip | BRCA2 And CDKN1A Interacting Protein |
| BFA | Bafilomycin A1 |
| Bif-1 | Endophilin-B1 |
| BIRB | BIRB796 |
| BMDM | Bone marrow derived macrophages |
| BrdU | 5-bromo-2-deoxyuridine |
| BTZ | Bortezomib |

## C

| | |
|---|---|
| CAMKK2 | Calcium/Calmodulin Dependent Protein Kinase Kinase 2 |
| CD | Common docking domain |

| | |
|---|---|
| Cdc25 | Cell division cycle 25 |
| CDO1 | Cysteine dioxygenase type 1 |
| C/EBPβ | CCAAT/enhancer-binding protein beta |
| CHX | Cycloheximide |
| CMA | Chaperone mediated autophagy |
| COPS5 | COP9 signalosome subunit 5 |
| COX2 | Cyclooxygenase |
| CreERT2 | Cre Recombinase -estrogen receptor T2 mutant |
| CSBP1 | Cytokine suppressive anti-inflammatory drug-binding protein |
| CXCL2 | Chemokine (C-X-C motif) ligand 2 |

## D

| | |
|---|---|
| DAPI | 4, 6-diamidino-2-phenylindole |
| DDA | Data-dependent acquisition |
| DLG1 | Discs large homolog 1 |
| DLK1 | Dual-leucine-zipper-bearing kinase 1 |
| DMEM | Dulbecco's Modified Eagle´s Medium |
| D-motif | Docking motif |
| DMSO | Dimethyl sulfoxide |
| DNA | Deoxiribonucleic acid |
| Dnajb6 | DnaJ Heat Shock Protein Family (Hsp40) Member B6 |
| DNAse | Deoxyribonuclease |
| DTT | Dithiothreitol |
| DUSP | Dual specificity phosphatase |

## E

| | |
|---|---|
| EDTA | Ethylenediamine tetraacetic acid |
| EGF | Epithelial growth factor |
| EGTA | Ethylene glycol tetraacetic acid |
| eIF4E | Eukaryotic initiation factor 4E |
| EpCAM | Epithelial cell adhesion molecule |
| ERK | Extracellular signal–regulated kinase |

## F

| | |
|---|---|
| FA | Formic acid |
| FACS | Fluorescence-activated cell sorting |
| FAD | Flavin adenine dinucleotide |





| | |
|---|---|
| FASP | Filter-aided sample preparation |
| FBS | Fetal bovine serum |
| FDR | False discovery rate |
| FIMO | Find individual motif occurences |
| FKBP8 | FK506 binding protein 8 |
| Fw | Forward |

## G

| | |
|---|---|
| GAPDH | Glyceraldehyde 3-phosphate dehydrogenase |
| GFP | Green fluorescent protein |
| Gln | Glutamine |
| Glu | Glutamate |
| Gly | Glycine |
| GRK5 | G Protein-Coupled Receptor Kinase 5 |
| GST | Glutathione S-transferase |

## H

| | |
|---|---|
| $H_2O_2$ | Hydrogen peroxide |
| HBS | HEPES buffered saline |
| hcAbs | Heavy chain antibodies |
| HECT | Homology to E6AP C terminus |
| HEPES | 4-(2-hydroxyethyl)-1-piperazineethanesulfonic acid |
| His | Histidine |
| hnRNPA1 | Heterogeneous nuclear RNP A1 |
| Hsp27 | Heat shock protein 27 |
| HTRA2 | High-temperature requirement A2 |

## I

| | |
|---|---|
| ID | Identification |
| IHC | Immunohistochemistry |
| IL-1 | Interleukin-1 |
| IL-6 | Interleukin-6 |
| Ile | Isoleucine |
| IP | Immunoprecipitation |

## J

| | |
|---|---|
| JIP | JNK-interacting protein |

| | |
|---|---|
| JLP | c-Jun NH2-terminal kinase-associated leucine zipper protein |
| JNK | c-Jun N-terminal kinase |

## K

| | |
|---|---|
| KA | Kinase assay |
| KD | Kinase dead |
| Kd | Dissociation constant |
| kDa | Kilo daltons |
| KI | Knock-in |
| KO | Knock-out |
| KSR | Kinase suppressor of Ras |

## L

| | |
|---|---|
| LB | Luria broth base |
| LC3 | Microtubule-associated protein 1A/1B-light chain 3 |
| Lck | Lymphocyte-specific protein tyrosine kinase |
| Leu | Leucine |
| LPS | Lipopolysaccharide |
| Lys | Lysine |

## M

| | |
|---|---|
| MAPK | Mitogen- activated protein kinase |
| MAPKAPK | MAPK-activated protein kinase |
| MAPKK | Mitogen- activated protein kinase kinase |
| MAPKKK | Mitogen- activated protein kinase kinase kinase |
| MBP | Myelin basic protein |
| M-CSF | Macrophage colony-stimulating factor |
| MDM2 | Mouse double minute 2 homolog |
| MEF | Mouse embryonic fibroblasts |
| MEKK | MAPK/ERK kinase kinase |
| Met | Methionine |
| MG | MG132 |
| MK2 | MAPKAPK2 (Mitogen- activated protein kinase kinase 2) |
| MKI | MAPK insert |
| MKP | MAPK phosphatase |
| MLK3 | Mixed-lineage kinase 3 |
| MNK | MAPK- interacting protein kinase |
| Mpp6 | MAGUK p55 subfamily member 6 |





| | |
|---|---|
| mRNA | Messenger RNA |
| MRS | Myogenic regulatory factor |
| MS | Mass spectrometry |
| MSK | Mitogen and stress activated protein kinase |

## N

| | |
|---|---|
| NCF1 | Neutrophil cytosolic factor-1 |
| NES | Nuclear-export signal |
| NGF | Nerve growth factor |
| NLS | Nuclear localization signal |
| NMR | Nuclear magnetic resonance |
| NT | Non-treated |

## O

| | |
|---|---|
| O/N | Overnight |
| OPA | O-phenanthroline |
| OP-Puro | O-propargylpuromycin |

## P

| | |
|---|---|
| p38α | MAPK14 (Mitogen- activated protein kinase 14) |
| PA200 | Proteasome activating protein 200 |
| PABP1 | Polyadenylate-binding protein 1 |
| PARP1 | Poly (ADP-ribose) polymerase 1 |
| PBS | Phosphate buffer solution |
| Pcmtd1 | Protein-L-isoaspartate O-methyltransferase domain containing 1 |
| PD | Pull down |
| PDB | Protein data base |
| PDGF | Platelet-derived growth factor |
| PF | PF-3644022 |
| PH | PH-797804 |
| P-H3 | Phospho Histone 3 |
| Phe | Phenylalanine |
| PIK3CD | Phosphoinositide-3-kinase |
| PLA | Proximity ligation assay |
| P-loop | Phosphate-binding loop |
| PMSF | Phenylmethylsulfonyl fluoride |
| PP2A | Protein phosphatase 2A |

| | |
|---|---|
| PP2AC | Catalytic subunit of protein phosphatase 2A |
| PPI | Protein-protein interactions |
| Ppm | Parts per million |
| PPM1A | Protein phosphatase 1A |
| PRDM16 | PR domain containing 16 |
| P-region | Proline rich region |
| PSM | Peptide spectrum matches |
| PSMD11 | Proteasome 26S Subunit, Non-ATPase 11 |
| PSSM | Position-specific scoring matrix |
| PTM | Post translational modification |
| PTP | Protein tyrosine phosphatase |
| PTPN7 | Protein tyrosine phosphatase non-receptor type 7 |
| PTPRQ | Protein tyrosine phosphatase receptor type Q |
| PyMT | Polyoma Middle T |

## Q

| | |
|---|---|
| qRT-PCR | Quantitative real time-Polymerase chain reaction |

## R

| | |
|---|---|
| RBR | RING-between-RING |
| RevD | Reverse D |
| RING | Really interesting new gene |
| RIPK1 | Receptor interacting serine/threonine kinase 1 |
| Rpm | Revolutions per minute |
| Rpn | Proteasome regulatory particle |
| Rsk | Ribosomal s6 kinase |
| RT | Room temperature |
| Rv | Reverse |

## S

| | |
|---|---|
| S.G | Sucrose gradient |
| SDS | Sodium dodecyl sulfate |
| SEM | Standard error mean |
| shRNA | short hairpin RNA |
| siRNA | small interfering RNA |
| SMG1 | Nonsense mediated mRNA decay associated PI3K related kinase |
| SMURF1 | SMAD specific E3 ubiquitin protein ligase |





| | |
|---|---|
| SSC | Side scatter |
| STEP | Tyrosine-protein phosphatase non-receptor type 5 |
| Strip1 | Striatin interacting protein 1 |
| STRIPAK | Striatin-interacting phosphatase and kinase |
| STRN | Striatin |
| STUB1 | STIP1 homology and U-box containing protein 1 |

## T

| | |
|---|---|
| TAB1 | TAK1-binding protein1 |
| TAK1 | Transforming growth factor β-activated kinase |
| TAO | Thousand-and-one amino acid |
| TCR | T-cell receptor |
| TGFβ | Transforming growth factor β |
| Thr | Threonine |
| TNFα | Tumoral necrosis factor alpha |
| TPL2 | Tumor progression loci 2 |
| TTP | Tristetraprolin |
| Tyr | Tyrosine |

## U

| | |
|---|---|
| Ub | Ubiquitin |
| UBC | Ubiquitin C |
| uPA | Plasminogen activator urokinase |
| UPS | Ubiquitin-proteasome system |
| UV | Ultraviolet |
| UVRAG | UV radiation resistance-associated gene protein |

## V

| | |
|---|---|
| Val | Valine |
| Vsp34 | Phosphatidylinositol 3-kinase catalytic subunit type 3 |

## W

| | |
|---|---|
| WB | Western blot |
| WT | Wild type |

## Z

| | |
|---|---|
| ZAK1 | Leucine zipper and sterile-α motif kinase 1 |
| ZAP-70 | ζ-chain-associated protein kinase 70 kDa |
| ZBED6 | Zinc finger BED-type containing 6 |

# Summary

Cells are often exposed to damaging internal and external stimuli and need to respond accordingly. One of the signaling pathways that is frequently activated by stress involves activation of the kinase p38α, which in turn can phosphorylate many substrates including phosphatases that inactivate the pathway. The binding between p38α and interacting molecules involves both docking-site mediated interactions and the transient enzyme-substrate interaction through the active site center. While the majority of the p38α protein partners undergo transient contacts, others are able to bind through more stable interactions, potentially allowing p38α to act as scaffolding molecule. So far, most of the functions attributed to p38α are mediated by its kinase activity, and therefore more studies are required to uncover p38α scaffolding functions. We have performed *in silico* screenings to identify p38α partners but we have not been able to find new proteins that interact with p38α in a stable manner. One of the best characterized effectors of p38α is the protein kinase MAPKAPK2 (MK2), which interacts via its C-terminal regulatory domain with the docking groove of p38α. Experiments using purified proteins have shown that non-phosphorylated p38α and MK2 can form a tight and rather stable complex in which structural constraints impede the interaction of both kinases with effectors and regulators. It is therefore critical to understand how the interaction between p38α and MK2 is regulated to ensure that they can separate from each other and phosphorylate the required substrates to mediate particular functions. We have found that in cells under homeostatic conditions, endogenous p38α and MK2 form a stable complex that is disrupted upon phosphorylation of both proteins. Depending on the length and intensity of the stimuli, p38α and MK2 undergo different fates. Transient stimulation leads to complex separation and MK2 degradation followed by an increase in MK2 gene expression, and the eventual re-assembly of the p38α:MK2 complex. In contrast, when cells are exposed to strong stimuli that lead to sustained p38α activation, as it is often the case with stress, both kinases remain phosphorylated, cannot bind to each other and eventually become destabilized, being unable to recover the stand-by state. Taken together, our study highlights the importance of docking interactions in the regulation of the p38α:MK2 complex dynamics, which may have implications for different processes regulated by p38α and MK2 signaling. In addition, we have also generated mice that express a kinase-dead form of p38α and provide some evidence of potential p38α kinase-independent functions *in vivo*. Overall, our results have shed light on the molecular regulation of this signaling pathway.

# Resum

Les cèl·lules estan exposades constantment a estímuls perjudicials provinents tant de l'interior com de l'exterior cel·lular. Aquests estímuls desencadenen en vies de senyalització que els permeten respondre en conseqüència. Una de les vies de senyalització que s'activa per estrès, és la via de la quinasa p38α. Un cop activada, p38α fosforil·la diversos substrats incloent fosfatases que finalment inactivaran la via. p38α pot interaccionar amb substrats i proteïnes reguladores a través dels seus dominis d'acoblament i els residus de fosforilació i activació. Majoritàriament, les proteïnes interaccionen amb p38α de manera transitòria a través de la reacció de fosforilació, però en alguns casos, p38α pot interaccionar de forma estable actuant com a proteïna d'assemblatge. Tot i que la funció quinasa de p38α està molt ben caracteritzada, la funció d'assemblatge està poc definida i per tant es requereixen més estudis per determinar aquest rol. Per caracteritzar aquesta funció, hem generat una cerca *in silico* que permet predir proteïnes que interaccionen amb p38α. Malauradament, cap de les proteïnes seleccionades s'han pogut unir de forma estable amb p38α i per tant, alternativament, ens hem focalitzat amb la quinasa MAPKAPK2 (MK2), ja que és un dels efectors principals de p38α. Concretament, MK2 utilitza la regió C-terminal per unir-se al lloc d'acoblament de p38α. Estudis basats en cristal·lografia han caracteritzat la unió d'ambdues quinases i suggereixen que l'estructura que formen com a complex proteic impedeix la seva interacció amb altres proteïnes. Per tal d'assegurar que les dues proteïnes puguin fosforil·lar als demés substrats i realitzar les corresponents funcions cel·lulars, és important entendre com es regula el complex p38α:MK2. En aquest estudi, hem vist que en condicions d'homeòstasis, p38α i MK2 formen un complex estable que s'acaba dissociant quan ambdues proteïnes estan fosforil·lades. Conseqüentment, la durada i intensitat de l'estímul determinarà l'efecte de la fosforilació tant per p38α com per MK2 donant lloc a diferents respostes. S'ha vist que una estimulació curta i transitòria, indueix la fosforilació d'ambdues proteïnes i alhora la degradació de MK2 seguida per un increment en la seva expressió gènica i la nova formació del complex. D'altra banda, una estimulació llarga i sostinguda dona lloc a una constant activació de p38α fent que les dues proteïnes romanguin fosforil·lades i no es puguin unir. La falta d'unió farà que les dues quinases es desestabilitzin i no puguin restablir el seu estat basal. Concretament, aquest estudi remarca la importància de les unions d'assemblatge de p38α en la regulació dinàmica del complex p38α:MK2, la qual podria tenir implicació en els processos regulats tant per p38α com per MK2. A més a més, hem generat un nou model de ratolí que expressa

una versió mutada de p38α afectant a la seva activitat catalítica per així, poder estudiar amb detall la contribució de les funcions independents de quinasa *in vivo*. En resum, els resultats obtinguts aporten un nou punt de vista en l'organització d'aquesta via de senyalització.

# Introduction

## Cellular signaling

The molecular basis of cell signaling emerged in the 60s with the discovery of nerve growth factor (NGF) and epidermal growth factor (EGF) by Rita Levi-Montalcini and Stanley Cohen, respectively. They demonstrated the involvement of these two molecules in the regulation of cell growth and differentiation. The discovery of NGF and EGF opened a new field of widespread importance to basic science. Nowadays, the understanding of cell signaling is one of the most dedicated areas of research.

The ability of cells to interact with and adapt to their environment is a key basic process of cell biology. In order to respond to changes in their surroundings, cells are able to receive and process signals from the extracellular milieu. The binding of signaling molecules to their receptors triggers signal transduction cascades involved in multiple cell responses such as metabolism, motility, proliferation, survival and differentiation (Graves & Krebs, 1999). The signals can be presented in a variety of contexts, for example soluble factors (chemicals, sugars, proteins, etc.), a ligand bound to another cell, or the extracellular matrix itself. To achieve a proper response, cells maintain a diversity of receptors on their surface that respond specifically to particular stimuli. The activity of a given receptor can be modulated by other signaling pathways in a several ways, generating the flexibility required for such a complex system to function correctly. In a simplified manner, a typical profile for a signaling pathway shows a curve determined by the rise and the decay of the triggered response (Lemmon et al., 2016). Transient or sustained stimulation of the same signaling pathway can dramatically alter the cellular outcome of receptor activation (Marshall et al., 1995).

### Post translational modifications in cell signaling

The information flow that a signaling pathway transmits from the plasma membrane to the nucleus, generally occurs through the enzymatic generation of post-translational modifications (PTMs). PTMs are reversible biochemical changes found on all types of proteins, from nuclear transcription factors to structural proteins, metabolic enzymes, and plasma membrane receptors (Liu et al., 2012). The addition of PTMs to proteins leads to changes in their physicochemical properties allowing the regulation of catalytic processes and protein assembly. More than 200 types of PTMs have been identified to target nucleic acids, metabolites, carbohydrates and phospholipids (Banks et al., 2000). Protein phosphorylation is considered the most frequent PTM in signal transduction, but other modifications such as ubiquitination and acetylation are also widespread (Wang et al., 2013) (**Figure 1**).

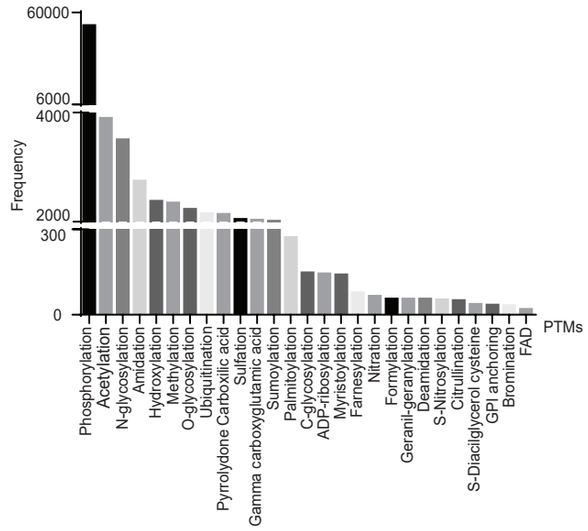


**Figure 1. Summary of experimentally identified PTMs.** The most frequent PTM is protein phosphorylation. The graph was adapted from (Khoury, Baliban, & Floudas, 2011).

Besides their role in transmitting stimuli, PTMs participate in the negative regulation of the signaling network. When signals flow downstream, immediate feedback regulations can occur by interactions and PTMs of target and upstream proteins. In the case of protein phosphorylation, a common mechanism of negative regulation is dephosphorylation by phosphatases (Lemmon et al., 2016), whereas in other cases, signal attenuation relies on the degradation of the activated proteins and receptors (Kang, Tian, & Benovic, 2014) (Irannejad & von Zastrow, 2014). Multiple degradation pathways operate within cells recognizing tagged-proteins with different PTMs such as ubiquitylation and acetylation (Hochstrasser, 1996) (Qian et al., 2013).

## Protein degradation pathways

Protein degradation is a mechanism that maintains cell homeostasis by removing damaged and unnecessary molecules. The two major processes that regulate protein degradation are autophagy and the ubiquitin-proteasome system (UPS). Autophagy regulates several cell responses by removing potentially dangerous cell components such as dysfunctional organelles and protein aggregates. Accordingly, autophagy serves as an adaptive mechanism to cope with cellular stresses such as hypoxia and nutrient deprivation (Lamb, Yoshimori, & Tooze, 2013) (Levine & Kroemer, 2008). Similarly, the UPS is involved in various critical functions, including cell survival and proliferation (Daniel Finley, 2009). Both systems contribute to protein quality control in an interconnected manner and communicate with each other via several mechanisms.







In general, **autophagy** occurs when the cell consumes part of itself (cytosol fractions, organelles and macromolecules) by fusing autophagosomes with lysosomes. Lysosomes are single-membrane vesicles containing various hydrolases that reach their enzymatic activity at the acidic pH of the lysosomal lumen. Depending on the type of cargo and delivery to the lysosomes, autophagy can be classified into chaperone-mediated autophagy (CMA), microautophagy or macroautophagy. In CMA, cytoplasmic proteins are recognized by chaperones through specific motifs (KFERQ) and transferred to the lysosome for proper degradation (Kon & Cuervo, 2010). In microautophagy, the cargo is directly engulfed by the lysosome itself, whereas, macroautophagy relies on autophagic adaptors to target misfolded protein aggregates to double-membrane vesicles called autophagosomes (Mizushima, et al., 2008). Macroautophagy is regulated by three major pathways. First, under starvation, autophagy can be induced by the recruitment of several autophagy-related proteins (Atg). In this case, Atg1, Atg17 and Atg13 form a complex that increases the activity of Atg1 and induces autophagy (Neufeld, 2010). A secondary pathway is mediated by Beclin1 which interacts with several cofactors (Ambra1, Bif-1, UVRAG) to activate autophagy induced by the lipid kinase Vps34 (Levine et al., 2008). Finally, the third pathway involves Atg3- and Atg7-mediated conjugation of microtubule-associated protein 1 light chain (LC3I) to the membrane lipid phosphatidylethanolamine to form LC3II (Ichimura et al., 2000). Present in the autophagosome membranes (inner and outer), LC3II serves as a recognition site for LC3-binding chaperones which deliver their cargo inside the autophagosome (Masaaki & Yoshinobu, 2010). Once the autophagosome is formed with the sequestered cargo inside, it is transported to the lysosome, where its outer membrane fuses with the lysosome and both the inner membrane and the cargo are degraded. The macromolecules derived from autophagy are released and recycled in the cytosol (**Figure 2A**) (Yang et al., 2013) (Glick, et al., 2010).

An increasing number of studies have shown that autophagy is involved in a number of human diseases, including cancer and neurodegenerative diseases. In this regard, several compounds have been generated to inhibit autophagy and have shown anti-cancer effects (Levine & Kroemer, 2008) (Lim et al., 2006). A commonly used autophagy inhibitor is Bafilomycin A1, an antibiotic derived from *Streptomyces griseus* that targets the proton pump $H^+$-ATPase complex inhibiting the passage of protons into the lysosomal lumen and, thereby, reducing the vesicle acidification that is essential for the degradation process (Yoshimori et al., 1991). Moreover, Bafilomycin A1 blocks the fusion between autophagosomes and lysosomes, thus causing an accumulation of autophagosome-associated molecules such as LC3II (González-Rodríguez et al., 2014).

The **UPS** is a different process mostly initiated by the conjugation of ubiquitin (Ub) to the substrate protein (Daniel Finley, 2009). Substrates can be modified with a single ubiquitin (monoubiquitination) or with a polyubiquitin chain (polyubiquitination) in

which one ubiquitin is conjugated to the next (Komander & Rape, 2012). Monoubiquitination has been thought to play a non-proteolytic function that regulates several processes by facilitating the interaction and activation of substrates. However, emerging evidence shows that monoubiquitins of substrates are also processed by the proteasome (Ronai, 2016).

The attached ubiquitin can be conjugated by another ubiquitin through any of its seven lysin residues or, alternatively, to the first methionine on the previously added ubiquitin molecule. This process can be repeated several times leading to polyubiquitination. In addition, ubiquitin can be also conjugated with ubiquitin-like modifiers such as SUMO, NEDD8 and ISG15 or it can be the substrate of other post-translational modifications such as phosphorylation (Kwon & Ciechanover, 2017).

The attachment of a ubiquitin molecule involves the activity of three enzymes. First, the ubiquitin-activating enzyme (E1) activates the carboxyl-terminal glycine of a ubiquitin in an ATP-dependent manner. Once activated, the ubiquitin is transferred to the ubiquitin-conjugating enzyme (E2). In the third step, a ubiquitin ligase (E3) links ubiquitin from E2 to a lysine residue of the target protein (**Figure 2B**). In some cases, E3 transfers E2-Ub into other amino acids such as serine, threonine, tyrosine or cysteine or at the N-terminal amine group of the target protein (McDowell & Philpott, 2013). Moreover, E3 ligases are able to specifically select their substrates by the recognition of short peptide motifs termed "degrons" (Zheng & Shabek, 2017). The need to specifically target a huge variety of substrates accounts for the diversity of human E3 ligases, with more than 600 reported to date (Morreale & Walden, 2016).

E3 ligases can be classified into three groups on the basis of the conserved domain and the mechanism by which ubiquitin is transferred from E2 to the substrate (Berndsen & Wolberger, 2014). E3 RING ligases are the most abundant type of ubiquitin ligases. They are characterized by the presence of a zinc-binding domain called RING (Really Interesting New Gene) or by a U-box domain, which adopts the same RING fold but does not contain zinc. The RING and U-box domains are responsible for both binding the ubiquitin-charged E2 and stimulating ubiquitin transfer by linking the E2-Ub and the substrate (Budhidarmo, et al., 2012) (Deshaies & Joazeiro, 2009). In contrast, the HECT (homology to E6AP C terminus) and the RBR (RING-between-RING) E3 ligases ubiquitinate substrates in a two-step reaction in which ubiquitin is transferred from the E2 to an active site cysteine in E3 and then from E3 to the substrate (Wenzel & Klevit, 2012).

The ubiquitinated-protein is then recognized and degraded by the proteasome. The proteasome is a multisubunit complex that exists in cells in two main forms, 20S and 26S species. The 20S proteasome is the catalytic core particle whereas the 26S is composed by the incorporation of a 19S regulatory subunit to both ends of the 20S proteasome. In particular, the 20S particle is formed by two α-rings and two β-rings with different peptidase activities. Together, they form two heteromeric rings with four seven subunits





($\alpha_{1-7}$, $\beta_{1-7}$, $\beta_{1-7}$, $\alpha_{1-7}$). These subunits are sequestered inside the core to avoid non-specific protein degradation (**Figure 2C**). The 19S regulatory subunit consists of a base and a lid complex. The base has an AAA-ATPase ring formed by Rpn (proteasome regulatory particle base subunit) 1-6 that binds to Rpn1, Rpn2, Rpn10 and Rpn13 (**Figure 2C**).

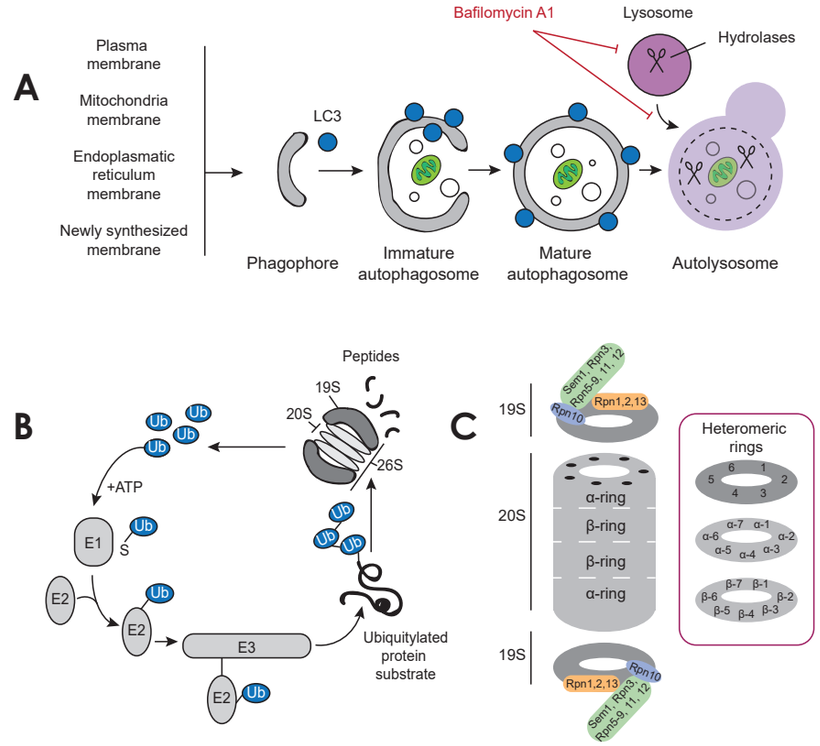


**Figure 2. Protein degradation mechanisms.** (**A**) Macroautophagy starts with the formation of the phagophore, a double membrane originated from the endoplasmic reticulum, mitochondria or plasma membrane. The cytoplasmic fraction is then engulfed into the phagophore, and the membrane elongates until giving rise to the autophagosome. This process requires the conjugation of LC3 proteins to phosphatidylethanolamine. As final step, the autophagosome fuses with the lysosome to form the autolysosome, where the cargo is degraded by the presence of hydrolases. Bafilomycin A1 inhibits autophagy by blocking the acidification of lysosomes and the formation of autolysosomes. Image adapted from (Vilchez, Saez, & Dillin, 2014). (**B**) Ubiquitin is activated by the E1 enzyme and subsequently transferred to the E2 Ub-conjugating enzyme. This enzyme then binds to a specific E3 ligase. Finally, the ubiquitin is transferred to the specific substrate. Repetition of this process generates a polyubiquitin chain that functions as a signal to target the substrate for proteasomal degradation. Deubiquitinating enzymes release the ubiquitin molecules from the substrate to be reused in subsequent reactions. The substrate is degraded to short peptides. Image taken from (Welchman, Gordon, & Mayer, 2005). (**C**) The 26S proteasome is formed by the 20S and the 19S subunits. The 20S is formed by two heteromeric rings (a and b, with seven subunits each). The 19S is formed by AAA-ATPases (Rpt 1-6) and the indicated subunits. Image taken from (Bedford, Paine, Sheppard, Mayer, & Roelofs, 2010).

Rpn1 and Rpn2 are scaffold proteins that bind to proteasome subunits and to other proteasome-associated proteins (Effantin, et al., 2009), whereas Rpn10 and Rpn13 act as ubiquitin receptors (D. Finley, 2009). On the other hand, the regulatory complex contains other proteins such as Rpn11 and Usp14 as deubiquitinating enzymes (Leggett

et al., 2002). Importantly, deregulation of the proteasome is associated with a number of diseases, including cancer (Manasanch & Orlowski, 2017). In this regard, several inhibitors have been developed to target the 20S catalytic core (Bortezomib, MG132) (Chen et al., 2011) (Han et al., 2009), as well as the regulatory subunit 19S (b-AP15, O-phenanthroline) (Deng et al., 2017) (Song et al., 2017).

For many years, the 26S-UPS was considered the primary route for proteasomal degradation, and many proteins such as cell cycle regulators (cyclins) and the tumor suppressor p53, have been identified as 26S-proteasome targets (Glotzer et al., 1991) (Vousden & Lane, 2007). On the other hand, proteins can be also targeted for degradation in a ubiquitin-independent manner. Intrinsically unstructured proteins that contain disordered regions can normally be degraded by the catalytic subunit 20S itself (Erales & Coffino, 2014) (Asher et al., 2006). Moreover, other types of proteasomes have been described in specific processes such as spermatogenesis. In this case, the proteasome contains the activator PA200 and catalyzes the degradation of acetylated proteins instead of ubiquitinated targets (Qian et al., 2013), indicating that other PTMs are also involved in protein degradation.

## Scaffold proteins in cell signaling

Besides protein degradation, signaling cascades require additional regulatory mechanisms such as proper protein localization within the cell and correct control of activation kinetics. Scaffold proteins specifically modulate the subcellular localization of proteins and facilitate complex formation, thereby playing an important role in the regulation of signal transduction pathways (Langeberg & Scott, 2015). The term "scaffold" has been widely used by the research community, however, there is no strict definition of the concept to date. Here we define scaffold protein as a molecule that allows interaction between several components regulating multiple functions within a signaling pathway.

Scaffold proteins can regulate signal transduction pathways in four major ways. First, they can act as platforms, allowing the formation of protein assemblies. By directing the signal in a cascade module formed by specific protein components, these protein complexes enhance signaling efficiency and specificity and prevent indirect interactions. Moreover, the binding between the scaffold protein and the signaling molecules can result in allosteric changes, thereby activating or inhibiting signaling (Burack & Shaw, 2000). Another important function of scaffold proteins is the modulation of subcellular localization. In this regard, these proteins can distribute components of the signaling cascade in a specific place inside the cell, such as the cell membrane or organelles (Good et al., 2011). In addition, scaffold proteins can regulate the strength of the signaling pathway by coordinating positive and negative feedback loops (Garbett et al,. 2014) (Pan et al.,2012). Finally, scaffold proteins might sometimes protect active signaling





molecules from inactivation and/or degradation. (**Figure 3**). The multiple functions of scaffold proteins can provide additional complexity to signaling cascades and give rise to distinct signaling thresholds.

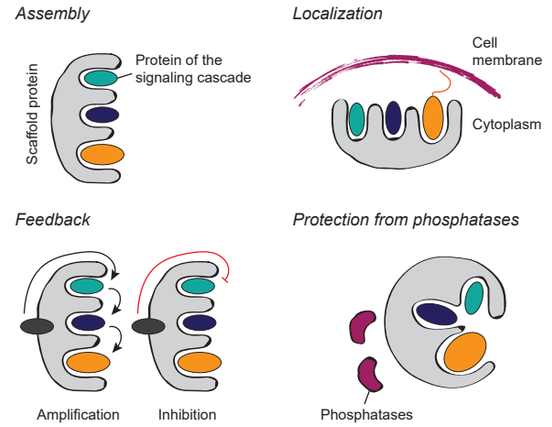


**Figure 3. Functions of scaffold proteins.** Scaffold proteins can have at least four functions: assembly of components of a signaling pathway, localization of molecules of a signaling pathway to a specific intracellular compartment, regulation of negative or positive feedback signals, and protection of active signaling intermediate proteins from deactivation by phosphatases. Scheme modified from (Shaw & Filbert, 2009).

## The mitogen-activated protein kinase signaling pathway

Signal transduction cascades start by sensing a stimulus that is amplified through PTMs. The signal is transmitted in a coordinated manner through scaffold proteins and signaling complexes until it is terminated by inactivating enzymes or protein degradation.

The mitogen-activated protein kinase (MAPK) signaling pathways are an example of signaling pathways that integrate all these regulatory mechanisms. MAPK pathways use scaffold proteins and enzymes to achieve a proper signal response. These pathways can be activated by a broad variety of stimuli, and they regulate many cellular responses, such as cell differentiation, proliferation and survival. These physiological processes mediated by MAPKs have been conserved during evolution from yeast to humans (Widmann et al., 1999).

The fourteen MAPKs described in mammals, have been classified into two groups. Canonical MAPKs comprise the extracellular signal-regulated kinases (ERK) 1/2, the c-Jun amino-terminal kinases (JNK) 1/2/3, the p38 family members (α, β, γ and δ), and the extracellular signal-regulated kinase 5 (ERK5). In contrast, atypical MAPKs are less

well-characterized and comprise extracellular signal-regulated kinase 3/4 (ERK3/4), 7/8 (ERK7/8) and Nemo-like kinases (NLK) (Coulombe & Meloche, 2007).

Canonical MAPKs share specific regulatory features and are expressed in all eukaryotic cells. The phosphorylation cascade of activation is organized in a MAPK module comprising a MAPK kinase kinase (MAPKKK), a MAPK kinase (MAPKK), and a MAPK. Upon stimuli, MAPKKKs are phosphorylated in serine (Ser) or threonine (Thr) residues and are activated through their interaction with other proteins. The activated MAPKKKs trigger the phosphorylation cascade, thus leading to the sequential activation of MAPKKs and MAPKs. Specifically, MAPKs are dually phosphorylated on a conserved motif (Thr-X-Tyr) located in the activation loop of the kinase domain (Coulombe & Meloche, 2007). Depending on the stimuli, different MAPKs are activated. Generally, ERK1/2 are activated in response to growth factors whereas JNK and p38 are more responsive to stress stimuli, such as cytokine stimulation, osmotic shock, and ionizing radiation (Pearson et al., 2001). MAPKs regulate a wide range of functions by phosphorylating downstream partners, including transcription factors, regulatory and structural proteins, as well as some phosphatases. Moreover, MAPKs can also catalyze the activation of several protein kinases termed MAPK-activated protein kinases (MAPKAPKs), such as the 90-kDa ribosomal S6 kinases (RSKs) (Carriere et al., 2008), the mitogen- and stress-activated kinases (MSKs) (Buxade et al., 2008), the MAPK-interacting kinases (MNKs), the MAPK-activated protein kinases 2 and 3 (MK2, 3), and MK5 (Shiryaev & Moens, 2010) (Ronkina et al., 2008) (**Figure 4**).
MAPKs phosphorylate their downstream substrates on a Serine or Threonine residue which are usually followed by a proline (SP/TP). This weak consensus provided by their catalytic site is insufficient for selective target recognition, and other determinants are needed to direct individual kinases towards their correct substrates. The specific binding is often conferred by dedicated interaction motifs located in both MAPKs and MAPK partners (substrates, activators and phosphatases) (Roux & Blenis, 2004).

Two types of docking motifs have been identified in MAPK substrates and cognate proteins, namely: the FXF motif and the docking motif (D-motif) (Sharrocks et al., 2000). The FXF motif is conserved in MAPK partners such as transcription factors (*e.g.* Elk1) (Jacobs et al., 1999), upstream activators (*e.g.* MKK7) and phosphatases (*e.g.* MKP1) (Liu et al., 2016), and it comprises two phenylalanines separated by one amino acid. The FXF motif is located 6-20 amino acids downstream of the phosphoacceptor site (**Figure 5A**). In contrast, the D-motif is conserved among MAPK-interacting molecules, and it consists of two or more basic residues followed by a short linker plus a cluster of hydrophobic residues. In activators (MAPKKs) and phosphatases (MKPs), the D-motif is located within the N-terminus (classical D-motif), whereas in substrates (MAPKAPKs) it is found in the C-terminus (reverse D-motif) (Tanoue & Nishida, 2003).





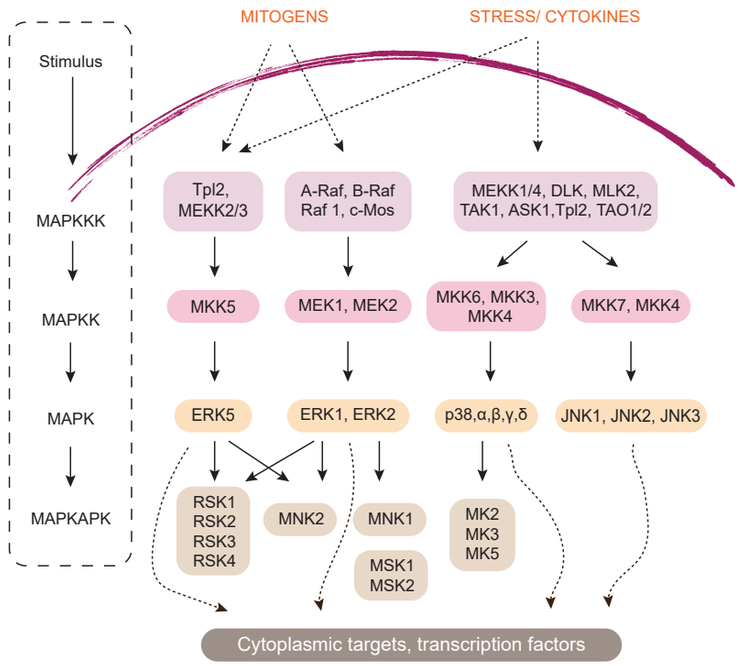


**Figure 4. Features of MAPK signaling.** Canonical MAPK signaling cascades lead to the activation of downstream targets. Mitogens and cellular stresses promote the activation of different MAPK pathways, which in turn phosphorylate and activate MAPKAPKs and other substrates, including both cytoplasmic targets and transcription factors. Graph adapted from (Cargnello & Roux, 2011).

In any case, the D-motif is located in a non-catalytic region of the MAPK interactors (**Figure 5A**). Classical MAPKs (ERK, JNK and p38) recognize the D-motif in downstream partners through docking sites that contain hydrophobic residues outside the catalytic domain. The most important docking site present in all MAPKs is the CD (Common Docking) region. The CD domain is located in the C-terminus part of the MAPK protein and it consists of a negatively charged region composed of two or three acidic amino acids. This domain is important for high affinity docking interactions and is required for ensuring efficient enzymatic reactions (Tanoue et al., 2000). Since the CD site is found in every MAPK, additional residues have been identified to regulate docking specificity. In fact, the ED domain contributes to substrate selectivity in ERK and p38 proteins. Together with the CD site, both regions form a negatively charged hydrophobic docking groove (Tanoue et al., 2001) (**Figure 5B**).

Given that the p38 and ERK docking grooves (containing the CD and ED) are similar in structure, it has been proposed that other docking determinants regulate the specificity of their enzymatic reactions. Recent studies suggest that the structural conformation of the intervening regions between the D-motifs and MAPK-docking sites mostly deter-

mines the MAPK docking specificity (Garai et al., 2012) (Zeke et al., 2015).

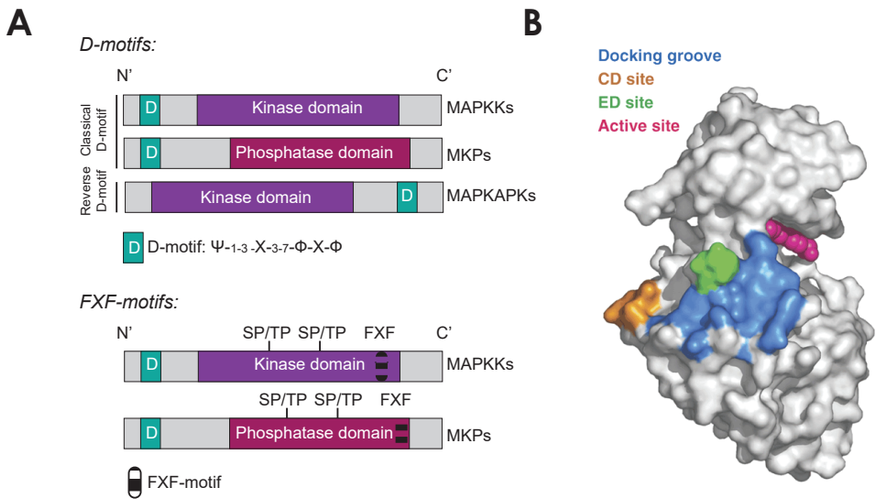


**Figure 5. Features of the MAPK docking motifs.** (**A**) Graphical representation of the D-motif (in which ϕ, ψ and X mark hydrophobic, positively charged, and any other amino acid, respectively) and the FXF motif among activators (MAPKKs), substrates (MAPKAPKs) and phosphatases (MKPs). Figure modified from (Tanoue & Nishida, 2003). (**B**) MAPK (ERK and p38) interactions through the indicated motifs with scaffold proteins, activating enzymes, phosphatases and substrates. Image modified from (Weston, Lambright, & Davis, 2002).

## Conformation of MAPKs in activation and catalysis

Protein kinases are dynamic structures and their functionality strongly depends on their conformational state. The active site of kinases is highly conserved and is located between two lobes, the N- and C-lobe, connected by the hinge region (McClendon et al., 2014) (**Figure 6**). This region determines the orientation of the N- and C- lobes during the catalytic process. In addition to binding to and releasing their substrates, kinases bind ATP at the P-loop and hydrolyze it. For this purpose, the structure of MAPKs is required to adopt various conformation transitions. The N-lobe undergoes significant structural rearrangements while the C-lobe is more rigid and shows less conformational flexibility, except for one conserved structural region called the activation loop (A-loop) (**Figure 6**). The A-loop starts with a highly conserved DFG motif (Asp-Phe-Gly) and extends to include the Thr-X-Tyr phosphorylation site (**Figure 6**) (Kung & Jura, 2016). During catalysis, the A-loop undergoes significant conformational changes and stabilizes the active state of the kinase (Huse & Kuriyan, 2002). In this state, referred to as "DFG in", the Asp DFG points to the active site while the Phe DGF points in the opposite direction. Furthermore, the Asp and Phe residues can exchange positions ("DFG out"), thereby preventing ATP binding and keeping the kinase in an inactive conformation. Importantly, these conformational changes in the A-loop are accompanied by





the αC helix, which is located in the N-lobe and contributes to maintaining the inactive conformation of the kinase. Although these structural transitions occur during the catalytic cycle, several studies also support the notion that these transitions are important for non-catalytic functions of kinases (Kung & Jura, 2016).

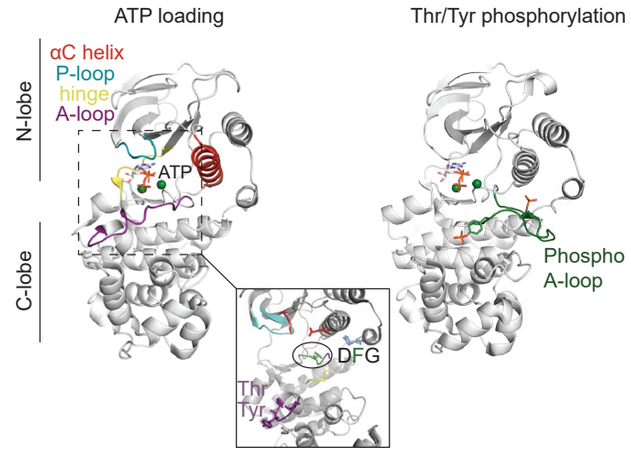


**Figure 6. Residues implicated in MAPK catalysis.** Representation of the active conformation of p38α MAPK showing the ATP loading (left image) and the phosphorylated protein (right image). Both structures illustrate the changes in the A-loop upon phosphorylation. The inset displays a close-up view of the active site, highlighting the DFG motif (the Phe residue is labeled in green). Images obtained using PyMol v2 software.

## Non-catalytic functions of MAPKs

A key function of MAPKs is to phosphorylate other proteins. However, MAPKs can also mediate cell function independently of their kinase activity. Kinases that use their kinase domain in a catalytic independent manner are called as pseudokinases (Jacobsen & Murphy, 2017). Using either MAPK-docking domains or functioning as pseudokinases, MAPKs can regulate some cellular processes in a non-catalytic manner, namely by allosteric regulation of other proteins, by acting as scaffolds, and even by direct interaction with DNA.

***Allosteric regulation of other kinases or enzymes***

Several MAPK cascade components can regulate the catalytic activity of other kinases through dimerization. For example, RAF kinases (A-RAF, B-RAF and C-RAF) function as MAPKKKs and can be activated through the formation of "side to side" dimers, in which one RAF molecule allosterically activates the other in a kinase-independent manner. This allosteric mechanism was observed primarily in the B-RAF kinase dead mutants found in human cancer (G466E, G466V and G596R). Despite their impaired

kinase function, these mutants were able to stimulate cell proliferation through C-RAF heterodimerization (Wan et al., 2004) (**Figure 7A**). In addition, kinases can allosterically regulate the activity of unrelated enzymes. ERK2, for instance, binds directly to the dual-specificity phosphatase MKP3, triggering a conformational change in its catalytic domain that enhances MKP3 phosphatase activity. Moreover, ERK2 has been proposed to use a similar mechanism to allosterically activate topoisomerase II and poly (ADP-ribose) polymerase I (PARP1) in a kinase-independent manner (Shapiro et al., 1999) (Cohen-Armon, 2007) (**Figure 7A**). Along this line, a recent biochemical study based on NMR spectroscopy proposed an allosteric enhancement of p38α kinase activity upon the binding of different substrate-derived peptides. The authors of that study found that docking interactions induce an increase in substrate affinity and ATP loading (Tokunaga et al., 2014). Another mechanism of allosteric regulation is found in JNK proteins, which, upon binding to certain peptides, can be autoinhibited, thus preventing spurious activity towards substrates (Laughlin et al., 2012).

***Scaffold regulation of MAPK signaling complexes***

As mentioned earlier, scaffold proteins regulate multiple functions by binding to several components within a signaling pathway. An example of scaffold protein is the JNK-interacting protein-1 (JIP1), which allows the recruitment of MAPKKKs, such as DLK and MLK, and MAPKKs such as MKK7, to induce the phosphorylation of JNK and enhance pathway activity (Zeke et al., 2016). A second example is JIP4, which does not activate JNK but serves as an activator of the p38 MAPK pathway by recruiting the p38 MAPK upstream activators. On the other hand, the scaffold protein Discs large homologue 1 (DLG1) coordinates alternative p38α activation, mediated by Lck and Zap70 tyrosine kinases, thus facilitating phosphorylation of the transcription factor NFAT (Round et al., 2007). Another example of scaffold protein is the adaptor Kinase Suppressor of Ras (KSR), which regulates the Ras/MAPK pathway by coordinating the assembly of the RAF/MEK/ERK module (Raabe & Rapp, 2002). In this case, KSR acts as a pseudokinase since this function depends on its kinase domain but is independent of its catalytic activity. Upon growth factor stimulation, KRS interacts with RAF to allow MEK phosphorylation (**Figure 7B**). Moreover, KSR also interacts with ERK, which then phosphorylates RAF and KSR to negatively regulate the MAPK pathway (McKay et al., 2011).

***Regulation of transcription***

The regulation of transcription by a non-catalytic MAPK function is still under investigation. Data profiling interactions between human proteins and DNA revealed that ERK and MAP4K2 regulate transcription by binding directly to DNA. Specifically, ERK uses a cluster of positively charged amino acids in the kinase domain to bind to the promoters of several genes that repress their transcription (**Figure 7C**). Kinase dead





mutations and ERK inhibitors had no effect on the ability of ERK2 to inhibit transcription, thereby indicating that this function is regulated in a kinase independent manner (Hu et al., 2009). On the other hand, it has been described that a kinase-inactive form of ERK5 retains transcriptional activity when Hsp90 dissociates from cdc37-ERK5 complex, indicating that, in some cases, ERK5 does not require kinase activity to induce gene transcription (Erazo et al., 2013).

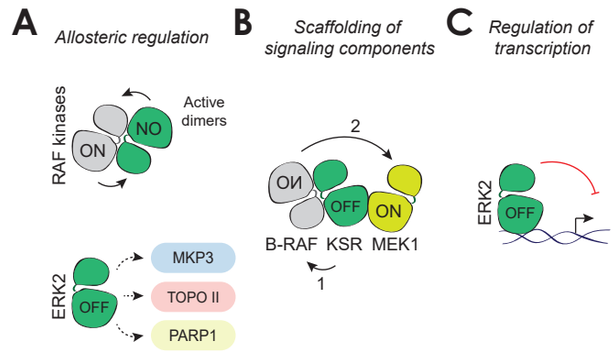


**Figure 7. Non-catalytic functions of MAPKs.** (**A**) Allosteric regulation of RAF family kinases and ERK2. (**B**) KSR activates B-RAF through dimerization and brings it to MEK. (**C**) ERK2 binds directly to promoters to repress transcription. Figure adapted from (Kung & Jura, 2016).

In summary, the non-catalytic functions of MAPKs have been focused primarily on the ERK signaling pathway because of its scaffolding function (Meister et al., 2013) (Witzel et al., 2012) (Brown & Sacks, 2009). Although ERK1/2 and p38α MAPKs are similar in structure with a common docking groove, the scaffolding role of p38α has not been addressed to date.

## p38 MAPK signaling pathway

The mammalian p38 MAPK family comprises four members: p38α, p38β, p38γ and p38δ. The most abundant family member is p38α which is highly expressed in many tissues, whereas p38β is usually found at low levels, except in brain. In contrast, p38γ is expressed at high levels only in skeletal muscle, and p38δ is found mainly in pancreas, kidney and small intestine (Cuenda & Rousseau, 2007). p38 MAPKs are encoded by four genes and share approximately 60% of identity in their overall amino acid sequence and more than 90% within their kinase domain (Coulthard et al., 2009). Despite the high homology, various phenotypes have been reported in mice lacking specific p38 MAPKs. Whereas p38β, p38γ and p38δ knock out (KO)mice are viable and fertile with no apparent health problems (Beardmore et al., 2005) (Sabio et al., 2005), p38α KO

mice are embryonic lethal due to placental defects (Adams et al., 2000) (Mudgett et al., 2000). Moreover, conditional deletion of p38α in the embryo also leads to lethality shortly after birth as result of developmental problems in the lungs (Hui et al., 2007). On the other hand, p38 MAPK members have notable differences regarding upstream activators and downstream effectors, as well as in their sensitivity to chemical inhibitors. However, in some cases, they have functional redundancy upon their genetic ablation (Sabio et al., 2005). For example, several embryonic phenotypes including defects in heart development, spina bifida, and exencephaly were observed in p38α and p38β double knockout embryos. However, these defects were absent in single gene knockouts, thereby indicating that the two isoforms compensate for each other with respect to these defects (del Barco Barrantes et al. 2011).

Upon stimuli, p38 MAPKs are activated by dual phosphorylation in their A-loop sequence (Thr-Gly-Tyr) by either MKK6 or MKK3, whose efficiency on the various p38 MAPKs varies (Alonso et al., 2000). Thus, MKK6 phosphorylate the four p38s, whereas MKK3 activates p38α p38γ and p38δ but not p38β (Cuadrado & Nebreda, 2010). In addition to MKK3 and MKK6, p38α can be also activated by MKK4 (a JNK activator). The relative contribution of MAPKKs to p38 MAPK activation depends mainly on the cell type and the stimulus received (Brancho et al., 2003) (Remy et al., 2010). Upstream in the pathway, 10 MAPKKKs have been identified in mammals to stimulate MKK3/6/4 which in turn leads to p38 MAPK activation (Cuadrado & Nebreda, 2010). These include the following: ASK1 (apoptosis signal-regulating kinase 1); DLK1 (dual-leucine-zipper-bearing kinase 1); TAK1 (transforming growth factor β-activated kinase); TAO (thousand-and-one amino acid) 1 and 2; TLP2 (tumor progression loci 2); MLK3 (mixed-lineage kinase 3); MEKK (MAPK/ERK kinase kinase) 3 and 4; and ZAK1 (leucine zipper and sterile-α motif kinase 1) (**Figure 8**). Similarly, the MAPKKKs involved in p38 MAPK activation also rely on the stimulus and the cell type. For example, ASK1 activates p38 MAPKs in response to tumor necrosis factor (TNFα) or oxidative stress (Tobiume et al., 2001) whereas MEKK3 responds to hyperosmotic shock. On the other hand, as shown in **Figure 4**, several MAPKKKs that trigger p38 MAPK activation can also activate JNK. These observations indicate, that the diversity and regulatory mechanisms of MAPKKK confer capacity to respond to many stimuli as well as to integrate signaling pathways (Cuevas et al., 2007).

Importantly, the regulation of signal intensity is required for proper transient activation and thus specific outcomes. Protein phosphatases are involved mainly in this inactivation process, targeting the Thr and/or Tyr residues from the p38 MAPK A-loop. In addition to generic phosphatases such as PP2A and PTP which can target the Thr and Tyr residues respectively, there is a group of MAPK phosphatases, called mitogen-activated protein kinases phosphatases (MKPs), which are classified on the basis of their preference for dephosphorylating Tyr, or both Tyr and Thr. MKPs are members of the dual specificity phosphatase (DUSP) family.





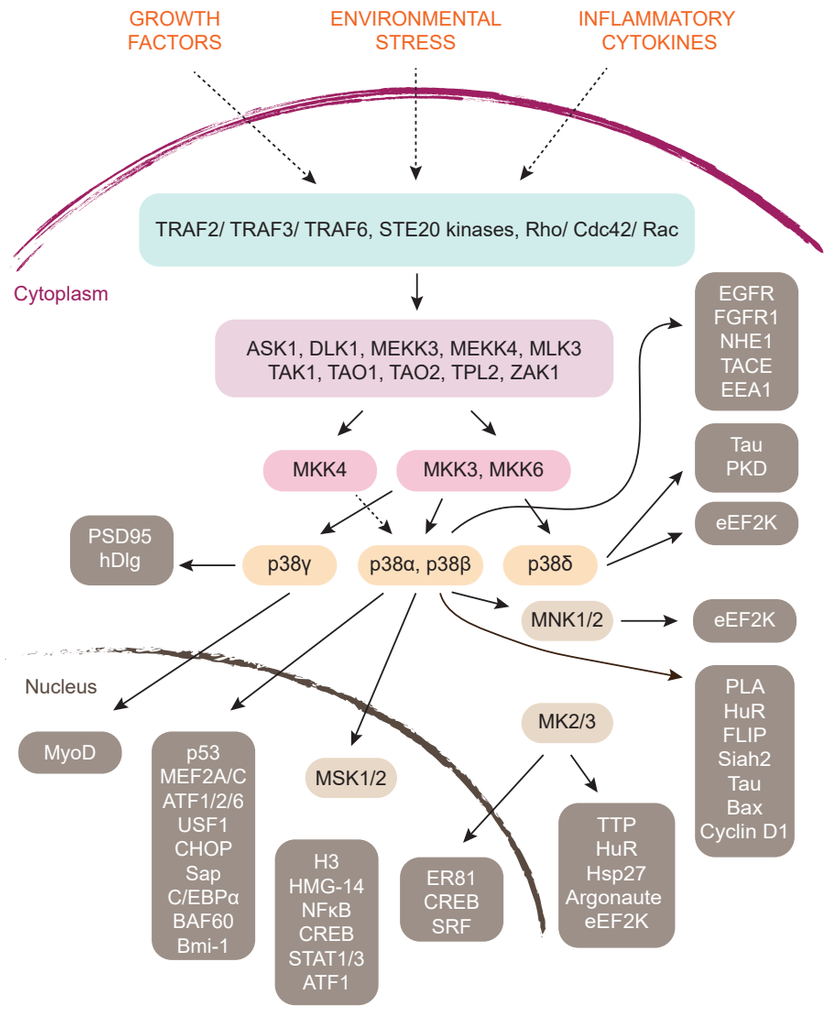


**Figure 8. The p38 MAPK pathway.** Stimuli such as growth factors, inflammatory cytokines and environmental stresses can activate p38 MAPKs, which in turn target protein kinases, cytosolic substrates, transcription factors or chromatin remodelers. Adapted from (Cuadrado & Nebreda, 2010).

There are 10 MKPs catalytically active in mammalian cells, and these all share a common structure consisting of an N-terminal regulatory domain and a C-terminal catalytic domain. The N-terminal contains the D-motif which mediates the ability of the phosphatase to recognize the MAPK substrate (Caunt & Keyse, 2013). The core of the D-motif in the MKPs is characterized by a cluster of two or three positively charged arginine (Arg) residues flanked by hydrophobic amino acids. Variations in the number of positively charged and hydrophobic residues are thought to contribute to the specificity

of MAPK binding (Tanoue et al., 2002). However, one single phosphatase can recognize different MAPKs, therefore, other parameters are required to specifically select the proper MAPK cognate. In some cases, different residues can distinguish the substrate selectivity between JNK, ERK and p38 MAPKs. Mutations in the conserved cluster of positively charged amino acids of MKP1 abolishes the binding to JNK1 but not to p38α or ERK2 (Slack et al., 2001). Regarding the binding selectivity between p38 and ERK, additional molecular determinants are required. In fact, it has been suggested that the interaction between p38 or ERK and PTP-SL, STEP or PTPN7 is influenced by intracellular redox conditions (Muñoz et al., 2003).
On the other hand, the control of p38 activity by phosphatases is often regulated by the p38 MAPKs themselves. For example, p38α can regulate MKP1 expression at a post-transcriptional level through the phosphorylation of MK2 upon exposure of cells to lipopolysaccharide (LPS) (Hu et al., 2007).

In addition to regulating negative feedback loops involving phosphatases, p38 MAPKs modulate many cellular processes by phosphorylating several proteins. These include nuclear proteins like transcription factors and regulators of chromatin remodeling and also a wide range of cytosolic proteins that regulate multiple processes, such as mRNA stability, protein degradation, apoptosis, cytoskeleton dynamics and cell migration.
In particular, p38α and p38β are able to phosphorylate a wide range of substrates, whereas p38γ and p38δ seem to target a lower number (Shi & Gaestel, 2002). In some cases, although substrates can be phosphorylated by more than one p38 MAPK (Corrêa & Eales, 2012), they usually show specificity among p38 MAPK members. As previously mentioned, the ability to phosphorylate proteins is influenced by binding sites through D-motifs and MAPK docking sites (**Figure 5**). The differences in the CD motifs of p38 MAP kinases (**Table 1**) might contribute to their ability to recognize substrates. It is also important to take into account that some substrates do not seem to have docking motifs and might use other mechanisms to facilitate their efficient phosphorylation (Cuadrado & Nebreda, 2010).

**Table 1 | CD properties of p38 members**
Table adapted from (Yu Shi & Matthias Gaestel, 2002).

| p38 | CD motif |
|---|---|
| p38α | DPDD |
| p38β | DPED |
| p38γ | DPED |
| p38δ | DPEE |





# Molecular determinants and functions of p38α MAPK

p38α is the prototypic member of the p38 MAPK family, and most of the published literature on p38 MAPKs refers to p38α (Wagner & Nebreda, 2009). It is encoded by the MAPK14 gene, and three p38α transcript variants have been identified (Exip, Mxi2 and CSBP1). Exip and Mxi2 lack different parts of the p38α protein. Mxi2 is identical to p38α in amino acids 1–280 but has a different C-terminus comprising 17 amino acids. In contrast, Exip has a unique 53-amino-acid C-terminus and is not phosphorylated by the usual p38 MAPK-activating treatments (Sudo et al., 2002). The CSBP1 isoform differs from p38α in an internal 25-amino-acid region, and its functional importance is still unclear (Lee et al., 1994).
Upon stimuli, p38α is phosphorylated on the TGY motif by upstream kinases (MKK3, MKK6 and MKK4) and then it activates different substrates depending on the stimuli and cell type. However, p38α can also be activated by alternative mechanisms. In this regard, p38α is phosphorylated on Tyr 323 by ZAP70 (ζ-chain-associated protein kinase 70 kDa) and Lck (Lymphocyte-specific tyrosine kinase) upon TCR (T-cell receptor) stimulation. The phosphorylation on Tyr 323 stimulates p38α autophosphorylation on the A-loop (TGY motif), thereby increasing its kinase activity (Salvador et al., 2005). In addition, p38α can bind to TAB1 (TAK1-binding protein1), which promotes p38α autophosphorylation on the A-loop. The later mechanism seems to be restricted mainly to some p38α functions in cardiomyocytes and myeloid cells (Ge et al., 2002) (Kim et al., 2005) (Li et al., 2005).
Activated p38α can phosphorylate many substrates on Ser or Thr residues, including transcription factors, protein kinases and cytosolic and nuclear proteins (Trempolec et al., 2013).

## p38α-mediated functions

The activities attributed to p38α include inflammatory response, cell differentiation, cell-cycle arrest, apoptosis, senescence, cytokine production, and regulation of protein synthesis (Cuadrado & Nebreda, 2010). For example, p38α regulates the differentiation of various cell types by phosphorylating transcription factors, such as C/EBPβ, which promotes adipocyte and lung cell differentiation (Engelman et al., 1998) (Ventura et al., 2007). p38α also controls skeletal muscle differentiation by regulating the sequential activation of myogenic regulatory factors (MRFs) and their transcriptional coactivators, including chromatin remodeling enzymes (Perdiguero et al., 2006). On the other hand, p38α negatively regulate cell cycle progression by targeting several substrates. p38α can induce G1/S arrest by transcriptional up-regulation of $p16^{INK4a}$, down-regulation of

cyclin D1 or activation of the p53/p21$^{Cip1}$ pathway (Lavoie et al., 1996) (Casanovas et al., 2000) (Kim et al., 2002) (Goloudina et al., 2003). Moreover, p38α contributes to G2/M cell cycle arrest (Mikhailov et al., 2004), which may be mediated by the phosphorylation of Cdc25B and Cdc25C, either directly by p38α or via activation of MK2 (Manke et al., 2005) (Karlsson-Rosenthal & Millar, 2006).

Another important function of p38α is the regulation of protein synthesis via MNK1, which phosphorylates eIF4E at Ser209 (Wendel et al., 2007). Moreover, p38α stimulates the expression of various inflammatory mediators, including TNFα, IL-1β, IL-6 and CXCl2 (Anderson, et al., 2008) (Qiu et al., 2015).

Consistent with all these functions, deregulation of the p38α signaling pathway is linked to several pathologies, such as inflammatory, cardiovascular and neurodegenerative diseases, as well as cancer (Kumar et al., 2003).

The set of substrates phosphorylated in each case most likely varies depending on each particular response and cell type. It has been shown that docking interactions via the non-catalytic region of MAPKs are important to establish specific protein-protein interactions for proper substrate recognition. In general, protein-protein interactions involves various mechanisms, depending on structural composition, protein affinity and whether the association is permanent or transient (see **Box 1**). As a kinase, p38α interacts mainly with downstream partners in a transient manner through residues that mediate the phosphotransfer reaction (Perkins et al., 2010). However, in some cases, the docking regions and structural domains of p38α are used to specifically bind to partners in a more stable fashion (Garai et al., 2012) (Tanoue et al., 2002).

**BOX 1**

| | |
|---|---|
| **Diversity of protein-protein interactions (PPI)**<br><br>PPIs plays different roles in biology and differ based on the composition, affinity and whether the association is permanent or transient. On the other hand, the local cell environment is critical to control the oligomeric state of interacting proteins. Moreover, other determinants such as protein concentration and binding energy will control protein interactions and thus protein complex formation.<br><br>*Information addapted from:*<br>(Nooren & Thornton, 2003) | COMPOSITION<br>Homo-and hetero-oligomeric complexes. PPIs occur between identical (**oligomers**) or non-identical chains (**heterooligomers**).<br><br>AFFINITY<br>Obligate and non-obligate. **Obligate** interactions occur when proteins are not found as stable structures on their own. Generally, their functionality depends on the complex formation. In contrast, in **non-obligate** PPIs, proteins exist independently.<br><br>ASSOCIATION<br>Transient and permanent. Based on the lifetime of PPIs. **Permanent** interactions are very stable and proteins only exist when the complex is formed. Whereas **transient** interactions associate and dissociate. They are classfied in two groups: Weak (when the interaction is broken and formed continously) and stable (when proteins require a molecular trigger to shift the oligomeric equilibrium). |





## p38α structural domains

p38α has a typical kinase structure that comprises two lobes (N- and C- lobes) linked by a flexible hinge (**Figure 6**). The ATP binding site is located between the two lobes and is composed by several residues such as K53, E71, R67, R70 and D168 (**Figure 9A**). Upon dual phosphorylation on the TGY motif, p38α is subjected to a large rearrangement that displaces the A-loop away from the ATP-binding site (Kuzmanic et al., 2017) (Zhang et al., 2011) (**Figure 9B**). Moreover, p38α and other MAPKs contain the MKI (MAPK insert), which forms a lipid-binding site (Diskin et al., 2008), and the L16 loop, which extends from the C- to the N-lobe. Conformational changes in the L16 loop have been associated with p38α activation and autophosphorylation (Diskin et al., 2007). The C-lobe segment of the L16 loop contains the acidic CD domain, which, together with the ED site, forms the hydrophobic groove (**Figure 9A**). As mentioned above, the CD has been identified in all MAPK members, whereas the ED site was found specifically in ERK1/2 and p38α proteins (Tanoue et al., 2000) (Tanoue et al., 2001). Although the CD and ED regions are involved primarily in MAPK docking specificity, other residues are required to distinguish between ERK1/2 and p38α interacting proteins. In fact, Gln120 and Ile116 have been proposed to specifically mediate p38α docking interactions. Located in the p38α docking groove, these two residues target the D-motif of p38α substrates and activators (MEF2A and MKK3 respectively) (Chang et al., 2002). On the other hand, Met194, Leu195, His228, Ile229 and Tyr258 residues are involved in the recognition of the FXF motif of substrates such as ATF2, MBP and Elk1. These residues are close to the A-loop that forms the p38α DEF pocket (Tzarum et al., 2013). In addition to the regulation of docking specificity, some p38α residues participate in other biochemical features. For example, Asp145 and Leu156 are involved in the regulation of the subcellular localization of MK5 through interaction with the MK5-nuclear localization signal (NLS) (Li et al., 2008). Moreover, mutations in Asp176 and Phe327 lead to p38α autophosphorylation, thereby enhancing the activity of this kinase (Diskin et al., 2004). There is also evidence that Tyr123 phosphorylation by GRK2 impairs p38α binding to and activation by MKK6 and reduce the ability of p38α to bind to and phosphorylate a range of substrates *in vitro* (Peregrin et al., 2006).

Some of these p38α residues were identified in crystal structures between p38α and different D-motifs containing peptides from p38α substrates and activators, and their biochemical contribution was determined by mutational studies. Since all these mutational studies were performed *in vitro*, further studies are needed to fully understand the relevance of such interactions for p38α signaling *in vivo* and how each of these regulatory mechanisms contribute to specific cell responses and tissue homeostasis.

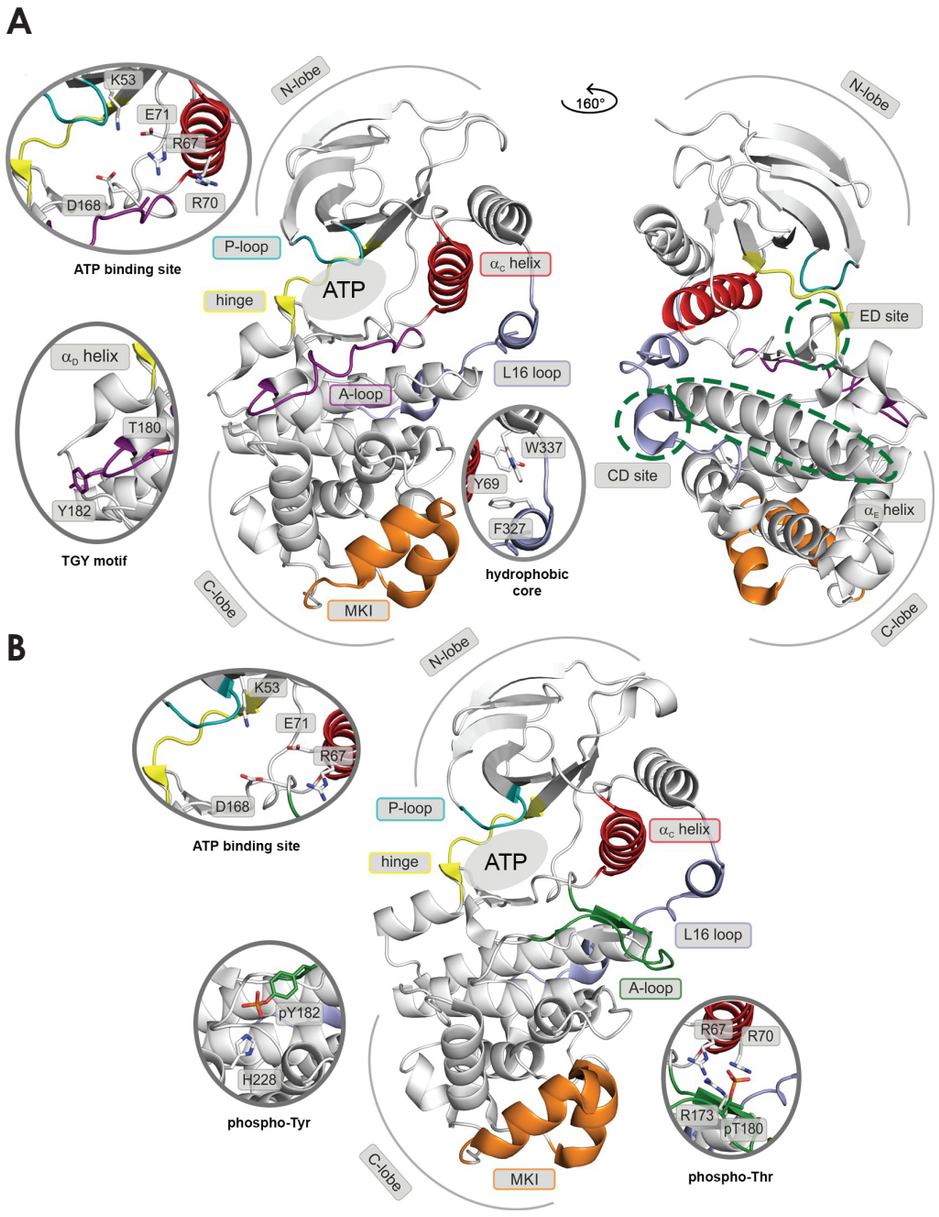


**Figure 9. Structural models of p38α.** (**A**) Inactive p38α (PDB ID: 3S3I), and (**B**) dually phosphorylated p38α (PDB ID: 3PY3). Main structural elements are colored as follows: A-loop in purple (inactive) and green (active), αC helix in red, L16 loop in slate, P-loop in cyan, hinge in yellow and MKI in orange. Key residues are shown as sticks and labeled. Different regions are indicated by the grey ellipse or green dashed ellipse. Image reproduced from (Kuzmanic et al., 2017).







# The p38a:MK2 complex

Although D-motif-containing peptides have been successfully crystalized with p38α (Chang et al., 2002) (Zhang et al., 2011) (McClure et al., 2005), only a few proteins, including MK2, TAB1 and some phosphatases, have been co-crystalized together with p38α (White et al., 2007) (ter Haar et al., 2007) (De Nicola et al., 2013) (Francis et al., 2011). Since p38α and MK2 are key regulators of several cell functions, their physical association is likely to be of physiological relevance.

## Crystal structure of the p38a:MK2 complex

p38α and MK2 show the typical kinase structure as monomers (**Figure 6**). In particular, MK2 is a multidomain protein consisting of an N-terminal proline-rich domain, a catalytic kinase domain and a C-terminal regulatory domain (amino acids 338-400) which contains an autoinhibitory domain (339-353) and a nuclear export and localization signal (NES and NLS). The NLS region contains the D-motif between the amino acids 370-389 (IKIKKI) and 358-389 (KRRKK).

The interface between p38α and MK2 proteins consists of five discontinuous contact regions, the MK2 activation segment (Tyr228-Tyr240), the MK2 helix αH (Asp345-Val365), the p38α loop β0a-β0b interaction to MK2 P loop β1'-β2', the MK2 Tyr264-Tyr284 region and the MK2 C-terminal region Asp366-390 (**Figure 10A**). The MK2 Tyr264- Tyr284 region comprises the regulatory phosphorylation domain of MK2 that interacts with the p38α TGY phosphorylation motif. On the other hand, the C-terminal end of the regulatory domain of MK2 binds to the p38α docking groove and has key interactions with the ED and CD regions (**Figure 10B**). These interactions show spatial conservation of the hydrophobic sequences from already characterized peptides accommodated in the hydrophobic groove. Like MEF2A and MKK3 peptides, MK2 also forms H bonds with p38α Gln120, His126 and Glu160. However, the binding to the p38α hydrophobic groove is in the opposite direction, thereby indicating that MK2 docking is another type of docking class, which is generally termed as reverse D-motif (White et al., 2007). Interestingly, the reverse D-motifs found in some proteins allow a clear discrimination between ERK and p38α in binding affinity. While the reverse D-motif of RSK1 displays high affinity to ERK2, its binding affinity to p38α is 20-fold lower. In contrast, the reverse D-motif of MK2 shows strong affinity to p38α but only a weak interaction with ERK2 (Garai et al., 2012).

p38α and MK2 bind in a parallel "face to face" orientation, which means that the ATP-binding sites and the binding grooves of the substrates are at the interface of the heterodimer but located at different sites. This orientation allows upstream activators to

phosphorylate the activation loop of p38α however, this conformation buries the substrate binding grooves and thus prevents the two kinases from phosphorylating their respective substrates (ter Haar et al., 2007) (Gaestel, 2015). This structure suggests that substrate phosphorylation is dependent on the heterodimer conformation.

Other studies based on steady-state kinetics and surface plasmon resonance provide molecular insights into the catalysis of the p38α:MK2 complex. It has been reported that phosphorylated p38α binds to phosphorylated GST-MK2 (1-400) with less affinity than the non-phosphorylated p38α:MK2 complex (Kd = 60 nM and 2.5 nM, respectively). However, the mechanisms by which phosphorylation attenuates the affinity are currently unknown (Lukas et al., 2004). Furthermore, the data suggest that any perturbation of the p38α and MK2 docking-interactions prevents the phosphorylation of MK2 (Lukas et al., 2004). This hypothesis has been applied for the identification of new p38α substrate-selective inhibitors.

Many p38α inhibitors with diverse chemical structures and modes of interaction have been designed on the basis of their ability to compete with ATP. However, most have failed in clinical trials due to poor efficiency or side effects (Sweeney & Firestein, 2006) (Zhang et al., 2007). Therefore, additional strategies have focused specifically on targeting the p38α docking groove and preventing the phosphorylation of D-motif-dependent partners such as MK2 (Davidson et al., 2004) (Willemen et al., 2014) (Shah et al., 2017).

The tight p38α and MK2 assembly observed *in vitro* has been used as a model to explain the mode of activation and subcellular localization (ter Haar et al., 2007) (Gaestel, 2015). However, there are controversies between published studies (Ben-Levy et al., 1998) (Gong et al., 2010). Some authors claim that these two proteins form a complex in the nucleus and that, upon stimuli, the proteins translocate into the cytosol. MK2 phosphorylation by active p38α leads to a conformational change that masks the NLS and unmasks the NES, thereby allowing the shuttling (Ben-Levy et al., 1998) (Gaestel, 2015) (Li et al., 2008). In contrast, other studies suggest that, upon stimuli, active p38α moves into the nucleus where it binds to and phosphorylates MK2 leading to its translocation from nucleus to cytoplasm (Gong et al., 2010). Although several hypotheses have been proposed, the exact mechanism remains unclear.





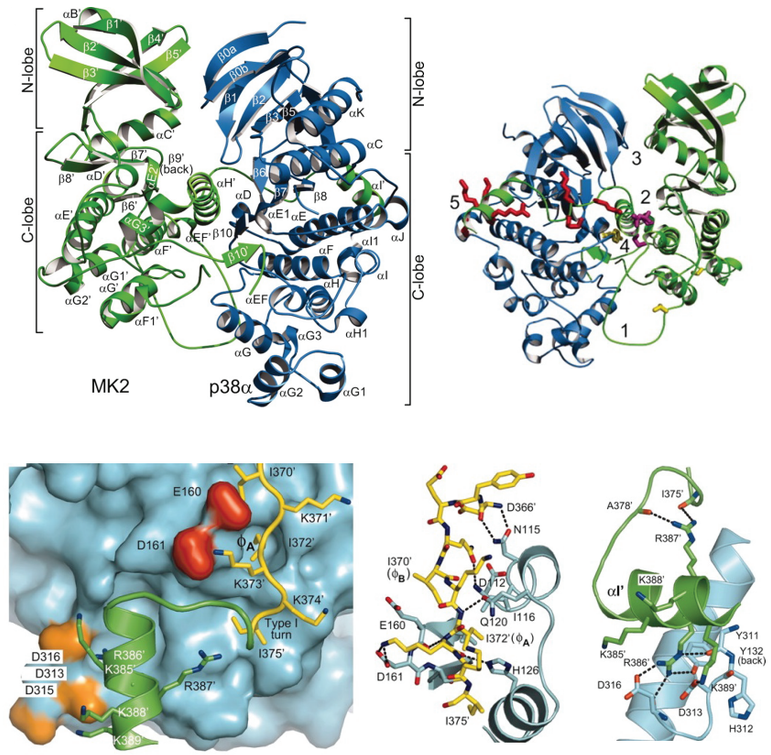


**Figure 10. Structure of the p38α:MK2 complex.** (**A**) In the left panel MK2 (green) and p38α (blue) secondary structures are shown as bundles for α-helices and arrows for β-strands. A prime (') suffix is used to denote MK2 residues and structural elements. In the right panel, the five intermolecular interface regions are shown as described in the main text. MK2 NLS is shown in red, MK2 NES is shown in magenta and the p38α and MK2 phosphorylation sites in yellow. Numbers (1-5) indicate the five discontinuous contact regions of the p38α:MK2 interface (**B**) p38α and MK2 docking interactions. The first part of MK2 NLS (371-KIKK-375) is shown in yellow and the second part of the MK2 NLS (385-KRRKK-389) is shown in green. p38α is represented as a cyan surface, the ED site is shown in red, the CD domain is shown in orange and the hydrophobic residues are represented as ϕ (right). Protein interactions between the p38α docking groove and the MK2 first part of the NLS (middle) and the MK2 second part of the NLS (left). Images reproduced from (White et al., 2007).

## Functions of the p38α:MK2 complex

The interaction between p38α and MK2 has been shown to be important *in vivo*. In fact, the amount of p38α is reduced in cells and mouse tissues lacking MK2. Analysis of various truncated forms shows that the MK2 C-terminus is indeed involved in p38α stabilization (Kotlyarov et al., 2002). Accordingly, MK2 protein levels are also reduced in p38α deficient cells. In this case, the levels of MK2 were restored upon the reintroduction of p38α but not its Exip isoform (Sudo et al., 2005). As mentioned previously, Exip is a 307-amino-acid protein that has a unique 53-amino-acid C-terminus and lacks the CD domain of p38α Therefore, the lack of p38α structural regions might prevent the stability of the MK2 protein. Moreover, the p38α and MK2 homologs in fission yeast

(Sty1 and Srk1, respectively) are also involved in mutual protein stabilization, indicating that this property is evolutionarily conserved (Lopez-Aviles et al., 2008). Although these observations demonstrate the requirement of either protein for its partner stability, the underlying regulatory mechanism is still unclear.

SDS-PAGE and chromatography analysis revealed two distinct MK2 isoforms, which might result from differential splicing. Although it has been suggested that the two isoforms interact with p38α, the binding details of the spliced isoform are still unknown (Gaestel, 2006). On the other hand, a rare human MK2 cDNA has been described, which encodes a different C-terminus that lacks both the NES and the NLS and, therefore, the D-motif (Zu et al., 1994). Since this coding mRNA is not adequately represented in expressed sequence tag libraries, this cDNA could be the result of a rare alternative-splicing event of the MK2 pre-mRNA (Gaestel, 2006).

Besides being interacting partners, p38α and MK2 are also functionally related. Several cell responses such as cell cycle, cell motility, metabolism and post-transcriptional regulation during inflammation, are mediated by the p38α-MK2 axis. As mentioned above, p38α-activated MK2 phosphorylates CDC25B and CDC25C in UV-treated osteosarcoma cells regulating the G2/M checkpoint (Bulavin et al., 2001) (Manke et al., 2005). Similar results were observed in fission yeast where the MK2 homolog Srk1 phosphorylates Cdc25 at the same sites as Chk1 and Chk2 (López-Avilés et al., 2005). In addition, the activation of p38α and MK2 usually results in the phosphorylation of Hsp27. These phosphorylations have been associated with the modification of oligomerization and chaperone properties of these substrates (Rogalla et al., 1999), as well as with regulation of the actin cytoskeleton (Guay et al., 1997). Remodeling of the cytoskeleton is a prerequisite for changes in cell shape and cell migration. In particular, the phosphorylation of Hsp27 has been implicated in cell motility through F-actin polymerization (Hedges et al., 1999). A recent report has also implicated the p38α-MK2 axis in the regulation of oxidative metabolism and mitochondrial function (Trempolec, 2017). Another important role for p38α and MK2 is the post-transcriptional regulation of gene expression during inflammation. Together, they regulate the mRNA stability of certain cytokines, such as TNFα and IL6, through a process that involves the AU-rich elements in the 3'-non-coding regions of the mRNAs and the phosphorylation of Tristetraproline (TTP) (Kotlyarov et al., 1999) (Neininger et al., 2002). Phosphorylation by MK2 increases the stability of TTP and its binding to 14-3-3 adaptor proteins, which prevents the mRNA destabilizing activity of TTP, thereby resulting in increased levels of its target mRNAs (Stoecklin et al., 2004) (Sandler & Stoecklin, 2008) (Hitti et al., 2006). For the proper control of inflammatory gene expression, TTP should be dephosphorylated by the PP2A phosphatase (Clark & Dean, 2016). Besides TTP, other MK2 targets, such as hnRNPA0 and PABP1, might contribute to TNFα expression (Rousseau et al., 2002). Furthermore, active MK2 also controls several mechanisms that regulate the stability of other mRNAs such as uPA, COX2 and IL1 (Ridley et al., 1998) (Tran et al., 2003).





It has recently been found that overexpressed p38α and MK2 proteins interact with RIPK1 and control its cytotoxic activity during inflammation (Menon et al., 2017). This observation indicates that other proteins might bind to p38α and MK2 when they are interacting.

So far, the binding between mammalian p38α and MK2 is well-established *in vitro*; however, how these two proteins are organized *in vivo* both in homeostasis and in response to different stimuli remains to be elucidated. Several parameters, including the local cell environment, are critical for the regulation of the oligomeric state of interacting proteins (**Box 1**). Therefore, further studies are needed to unravel how binding between endogenous p38α and MK2 is regulated in cells.

Given that the p38α:MK2 crystal structure shows both protein docking grooves buried within the complex, it has been proposed that the fully active p38α:MK2 complex acts cooperatively to phosphorylate downstream partners and structures (Gaestel, 2015). However, it is still unclear how p38α and MK2 are organized for proper substrate phosphorylation.

As the D-motif is critical for tight and stable binding of MK2 to p38α, other D-motif-containing proteins might similarly form a protein assembly with p38α. Biochemical studies have reported that p38α interacts not only with MK2 but also with other proteins containing canonical D-motifs, such as the PTPN7 and MKP1 phosphatases (Saxena et al., 1999) (Hutter et al., 2000), the MKK6 activator (Stein et al., 1996) and the ATF2 substrate (Raingeaud et al., 1995). These observations suggest that the presence of the D-motif sequence might allow the identification of proteins that can interact with the p38α docking groove. These new p38α interactors should contribute to defining new p38α protein complexes with specific scaffolding and kinase functions.

# Aim of the work

The main goal of this study was to investigate kinase-independent scaffolding functions of p38α to better understand the mechanistic principles that govern this signaling pathway.

## Specific objectives

- Identification of new p38α interacting partners.

- Investigation of new physiological roles of p38α-structural domains mediated by the high affinity binding to MK2.

- Characterization of the p38α:MK2 complex.

- Generation and characterization of mice expressing kinase-dead p38α to define the contribution of p38α catalytic activity to specific processes.

# Material & Methods

# Materials

## General buffers and solutions

Buffers and solutions used in this thesis are specified below, or in the corresponding sections.

**PBS 10X**
1.37 M NaCl
27 mM KCl
100 mM $Na_2HPO_4$
17.5 mM $KH_2PO_4$
pH 7.4

**Running Buffer 10X**
0.25 M Tris base
2 M glycine
1% SDS
pH 8.3

**Transfer Buffer 10X**
0.2 M Tris base
1.5 M glycine

**Protein Loading buffer 5X**
250 mM Tris pH 6.8
50% glycerol
250 mM DTT
10% SDS
0.1% bromophenol blue

**Ponceau Red**
0.1% Ponceau Red powder
5% acetic acid

HBS buffer (2X)
50 mM HEPES
280 mM NaCl
1.5 mM $Na_2HPO_4$
pH 7.12

**IP buffer**
50 mM Tris-HCl (pH 7.5)
150 mM NaCl
5 mM EGTA
5 mM EDTA
1% NP-40
20 mM NaF
1 mM Na orthovanadate
1 mM PMSF
2.5 mM benzamidine
10 μg/ml pepstatin A
1 μM mycrocystin
10 μg/ml leupeptin
10 μg/ml aprotinin

**Coomassie staining solution**
0.5% Coomassie Blue R250
10% acetic acid
45% methanol

**Coomassie distaining solution**
25% methanol
7% acetic acid

**TBS 1X**
0.1 M Trizma base
1.5 NaCl

## Commercial reagents and kits

### *Mouse work*

| Reagent | Company | Reference |
|---|---|---|
| 4-OHT | Sigma | H6278 |
| Corn oil | Sigma | C8267 |
| Methylcellulose | Sigma | M7140 |

### *Cell culture*

| Reagent | Company | Reference |
|---|---|---|
| 4-OHT | Sigma | H7904 |
| Actinomycin D | Sigma | A1410 |
| Anisomycin | Sigma | L4005 |
| Bafilomycin A1 | Sigma | B1793 |
| b-AP15 | Selleckchem | S4920 |
| BIRB796 | Axon MedChem | 1358 |
| Blasticidin | Invitrogen | A11139-03 |
| Bortezomib | Selleckchem | PS-341 |
| Bromodeoxyuridine (BrdU) | Roche | 10280879001 |
| Calcium Chloride | Sigma | 449709 |
| CMPD1 | Santa Cruz | sc-203138 |
| Collagenase A | Roche | 10103586001 |
| Cycloheximide | Sigma | C6255 |
| Dispasell | Roche | 04942078001 |
| DMEM | Sigma | 5796 |
| DMSO | Sigma | D8418 |
| DNAse | Sigma | D4513 |
| FBS | ThermoFisher | E6541L |
| Glutamine | LabClinics | M11-004 |
| $H_2O_2$ | Sigma | H1009 |
| Hyaluronidase | Sigma | H3506 |
| Hygromycin B | Invitrogen | 10687-010 |
| Lipofectamine RNAi MIX | ThermoFisher | 13778150 |
| LPS | Sigma | L4005 |
| MG132 | Sigma | A9789 |
| Mr.Frosty container | ThermoFisher | 5100-0001 |
| Neon transfection pipette | ThermoFisher | MPP100 |
| Neon transfection pipette station | ThermoFisher | MPS100 |







| | | |
|---|---|---|
| O-phenantroline | Merk millipore | S1078 |
| PBS 10X | Sigma | D1408 |
| PF-3644022 | Sigma | PZ0188 |
| Penicillin/Streptomycin | LabClinics | P11-010 |
| PH-797804 | Selleckchem | S2726 |
| Polybrene | Sigma | H9268 |
| Puromycin | Sigma | P9620 |
| TC10 Automated cell counter | BioRad | S06BR2077 |
| Tetracyclin | Sigma | 87128-25G |
| TGFβ | Prepotech | 100-21 |
| Trypsin | Sigma | T3924 |
| UV-Crosslinker | Amersham bioscience | 20140847 |
| Zeozin | Invitrogen | R250-01 |

### *Cellular and molecular biology*

| Reagent | Company | Reference |
|---|---|---|
| Acetic acid | Panreac | 131008.1611 |
| Acrylamide 40% 29:1 | BioRad | 161-0146 |
| Agarose beads | Santa Cruz | Sc-2002 |
| Ampicillin | Vitro | CAY-14417.25 g |
| Aprotinin | Sigma | A6279 |
| APS | Sigma | A3678 |
| ATP | GE Healthcare | 27-1006-01 |
| ATP ($\gamma$-$^{32}$P) 500 μCi | Perkin Elmer | BLU002A500UC |
| Control agarose beads | Chromotek | Bab-20 |
| Benzamidine | Sigma | B6506 |
| Bromophenol blue | Sigma | B8026 |
| BSA | Sigma | A7906 |
| Complete protease inhibitors | Roche | 11873580001 |
| dNTPs | ThermoFisher | R0192 |
| DTT | GE Healthcare | 17-1318-02 |
| Dyalisis membrane (12-14KD) | SpectrumLabs | 132676 |
| ECL prime WB detection | GE Healthcare | RPN2232 |
| EDTA | Sigma | E46758 |
| EGTA | Sigma | E4378 |
| Ethanol | Panreac | 141086.1214 |
| Glycerol | Sigma | 49782 |
| Glycine | Sigma | G7126 |
| Glutation sepharose 4B | GE Healthcare | 17-0756-01 |
| HEPES | GIBCO | 15630-049 |

| | | |
|---|---|---|
| IPTG | Sigma | I6758 |
| L-glutathione reduced | Sigma | G4251-10G |
| Leupeptin | Sigma | L2884 |
| Luria Broth Base 2500g | Invitrogen | 12795-084 |
| Lysozime | ThermoFisher | 89833 |
| Magnesium cloride | Merck millipore | 1.05833.1000 |
| Methanol | Panreac | 131091.1214 |
| MK2-Trap_A | Chromotek | mt-20 |
| Mycrocystin | Enzo LifeScience | ALX350012 |
| Nitrocellulose membrane 0.2 µm | GE Healthcare | 10600002 |
| NP40 | AppliChem | A16960250 |
| Paraformaldehyde 16% | Electron Microscopy Sciences | 15710 |
| Pepstatin A | Sigma | P4265 |
| Percellys 24 homogenizer | Bertin technologies | 03119200RD000 |
| PMSF | Sigma | P7626 |
| Ponceau Red | Sigma | P3504 |
| ProLong Gold antifade mountant with DAPI | Life Technologies | P36935 |
| Propidium Iodide | Sigma | P4864 |
| Proteinase K | Roche | 03115852001 |
| Random primers | Invitrogen | 48190-011 |
| Rnase A | Roche | 10109142001 |
| RNAsin 2500U | Promega | N211 |
| Sarcosyl | Sigma | L9150-50G |
| SDS | Sigma | 71725 |
| Sodium chloride | Sigma | 433209 |
| Sodium fluoride | Sigma | S7920 |
| Sodium orthovanadate | Sigma | S6508 |
| Sucrose | Sigma | 50389 |
| Superfrost glass slides | VWR | J1800AMNZ |
| Superscript IV reverse transcriptase | Invitrogen | 18090010 |
| SYBR Select master mix | ThermoFisher | 4472942 |
| TEMED | Sigma | T9281 |
| Triton X-100 | Sigma | T9284 |
| TRIZMA base | Sigma | T6066 |
| TRIZMA HCl | Sigma | T3253 |
| Tween 20 | Sigma | P7949 |
| Triton X-100 | Sigma | T9284 |
| Trizol | ThermoFisher | 15596026 |
| β-mercaptoethanol | Sigma | M7154 |







### *Histology work*

| Reagent | Company | Reference |
|---|---|---|
| 10% buffered formalin | Sigma | HT501128 |
| Diaminobenzidine | Dako | K346811 |
| DPX mounting media | Leica | 3808600E |
| Peroxidase blocking buffer | Dako | S2023 |
| Sodium citrate | MERK | 1064485000 |
| Superfrost glass slides | VWR | J1800AMNZ |

### *Commercial kits*

| Kit | Company | Reference |
|---|---|---|
| Duolink in situ detection (PLA) | Sigma | DUO92007 |
| FITC Mouse Anti-BrdU set | BD Biosciences | 556028 |
| Gateway LR clonase enzyme mix | Invitrogen | 11791020 |
| GenElute Plasmid miniprep kit | Sigma | PLN350-1KT |
| MEF Starter Nucleofector Kit | Lonza | V4XP-4012 |
| Mycoalert | Lonza | LT07-318 |
| Neon Transfection system kit | ThermoFisher | MPK10025 |
| Click-IT Plus OPP protein synthesis kit | ThermoFisher | C10456 |
| PureLink on column DNAse | Invitrogen | 121-85-010 |
| QIAfilter plasmid maxi kit | Quiagen | 12263 |
| QuickChange site-directed mutagenesis kit | Aligen technologies | 200518 |
| RC DC Protein Assay Kit I | Dako | S2023 |
| BioRad | 5000111 | S2023 |

# Methods

## Mouse work

Mice were housed according to national and European Union regulations, and protocols were approved by the animal care and use committee of the Barcelona Science Park (PCB-CEEA). Animal handling was performed by Dr. Ana Igea Fernández.

***Generation of p38α kinase dead mice***

The targeting strategy to generate p38α kinase dead (KD) mice was designed by Drs. Stephen Furrow, Ivan del Barco and Angel R. Nebreda. The mice were generated by the

Mouse mutant core facility of IRB Barcelona.

Briefly, a p38α WT mini-gene cassette, including exons 2-12 and the 3'UTR, was incorporated between the exons 1 and 2 of the Mapk14 locus encoding p38α. This mini gene contained around 500 bp of intron sequence immediately upstream of the coding sequences in an effort to maintain the appropriate splicing signals. In addition, a mutation was introduced in exon 2 changing the lysine 53 to methionine (K53M*). For selection of targeted embryonic stem cells, a Frt flanked neo resistance gene driven by the β-actin promoter was included in the construct. The whole cassette was flanked by LoxP sites to allow conditional removal and thus, expression of the mutant form of the gene (**Figure 11**).
Animals with the modified allele are referred as p38α knock-in mice (KI). These mice normally express p38α WT from the mini-gene, but Cre-mediated excision of the cassette allows expression of the p38α K53M mutant p38α KD.


**Figure 11. Graphical representation of the targeting strategy to generate the p38α KI allele.**

***Generation of PyMT mice with inducible Cre***
PyMT p38α$^{KI/KI}$ UBC-Cre-ERT2 or PyMT p38α$^{lox/lox}$ UBC-Cre-ERT2 female mice were generated by crossing p38α$^{KI/KI}$ or p38α$^{lox/lox}$ (Ventura et al., 2007) with MMTV-PyMT, provided by William Muller (McGill University, Canada) and UbiquitinC (UBC)-Cre-ERT2 mice (Ruzankina et al., 2007), being all mostly in FVB background.

***Animal treatments and tumor measurements***
PyMT breast tumors were monitored twice a week with a caliper using the formula V= (π x length) x wide$^2$ and experiments were started when tumors reached 150-200mm$^3$, usually around 2-3 months old.
For p38α deletion or expression of the kinase dead form, mice were intraperitoneally injected each day for five alternative days with 1 mg/ml of 4-OHT dissolved in 10% ethanol and 90% corn oil (**Figure 12**). The inhibition of p38α was confirmed by western-blotting using lysates of tumors treated with 300 mM of NaCl for 15 min.







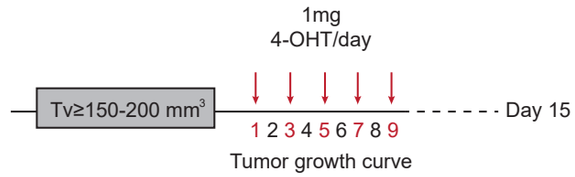


**Figure 12. Graphical representation of mice treatment with 4-OHT**

***Mouse genotyping***
DNA was extracted from tails for mouse genotyping. Samples were sent to Transnetyx for processing. Alternatively, mice were genotyped in house using the following primers (**Table 2**).

**Table 2 | Primers used for mouse genotyping**

| Gene | Fw sequence 5'-3' | Rv sequence 5'-3' | Band size |
|---|---|---|---|
| CRE | acgagtgatgaggttcgcaag | cccaccgtcagtacgtgagat | 520 bp |
| p38α lox | atgctactgtctgcgcctctct | cagcttcttaactgccacacga | WT: 121 bp, Flox:188 bp |
| p38α KI | tgtcactcttcccacacttgaggac | gcctgaaagcagccaaataatagga | WT: 243bp, KI: 293 bp, KD: 353 bp |
| PyMT | ggaagcaagtacttcacaaggg | ggaaagtcactaggagcaggg | 540bp |

## Cell culture

For standard culture, cells were maintained in Dulbecco's Modified Eagle´s Medium (DMEM) supplemented with 10% heat inactivated fetal bovine serum (FBS), 1% L-Glutamine and 1% penicillin-streptomycin at 37°C and 5% $CO_2$.

***Cell lines***
Fibroblasts and epithelial cells derived from PyMT-induced tumors, colon fibroblasts, bone marrow derived macrophages (BMDM) and p38α$^{KI/KI}$ MEFs were generated in our laboratory coming as explained below. U2OS (osteosarcoma) and HEK293-T (embryonic kidney, transformed) cells were purchased from ATCC. Murine MSCs were obtained in our laboratory as described (Soleimani & Nadri, 2009). MK2 deficient MEFs were a kind gift from Dr. Matthias Gaestel (MH-Hannover, Germany), and were obtained from MK2 KO mice and immortalized by co-transfecting with pSV40Tag encoding the SV40 large T antigen (Kotlyarov et al., 1999). Most of the experiments were performed by using breast cancer fibroblasts unless otherwise indicated in the corresponding sections.

***Cell generation***

*Generation of breast cancer fibroblasts or epithelial cells from PyMT tumors.* Tumors from PyMT p38α$^{lox/lox}$ or p38α$^{KI/KI}$ UBC-Cre-ERT2 female mice were chopped using razors and digested at 37°C rocking for 1 h in DMEM medium containing Collagenase A (1 mg/ml) and Hyaluronidase (1.5 units/ml). After digestion, cell suspension was filtered through a 70 µm cell strainer and centrifuged 5 min at 1500 rpm. The cell pellet was resuspended in 10 ml DMEM and centrifuged at 1500 rpm for 30 s. The supernatant was discarded, and the cell pellet was resuspended and spun again four more times. The final cell pellet was plated. Cells were passaged until spontaneously immortalized, usually after 16 passages. For breast cancer fibroblasts isolation, PDGFα$^{+}$, EpCAM$^{-}$ and CD45$^{-}$ cells were sorted using FACS Aria flow cytometer whereas EpCAM$^{+}$ breast cancer epithelial cells were verified using Gallios Flow cytometer (more methods details in section ***Flow cytometry analysis***).

*Colon fibroblasts* were isolated from p38α$^{lox/lox}$ UBC-Cre-ERT2 mice. Colons were dissected, opened longitudinally and washed with cold PBS, incubated with 8 mM EDTA at 37°C for 15 min. Supernatants were centrifuged at 1200 rpm for 5 min at 4°C, and pelleted cells were digested with Dispase II (0.5 mg/ml) at 37°C for 25 min to isolate epithelial cells. To obtain lamina propria (mesenchymal cells and leucocytes) colon pieces were collected, cut (2-3 mm) and digested with collagenase A (1.75 mg/ml) at 37°C for 45 min. Cells were sorted in a FACS Aria flow cytometer (BD Biosciences) using CD45$^{-}$, CD31$^{-}$, CD140α$^{+}$ and CD140β$^{+}$ (more details in section ***Flow cytometry analysis***).

*Generation of bone marrow derived macrophages (BMDM).* Bone marrow precursor cells were isolated from femurs and tibias of p38α WT mice and cultured in complete DMEM as previously described (Bailon et al., 2010). To generate macrophages form bone marrow derived precursor cells, we used the conditioned media (L-cell) of the mouse fibroblast cell line L929 (ATCC CCL 1, NCTC clone 929), which produces large quantities of M-CSF during proliferation. This is the only growth factor produced by these fibroblasts affecting macrophages. L929 cells were grown in 150 mm flasks up to confluence and after 7 days the supernatant was removed, centrifuged to remove the cells in suspension, and kept in aliquots at -80 °C until the moment of use. Once thawed, the aliquots were stored at 4°C to prevent degradation of M-CSF. For proper cell differentiation, bone marrow precursor cells were treated with L-cell for 6 days. Before LPS treatments, cells were deprived from L-cell for 18 h in DMEM (10% FBS, 1% P/S) to synchronize the culture and render the cells quiescent.

*Generation of cells expressing constitutively active MKK6.* U2OS were transfected with pcDNA6-MKK6DD and selected with 4 µg/ml Blasticidin S HCl and 35 µg/ml Zeozin. To induce MKK6DD expression, cells were treated with 1 µg/ml Tetracycline or the corresponding amount of ethanol as described (Trempolec et al., 2017).

*Generation of p38α$^{KI/KI}$ MEFs.* MEFs were generated from p38α$^{KI/KI}$ 14.5 embryos as described (Ambrosino et al., 2003) and were immortalized by transfecting 5 µg of p129-







SV40 large T plasmid (provided by Dr. Travis Stracker (IRB Barcelona)) using MEF Starter Nucleofector Kit.

***Cell maintenance***

For sub-culturing, cells were washed once in PBS and incubated in 1 ml trypsin at 37°C until detached. Then, complete media was added, and cells were diluted as desired depending on the confluence and re-plated in a new culture dish. In the case of differentiated BMDM, cells were harvested by using cell scrappers and plated with the same media until they attached. 18 h before treatment media was changed to render the cells quiescent.

***Cell collection***

For harvesting, cell cultures were washed with PBS and trypsinized. Cells were resuspended in 5 ml of complete fresh media and the suspension was transferred to a 15 ml conical tube and centrifuged at 1000 rpm for 5 min. Afterwards, media was aspirated, and the pellet was washed in 3 ml of PBS. Cell suspension was centrifuged again in the same conditions and supernatant was discarded. Cell pellet was resuspended according to the following procedures.

***Cell counting***

Cells were harvested and placed in a 15 ml tube with 5 ml of DMEM. Cells were resuspended carefully up and down until a homogeneous suspension was obtained. 10 µl of cell solution were added to counting slides and the cell number was determined using a TC10 Automated cell counter.

***Cell freezing and thawing***

For freezing, cells from a 70-85% confluent p10 cm culture dish were collected as above and resuspended in freezing media consisting of 90% FBS and 10% DMSO and transferred to 1-2 1.5 ml cryo-tubes. Cryo-tubes were stored in a Mr. Frosty container at -80°C for up to one week and then transferred to liquid nitrogen for long term storage. For thawing, frozen cells were quickly placed in a 37°C water bath until completely thawed. Then cells were transferred to a p10 cm plate with 10 ml of media. Next day, the media was replaced by 10 ml of fresh DMEM to remove remaining DMSO in culture.

***Mycoplasma detection***

Cells were routinely tested for mycoplasma using Mycoplasma Detection Kit. 100 µl from the cell media were taken and centrifuged for 5 min at 200 g. The supernatant was transferred to a test tube. 100 µl of MycoAlert reagent (A) were added and luminescence was measured after 5 min incubation. Then, 100 µl of MycoAlert substrate (B) were added and luminescence was measured after 10 min incubation. The ratio of B/A

was used to determine the mycoplasma status according to manufacturer´s parameters.

***Cell treatments***

*Modification of endogenous p38α expression.* For depletion of p38α or expression of p38α kinase dead mutant, cells were treated with 60 μg Tat-Cre protein (Peitz et al., 2002) or with 100 nM 4-OHT for 4 or 2 days, respectively. 4-OHT is the active metabolite of tamoxifen used to activate Cre-ERT2, in which the Cre recombinase is fused to the ligand-binding domain of the estrogen receptor. The resulting protein, Cre-ER, is confined to the cytoplasm but in the presence of tamoxifen, Cre-ER translocates to the nucleus, where it catalyzes the recombination of the target DNA sequences flanked by loxP (lox) sites. The Tat-Cre protein was used when cells do not express Cre-ER, as it can enter the cell and induce the recombination of lox-flanked DNA sequences.

*p38 MAPK pathway stimulation:* Several agents were used to activate the p38α pathway. In all cases, cells were plated at 60-70% confluence and attached in a p10 cm plate. Incubation times for the different treatments are indicated in each experiment.

- UV radiation: cell media was removed and placed into 15 ml tubes, and plates were introduced into a UV crosslinker apparatus. UV radiation intensities were determined according to the experiment. After stimulation, the media was added back to the cells.
- NaCl: 200 mM NaCl was used to induce osmotic stress.
- $H_2O_2$: 100 μM $H_2O_2$ was used to generate oxidative stress.
- Anisomycin: This is an antibiotic produced by *Streptomyces griseolus* that inhibits protein synthesis, and it was used at 20 μM.
- Lipopolysaccharide (LPS): LPS is a component of the Gram negative bacteria outer membrane and it was used at 10 ng/ml to activate p38α signaling in BMDM. Before LPS treatment, cells were deprived form L-cell media for 18 h at day 6 of differentiation as mentioned above.
- Transforming growth factor β (TGFβ): TGFβ is a multifunctional cytokine that activates Smad proteins and MAPK pathways, and it was used at 5 ng/ml.

*MAPK inhibitors.* Two different p38α inhibitors were used. BIRB796 is a p38α allosteric inhibitor (Pargellis et al., 2002) that was used at 10 μM and was added 2 h prior to p38α stimulation. PH-797804 is an ATP competitive inhibitor (Xing et al., 2009) that was used at 2 μM and was added 2 h before stimulation. MK2 was inhibited using the ATP competitive inhibitor PF-3644022 (Mourey et al., 2010) at 10 μM, which was added 2 h before p38α pathway stimulation. The p38α docking groove was blocked by using the CMPD1 inhibitor at 10 μM for different times, as indicated in the corresponding experiments. All stock aliquots were prepared in DMSO and stored at -20ºC.

*Protein degradation inhibitors.* Autophagy and proteasome degradation pathways were inhibited by using different compounds. The 20S proteasome subunits were inhibited with 20 μM MG132 or 100 nM Bortezomib, whereas the 19S regulatory subunits were







blocked with 3 μM b-AP15 or 200 μM O-phenanthroline. Autophagy was inhibited using 400 nM Bafilomycin A1. All inhibitors were added 2 h before p38α stimulation and incubated for the indicated times. All compounds were dissolved in DMSO and stored at -20ºC.

***Cell transfection***

*Calcium chloride method.* 293T cells at 70% confluency were used for cell transfection. DNA (5-10 μg) was dissolved in 450 μl of sterile water, and 50 μl of 2.5 M $CaCl_2$ were added drop by drop and incubated for 5 min at RT. Afterwards, 500 μl of 2X HBS were added drop-wise with bubbling and incubated for 20-30 min at RT. The final mix (1 ml) was added to 293T cells and incubated overnight (O/N). Next day, the media was replaced by fresh DMEM to avoid $CaCl_2$ toxicity. Unless otherwise indicated, experiments were performed 24 h after changing the media. The following constructs were used for transfection.

- p38α mutants: pcS2-MT plasmids containing 6x Myc-tagged p38α WT or mutated forms were provided by Dr. Jalaj Gupta. The mutations were generated using the QuickChange site-directed mutagenesis kit. The primers used are indicated in **Table 3**.
- Tagged proteins: pDEST Flag constructs containing CDO1, COPS5, FKBP8 and NCF1 proteins were obtained by cloning from pDONOR plasmids using the Gateway system. Briefly, 1,5 μl of vector (150 ng/μl) and 2,5 μl (150 ng/μl) of insert were mixed with 1 μl of LR clonase in a volume of 4 μl. The mixture was incubated at 25°C for at least 1 h. After incubation, 1 μl of Proteinase K was added and incubated for 20 min at 37°C. Then, 2-3 μl of the mixture were transformed into 20 μl of DH5α E.coli. The Flag-MK2 construct, as well as Myc and GFP constructs used in different assays were obtained as indicated below (**Table 4**). DNA was purified using a plasmid miniprep kit following the manufacturer's procedure.

**Table 3 | Primers used for the generation of p38α mutants**

| Mutant | Fw sequence 5'-3' | Rv sequence 5'-3' |
|---|---|---|
| T123A | gtgccagaagctggccgacgaccacgttcag | ctgaacgtggtcgtcggccagcttctggcac |
| T123D | gtgccagaagctggacgacgaccacgttcag | ctgaacgtggtcgtcgtccagcttctggcac |
| Q120A | caacatcgtgaagtgcgcgaagctgaccgacg | cgtcggtcagcttcgcgcacttcacgatgttg |
| D176A | gggctggctcggcacactgcagatgagatgacag-gctac | gtagcctgtcatctcatctgcagtgtgccgagccagccc |
| F327S | gacccttatgaccagtccagtgaaagcagggacc | ggtccctgctttcactggactggtcataagggtc |
| D145G | ctgaagtatatacattcggctggcataattcacagg-gacctaaag | ctttaggtccctgtgaattatgccagccgaatg-tatatacttcag |
| E160T | gcccagcaacctagctgtgaacacagactgtgagct-caagattc | gaatcttgagctcacagtctgtgttcacagctaggttgct-gggc |

| | | |
|---|---|---|
| D161T | caacctagctgtgaacgaaacctgtgagctcaagat-tctg | cagaatcttgagctcacaggtttcgttcacagctaggttg |
| I116A | gcggacctgaacaacgccgtgaagtgccagaag | cttctggcacttcacggcgttgttcaggtccgc |
| D313-15-16N | gctcagtaccacaaccctaataatgagcctgttgct-gaccc | gggtcagcaacaggctcattattagggttgtggtact-gagc |

**Table 4 | Plasmids used for transient transfection**

| Plasmid | Company | Reference |
|---|---|---|
| pCMV6-Myc-DKK-Bccip | Origene | MR204529 |
| pCMV6-Myc-DKK- Mpp6 | Origene | MR224477 |
| pCMV6-Myc-DKK- Pcmtd1 | Origene | MR205454 |
| pCMV6-Myc-DKK- Strip1 | Origene | MR210201 |
| pcDNA5 FRT/TO FLAG MK2 | MRC Dundee | DU45476 |
| pcDNA3 MYC MK2 | - | Provided by Dr.Matthias Gaestel (Ronkina et al., 2011) |
| GFP p38α | - | Nebreda's lab |

*Lipofectamine method.* siRNAs (50 nM) were transfected into U2OS cells or breast cancer fibroblasts using Lipofectamine RNAi MIX transfection reagent following the manufacturer's protocol. After transfection, cells were incubated 24 h in antibiotic free media, split and analyzed 48 h later. The siRNAs used are indicated in **Table 5**.

**Table 5 | siRNAs used for transient transfection**

| siRNA | Target sequence 5'-3' | Company |
|---|---|---|
| siLuciferase (siCntrl) | cguacgcggaauacuucgadtdt | Microsynth |
| siSMURF1 | ccagcacuaugaucuauautt | Ambion Life Technologies |
| siSTUB1 | gagcuaugaugaggccauctt | Ambion Life Technologies |
| siMDM2 | gccauugcuuuugaaguuatt | Ambion Life Technologies |
| siStrip1 | uuuaucagagccuugugcucccguc | Invitrogen |

***Retroviral infection***

Retroviruses were produced in 293T cells by transfecting the desired retroviral plasmid along with pCL-ECO (packaging vector). 48 h after transfection, viruses were diluted 1:2 with DMEM containing 8 μg/ml polybrene. Breast cancer fibroblasts or MK2 KO MEFs at around 60% confluency were infected with the supernatant from 293T cells (48h post-transfection) and then again with the second supernatant (72 h post-transfection). Infected cells were selected in puromycin (1 μg/ml) for one week to generate stable cell lines. Retroviral vectors to express p38α mutants were generated by sub-cloning from the plasmids described above (**Table 3**) into the pBabe-puro vector.







MK2 WT, MK2 N-term, HA-MK2 WT and the MK2 D-(R) were cloned from pMMP3-IRES-EGFP-D-MK2 WT plasmid (Ronkina et al., 2007) into a pbabe-hygro vector by the DC-Biosciences company.

***Lentiviral infection***

For a 10 cm plate, 5 μg of shRNA plasmid were transfected (1:1) along with packaging vectors VSV-G, RRE and RSV.

pLKO.1 shRNA for HSP27 and MK2 were obtained from the Functional Genomics facility of IRB Barcelona. Sequences are shown in **Table 6**.

**Table 6 | Sequences of the shRNAs used.**

| shRNA | Target sequence 5'-3' |
|---|---|
| shHsp27_1 | accctctatcacggctactat |
| shHsp27_2 | cacggaagtcaatgaagtcta |
| shMK2_1 | ccgggcatgaagactcgtatt |
| shMK2_2 | tccgtgttatacaccatacta |

***Cell electroporation***

BMDMs and MK2 deficient MEFs were electroporated by using a Neon transfection system kit, pipette and pipette station.

After differentiation, BMDMs ($20x10^6$) were resuspended in 100 μl of buffer R (provided in the kit). The cell suspension was mixed with 800 nM of siRNA (**Table 5**) and cells were electroporated with 2 pulses of 1400V for 20 ms. Cells were transferred into 6,6ml of media to reach a final siRNA concentration of 12 nM. Then, 1 ml of cells ($3x10^6$) were plated in a 60 cm plate.

MK2 KO MEFs ($8x10^6$) were resuspended in 100 μl of buffer R. Cells were mixed with 6 μg of pcDNA3 MK2 WT (Ronkina et al., 2011) (provided by Dr. Matthias Gaestel (MH-Hannover, Germany). Then, cells were electroporated with 1 pulse of 1350V during 30 ms and plated in a 10 cm plate.

## Cellular and molecular biology

***Protein detection by western blotting***

*Protein extraction:* For protein extraction, samples were lysed in IP buffer. Tissue samples were homogenized using the Percellys instrument whereas cells were washed twice with PBS and scrapped. Samples were incubated for 15 min on ice and then centrifuged at 16000 ×g at 4°C for 15 min. Then, supernatants were placed in new Eppendorf tubes. Cell lysates were processed by western blotting or frozen at -80°C.

*Protein quantification:* Total protein was quantified using RC DC protein assay kit ac-

cording to manufacturer's instructions. Protein concentration was measured at 750 nm using a spectrophotometer (BioTek, #FLx800), and a BSA standard curved as a reference.

*Western blot:* 50 µg of protein were resuspended in loading buffer 1X and boiled for 5 min at 95°C. Then, samples were loaded onto different types of SDS-polyacrylamide gels depending on protein size. Gel composition is shown in **Table 7**.



**Table 7 | Composition of SDS-polyacrylamide gels**

| | Resolving | | | | Stacking |
|---|---|---|---|---|---|
| **% Acrylamide** | **14%** | **12%** | **10%** | **8%** | **5%** |
| MQ (ml) | 6,1 | 6,9 | 7,7 | 8,5 | 5.8 |
| Acrylamide 40% 29:1 (ml) | 5,6 | 4,8 | 4 | 3,2 | 1 |
| 1,5M Tris pH 8,8 (R) or 6.8 (S) (ml) | 4 | 4 | 4 | 4 | 1 |
| SDS 10% (µl) | 160 | 160 | 160 | 160 | 80 |
| APS (µl) | 160 | 160 | 160 | 160 | 80 |
| TEMED (µl) | 16 | 16 | 16 | 16 | 8 |

Proteins were separated by SDS-PAGE at 100 V for 2 h. After electrophoresis, proteins were transferred from polyacrylamide gels to a nitrocellulose membrane using a wet-transfer system (BioRad). Ponceau red was used to determine transfer quality and efficiency. After washing out the Ponceau red with PBS, membrane was blocked for 1 h in 5% non-fat dry milk in PBS at RT. Then, primary antibody was added to the membrane and incubated O/N at 4°C. The next day, the membrane was washed three times with TBS-0,05 % Tween and incubated with the secondary antibody diluted in 1% non-fat milk in TBS- 0,05% Tween for 1 h at RT. Finally, membranes were washed as previously mentioned and proteins were detected using Odyssey Infrared Imaging System. Antibodies are indicated in **Table 8**.

***Protein detection by Immunofluorescence***

293T cells grown in coverslips were washed with PBS and fixed for 20 min in ice-cold methanol (-20°C). After fixation, cells were placed in a petri dish covered with aluminum foil with a strip of wetted Whattman paper around the inside wall of the plate to avoid coverslips from drying out. Then, coverslips were washed again with PBS and blocked for 1 h with PBS-BT solution (3% BSA, 0.1% Triton X-100, 0.02% Azide in PBS) at RT. Primary antibodies were incubated O/N at 4°C. The next day, coverslips were washed with PBS-BT buffer and secondary antibodies were incubated for 1h at RT. Coverslips were placed into superfrost glass slides with ProLong Gold antifade DAPI mountant. Primary and secondary antibodies were diluted with PBS-BT and are indicated in **Table 9**.

**Table 8 | Primary and secondary antibodies used by western blotting**

| Antibodies for western blotting | | | | |
|---|---|---|---|---|
| **Antibody** | **Dilution** | **Buffer** | **Company** | **Reference** |
| c-Myc | 1:1000 | 1% BSA (PBS) | Abcam | Ab9132 |
| Dnajb6 | 1:500 | 1% BSA (PBS) | Santa Cruz | sc365574 |
| Flag | 1:1000 | 1% BSA (PBS) | Sigma | F3165.2MG |
| GAPDH | 1:5000 | 1% BSA (PBS) | Sigma | G8795 |
| GFP | 1:1000 | 1% BSA (PBS) | Santa Cruz | sc9996 |
| GST | 1:1000 | 1% BSA (PBS) | Santa Cruz | sc138 |
| Goat IgG (AlexaFluor 680) | 1:5000 | 1% milk (TBS-T) | Invitrogen | A21084 |
| HA | 1:1000 | 1% BSA (PBS) | Abcam | 3F10 |
| HSP27 | 1:1000 | 5%BSA (TBS-T) | Santa Cruz | sc-1049 |
| HSP27 phospho-S82 | 1:1000 | 5%BSA (TBS-T) | Cell Signaling | 2401 |
| Lamin A/C | 1:1000 | 1% BSA (PBS) | Santa Cruz | sc20681 |
| LC3 | 1:1000 | 1% BSA (PBS) | BioNova cientifica | PM036 |
| MK2 | 1:500 | 5%BSA (TBS-T) | Cell Signaling | 3042 |
| MK2 phospho-T334 | 1:500 | 5%BSA (TBS-T) | Cell Signaling | 3007 |
| MKK6 | 1:500 | 1% BSA (PBS) | Homemade | (Ambrosino et al., 2003) |
| Mpp6 | 1:500 | 1% BSA (PBS) | Santa Cruz | sc393429 |
| Mouse IgG (AlexaFluor 680) | 1:5000 | 1% milk (TBS-T) | Invitrogen | A21057 |
| Mouse IgG (AlexaFluor 800) | 1:5000 | 1% milk (TBS-T) | Rockland | 611-131-122 |
| PCMT1 | 1:500 | 1% BSA (PBS) | Santa Cruz | sc100977 |
| PP2A C subunit | 1:1000 | 5%BSA (TBS-T) | Cell Signaling | 2038T |
| p38α | 1:1000 | 1% BSA (PBS) | Santa Cruz | sc-535 |
| p38α | 1:1000 | 1% BSA (PBS) | Santa Cruz | sc81621 |
| p38 phospho-T180/Y182 | 1:1000 | 5%BSA (TBS-T) | Cell Signaling | 9211 |
| p53 | 1:1000 | 5%BSA (TBS-T) | Cell Signaling | 2524S |
| Rabbit IgG (AlexaFluor 680) | 1:5000 | 1% milk (TBS-T) | Invitrogen | A21076 |
| Smad3 phospho-S424/425 | 1:500 | 5%BSA (TBS-T) | Cell Signaling | 9520S |
| Spectrin 1β | 1:500 | 1% BSA (PBS) | Santa Cruz | sc515592 |
| Strip1 | 1:1000 | 1% BSA (PBS) | Abcam | Ab199851 |
| Tubulin | 1:10000 | 1% BSA (PBS) | Sigma | T9026 |
| Ubiquitin | 1:1000 | 1% BSA (PBS) | Enzo Biosciences | BML-PW88100100 |

***Protein detection by Immunohistochemistry (IHC)***

Tissues were fixed with formalin for 24 h at RT, washed once with 70º ethanol and embebed in paraffin. IHC staining was performed by Elisabeth Llonch and the Histopathology facility unit of IRB Barcelona. Briefly, tissue sections on slides were de-waxed in xilol for 10-15 min and then re-hydrated in descending series of ethanol solutions (100%, 95%, 75%, 50% and water). Then, antigen unmasking was performed with citrate buffer (10 mM sodium citrate, pH 6) for 20 min at 97°C. Afterwards, endogenous peroxidase activity was blocked for 10 min at RT using peroxidase blocking buffer. Then, slides were washed and incubated for 1 h with the primary antibodies (**Table 10**). Slides were washed with water and incubated with HRP-conjugated secondary antibodies (**Table 10**). Signals were visualized with diaminobenzidine and tissue slides were mounted with DPX mounting medium after washing with PBS.

**Table 9 | Primary and secondary antibodies used for Immunofluorescence**

| Antibodies for Immunofluorescence | | | |
|---|---|---|---|
| **Antibody** | **Dilution** | **Company** | **Reference** |
| c-Myc | 1:200 | Abcam | Ab9132 |
| Flag | 1:200 | Sigma | F3165.2MG |
| GFP | 1:200 | Santa Cruz | sc-9996 |
| Rabbit IgG (Alexa Fluor 488) | 1:400 | Invitrogen | A-21441 |
| Mouse IgG (Alexa Fluor 555) | 1:400 | Invitrogen | A-21422 |
| GST | 1:1000 | Santa Cruz | sc138 |
| Tubulin | 1:10000 | Sigma | T9026 |
| Ubiquitin | 1:1000 | Enzo Biosciences | BML-PW88100100 |

**Table 10 | Primary and secondary antibodies used for Immunohistochemistry**

| Antibodies for Immunohistochemistry | | | |
|---|---|---|---|
| **Antibody** | **Dilution** | **Company** | **Reference** |
| Ki67 | 1:1000 | Abcam | 15580 |
| P-H3 | 1:3000 | MERK Millipore | 06-570 |
| BrightVision poly HRP anti Rb | 150 µl | Immunologic | DPVR110HRP |

***Flow cytometry analysis (FACS)***

Flow cytometry analysis was performed in the Cytometry facility from University of Barcelona.

*Epithelial cell status verification.* Cells lines derived from PyMT-induced mouse mammary tumors were tested for the EpCAM marker that is commonly expressed in epithelial cells. Cells were collected, washed in PBS and resuspended in 100 µl of fresh DMEM containing 2 µl of EpCAM antibody (**Table 11**). After 1 h of incubation, cells were washed with PBS and resuspended in 500 µl of fresh DMEM. 10.000 cells were acquired on Gallios Flow cytometer and FlowJo software was used for analysis.

*Breast cancer and colon fibroblasts isolation.* 5 x $10^6$ cells were resuspended in 500 µl of 3% FBS in PBS and stained with PDGFα, EpCAM and CD45 antibodies (**Table 11**) for 30 min on ice. Isotype controls (**Table 11**) and single antibody stainings were included as controls. Afterwards, cells were washed with 3% FBS in PBS and finally resuspended in 2 ml of the same buffer. For fibroblasts isolation, PDGFα$^+$, EpCAM$^-$ and CD45$^-$ cells were sorted using FACS Aria flow cytometer.

*Detection of global protein synthesis in living cells.* Growing cells were treated with O-propargyl-puromycin (OP-Puro) for 30 min. Then cells were harvested, fixed (3.7% Paraformaldehyde in PBS) and permeabilized (0.5% Triton in PBS). To stain OP-Puro positive cells, Click-iT Alexa-488 cocktail reagent was prepared following the manufacturer's protocol and added to the cell pellet and incubated during 30 min at RT protected from light. Finally, cells were washed twice with PBS and OP-Puro positive cells were analyzed using the BD Aria Fusion FACS.

*BrdU cell labeling.* Growing cells were treated with 10 µM BrdU for 2 h, harvested and fixed with cold 70% ethanol for at least 24 h at -20°C. After fixation, cells were centrifuged at 1000 rpm for 5 min and washed once with PBS. Afterwards, the cell pellet was resuspended in an ice-cold denaturizing solution (0.1 M HCl, 0.5% Tween 20 in $H_2O$) and incubated for 10 min on ice. After centrifugation, cells were resuspended in $H_2O$ and incubated at 95°C for 5 min. Cells were centrifuged again, washed once in blocking buffer (1% BSA, 0.5% Tween 20 in PBS) and resuspended in 100 µl of blocking buffer containing 10 µl of anti-BrdU-FITC (included in the FITC Mouse Anti-BrdU set). After 1 h of incubation at RT in the darkness, cells were washed once in blocking solution and resuspended in PI staining solution (10 µg/ml PI, 200 µg/ml RNAase A, 0.05% Tween 20 in PBS). Cells were acquired on a Gallios flow cytometer and FlowJo software was used for analysis.

**Table 11 | Antibodies used in flow citometry**

| Antibodies for FACS | | | |
|---|---|---|---|
| **Antibody** | **Dilution** | **Company** | **Reference** |
| CD31 PeCy7 | 1:200 | Biolegend | 102417 |
| CD45 APC/PerCpCy5.5 | 1:200 | BD pharmigen | 550539 |
| EpCAM FITC | 1:100 | Santa Cruz | sc-53532 |
| PDGFα PE | 1:100 | eBioscience | 12-1401-81 |
| PDGFβ PE | 1:25 | eBioscience | 17-1402-82 |
| Isotype- FITC | 1:200 | BD pharmingen | 556923 |

| | | | |
|---|---|---|---|
| Isotype- PE | 1:100 | Santa Cruz | sc2866 |
| Isotype- APC | 1:200 | eBioscience | 17-4031-81 |
| Isotype- PeCy7 | 1:200 | Biolegend | 400521 |
| Isotype- PerCpCy5.5 | 1:200 | Biolegend | G0114F7 |

***Gene expression analysis by qRT-PCR***

*RNA extraction:* Cells were washed twice with PBS, resuspended in 500 µl Trizol and placed in a 1.5 ml Eppendorf tube. 100 µl Chloroform were added, and tubes were centrifuged 15000 ×g at RT for 10 min. Two liquid phases were generated and the fraction with less density was transferred into new tubes. 200 µl of 70° ethanol were added and mixed with samples. The RNA extraction was followed by using PureLink RNA mini kit. DNAse treatment was performed using on-column DNase treatment following manufacturer's instructions.

*cDNA synthesis:* RNA samples were quantified using Nano Drop. 1 µg RNA was used for cDNA synthesis with SuperScript IV reverse transcriptase, RNAsin and random primers following Invitrogen's instructions.

*qRT-PCR:* 5 ng of cDNA, 5 µl SYBR green reagent and 0.2 µl of gene specific Fw and Rv primers were mixed in a 10 µl final volume. The plate was sealed, centrifuged for 1 min at 200 ×g and run as follows: 50°C for 2 min, 95°C for 10 min, 40 cycles of denaturation at 95°C for 15 s, annealing and elongation at 60°C for 1min, and three final steps of 95°C for 15 s, 60°C for 1min and 95°C for 15 s. mRNA levels were analyzed in triplicates and normalized to the GAPDH expression level. Primers are shown in **Table 12**.

**Table 12 | Primers used in qRT-PCR**

| Gene | Fw sequence 5'-3' | Rv sequence 5'-3' |
|---|---|---|
| CXCL2 | gctgtcaatgccctgaagaccctgc | gtacgatccaggcttcccgggtg |
| GAPDH | cttcaccaccatggaggaggc | ggcatggactgtggtcatgag |
| IL6 | gaggataccactcccaacagacc | aagtgcatcatcgttgttcataca |
| MK2 | gtcagaagtatcagaagaagtg | ggttcatgaattctgtgatgg |
| TNFα | ccagaccctcacactcagatc | cacttggtggtttgctacgac |
| SMURF1 | gagagcttcgatgaagaaag | gaatgtcgatccggttaaag |
| STUB1 | tggaacagcattgaggag | atgtacttgtcgtgcttg |
| MDM2 | tgaggagcaggcaaatg | gtctaaccagggtctcttg |

***Protein expression and purification***

Expression constructs for GST fusion proteins were cloned into pDEST15 plasmid by Dr. Natalia Trempolec using Gateway cloning technology or were kindly supplied by other laboratories. GST-p38α mutants were generated using QuickChange site-directed mutagenesis with the indicated primers (**Table 13**).







**Table 13 | Primers used for GST-p38α mutant generation**

| Mutant | Fw sequence 5'-3' | Rv sequence 5'-3' |
|---|---|---|
| E178A | cggcacacagatgatgcaatgacaggctacg | cgtagcctgtcattgcatcatctgtgtgccg |
| P322R | gaaccagtggccgatcgttatgatcagtcctttg | caaaggactgatcataacgatcggccactggttc |
| R49Q | gacacaaaaacggggttacaagtggcagtgaagaagctc | gagcttcttcactgccacttgtaaccccgtttttgttc |
| R136Q | ccttatctaccaaattctcaaggtctaaagtatatac | gtatatactttagaccttggagaatttggtagataagg |

GST-tagged proteins were obtained as describe below:

*Bacteria transformation.* 100-200 ng of GST-expression plasmids (**Table 14**) were added to 50 µl of chemo-competent BL21 E.coli and incubated on ice for 20 min. Samples were placed in a thermoblock at 42°C for 45 sec and then put back on ice for 2 more min. Then, 700 µl of LB media were added and the bacteria were incubated with light shacking for 1 h. Afterwards, bacteria suspension was plated onto pre-warmed plates containing ampicillin (Amp) and incubated O/N.

*GST-protein expression.* After transformation, one bacterial colony was grown O/N in 25 ml of LB containing Amp (50 µg/ml). Next day, the whole culture was mixed with 475 ml of LB+Amp and grown until it reached an 0.4-0.5 OD595 nm. Then, 1 mM IPTG was added and the culture was incubated for 3 more h at 37°C.

*GST-protein purification.* The bacterial culture was centrifuged at 4000 rpm for 20 min at 4°C. After centrifugation, the pellet was either frozen at -20°C or processed for protein purification. The pellet was incubated in 5 ml of lysozyme solution (100 µg/ml lysozyme in PBS) for 15 min on ice. Then, 5 mM DTT, 1 mM PMSF and 0.5% Sarcosyl were added for bacterial lysis. Next, lysates were sonicated at 30% amplitude for 15 seconds (on/off for 3-4 cycles) and incubated with 1% Triton X-100 to solubilize proteins. Cell lysates were centrifuged at 11000 xg for 12 min at 4°C, and the supernatants were incubated with 100 µl of Glutathione Sepharose beads (previously washed twice in PBS) for 2 h rotating at 4°C. Then, beads were washed with cold-PBS and resuspended in 300µl of elution buffer (20 mM glutathione in 50 mM TrisHCl pH 8.5). After 5-10 min incubation on RT, GST-proteins were released from the beads by centrifugation for 2 min at 200 xg. At each step, 20 µl samples were collected for SDS-PAGE analysis to check the purification procedure.

*Dialysis.* Eluted proteins were dialyzed O/N against 2-5 l of 20 mM TrisHCl pH 8, 50 mM NaCl, 0.1 mM EDTA, 0.5 mM DTT and 5% glycerol.

***Kinase assay***

p38α was activated by incubating 4 µg of bacterially expressed GST-p38α with 1 µg of MBP-MKK6DD (constitutively active MKK6) in kinase buffer (50 mM TrisHCl pH 7.5, 10 mM $MgCl_2$, 2 mM DTT, 100 µM Na vanadate, 1 mM PMSF, 10 µg/ml aprotinin and

10 μg/ml leupeptin) supplemented with 10 mM ATP for 1 h at 30°C. Kinase assays were performed with 1 μg of GST-protein substrate and 0.5 μg of active p38α in kinase buffer supplemented with 100 μM of cold ATP and 2 μCi γ-$^{32}$P-ATP for 30 min at 30°C. Reaction was stopped by adding 5 μl of 5X loading sample buffer. Proteins were separated by SDS-PAGE, stained with Coomassie for 1h and distained for 2 h. Gels were placed on Whatman paper, covered with foil and placed on a gel dryer. Then, gels were analyzed by autoradiography.

**Table 14 | GST-expression constructs**

| GST-protein | Plasmid | Source | Reference |
|---|---|---|---|
| CAMKK2 | pDEST15 | Home-made | |
| CDO1 | pDEST15 | Home-made | |
| FKBP8 | pDEST15 | Home-made | |
| GFP | pGEX | Home-made | |
| GRK5 | pGEX | Provided by Dr. Jeffrey Benovic | (Carman et al., 1999) |
| hnRNPA1 | pDEST15 | Home-made | |
| HTRA2 | pDEST15 | Home-made | |
| p38α E178A | pGEX | Home-made | |
| p38α P322R | pGEX | Home-made | |
| p38α R49Q | pGEX | Home-made | |
| p38α R136Q | pGEX | Home-made | |
| p38α WT | pGEX | Home-made | |

***p38α mutant immunoprecipitation and kinase assay***

6X Myc-tagged p38α mutants (**Table 3**) were overexpressed in 293T cells together with constitutively active MKK6DD to induce p38α activation. Agarose beads were coupled with home-made c-Myc hybridoma and incubated with 500 μg of cell lysates rotating O/N at 4°C.

The next day, beads were recovered by centrifugation (200 xg for 2 min), washed and used for kinase assays. The immunoprecipitated p38α mutants were incubated with 1μg of purified GST-MK2 and 100 μM ATP in a total volume of 30 μl of kinase buffer (50 mM Tris pH 7.5, 10 mM $MgCl_2$, 1 mM DTT, 2 μM Microcystin) for 30 min at 30°C. Reaction was stopped by adding 1X sample loading buffer and boiling for 5 min. Proteins were resolved by SDS-PAGE, transferred onto a nitrocellulose membrane and detected with antibodies that recognize the phosphorylated MK2.

***MK2 immunoprecipitation***

Single-domain antibodies against MK2 called Nano-Traps (MK2-Trap_A) were used for endogenous MK2 immunoprecipitation. In contrast to conventional antibodies, Nano-traps takes advantage of Camelids species that possess a second type of antibodies named heavy chain antibodies (hcAbs). HcAbs bind their antigen with a single monomeric variable domain (nanobody) with excellent binding properties (Harmsen & De Haard, 2007) whereas the binding region of common IgG consists of two domains (VH and VL) which tend to dimerize or aggregate because of their lipophilicity. As a result, Nano-traps allow fast, reliable and efficient immunoprecipitations. Binding agarose beads were used as negative controls. Cells were processed using the manufacturer's protocol. Briefly, 25μl of MK2-Trap_A or binding agarose beads were incubated O/N with 500μg of cell lysates rotating at 4°C. The next day, beads were recovered by centrifugation (200 xg for 2 min), washed three times with wash buffer (10 mM Tris HCl pH 7.5; 150 mM NaCl; 0.5 mM EDTA), resuspended in 1X loading buffer and boiled for 5 min at 95°C. Immunoprecipitated proteins were analyzed by western blotting.







***GST-pull down***

*Binding of GST-fused recombinant proteins to the beads*. 40 μl of glutathione beads were washed three times in PBS and incubated with 5 μg of GST recombinant protein (**Table 14**) in 500 μl of PBS with 1X Complete protease inhibitors (Roche). The mixture was incubated for 2 h rotating at 4°C. Then, bead-bound GST-proteins were recovered and washed three times with PBS.

*Pull down:* 500 μg of lysates from 293T cells expressing the protein of interest were incubated with previously prepared beads for at least 3 h at 4°C rotating. Then, beads were washed three times with PBS and once with IP buffer. Afterwards, beads were resuspended in 1X loading buffer, boiled for 5 min at 95°C and analyzed by western blotting.

***Proximity ligation assay (PLA)***

U2OS cells transfected with the required plasmids (details in ***cell transfection*** section), were grown on coverslips, washed with PBS and fixed for 20 min with ice-cold methanol (-20°C). After fixation, cells were incubated with anti-Myc and anti-Flag primary antibodies (**Table 8**) as for a normal immunofluorescence. The next day, PLA was performed following manufacturer's instructions. Briefly, anti-mouse and anti-rabbit probes were diluted 1:5 in blocking buffer (provided in the kit) and incubated 20 min at RT. Then, coverslips were incubated with the probe for 1 h at 37°C in a humid chamber. After incubation, coverslips were washed with buffer A (0.01 M Tris HCl, 0.15 M NaCl and 0.05% Tween 20) and incubated with the ligation reaction (ice-cold ligase diluted 1:40 in 1X ligation buffer provided in the kit) for 30 min at 37°C in humidity chamber. Coverslips were washed again with buffer A and incubated in the amplification reaction (polymerase diluted 1:80 with 1X amplification buffer supplied in the kit) for 100 min at 37°C in humidity chamber. The, samples were washed three times with buffer B (0.2 M Tris HCl, and 0.1 M NaCl) and dried. Coverslips were placed in superfrost glass slides with ProLong Gold antifade DAPI mountant and analyzed for DAPI and alexa555.

***Sucrose gradients***

Breast cancer fibroblasts were trypsinized, harvested and resuspended in 25 mM HEPES, 0.1 mM EDTA, 12.5 mM $MgCl_2$, 10% Glycerol, 0.1 M KCl, 0.1% NP-40, 1 mM DTT and 1x Complete protease inhibitors (Roche). Cell lysates were incubated for 15 min on ice and centrifuged 15 min at 16000 xg. 1 mg of lysates was loaded on top of a 4 ml linear sucrose gradient (20–28%) prepared in the same buffer. Gradients were centrifuged at 156,500 xg in a Beckman Coulter MLS-50 rotor for 16 h at 4 °C. Fractions of 930 µl were collected from the top and then analyzed by western blotting.

***MK2 protein half-life analysis***

Breast cancer fibroblasts were treated or not with p38α inhibitors and exposed to 50µM cycloheximide. Cells were collected at timed intervals for up to 6 h and subjected to western blotting using anti-MK2 antibody. Tubulin was used as a loading control. The intensity of the bands was determined using the ImageJ software and the half-life was determined from fitting the data to an exponential one phase decay equation using the GraphPad Prism computer program (GraphPad Software, Inc., La Jolla, CA, USA).

***MK2 mRNA stability***

BMDM were treated with p38α or MK2 inhibitors for 2 h, stimulated with LPS for 4 h more, and then treated with 5µg/ml actinomycin D for the indicated times. Total RNA was isolated and MK2 mRNA was analyzed by RT-PCR.

***Subcellular fractionation assay***

At least $1x10^6$ cells were harvested and resuspended in 200 µl 10 mM Hepes pH 7.5, 10 mM KCl, 5 mM $MgCl_2$ and protease inhibitors (Buffer A) and incubated for 15 min on ice. NP40 was added to a 0.3% final concentration followed by an incubation of 10 min more on ice. Lysates were centrifuged for 5 min at 3500 rpm to obtain cytoplasmic and nuclear fractions (supernatant and pellet, respectively). The nuclear pellet was washed once in Buffer A and incubated with 100 µl of 20 mM Hepes pH 7.5, 200 mM NaCl, 1% NP-40, with protease inhibitors and 2-3 U/µl DNAse (Buffer B) for 30 min at 37°C. Then, lysates were centrifuged at 14000 rpm for 5 min and the supernatant contained the soluble nuclear proteins. Proteins of both fractions were analyzed by western blotting. GAPDH and Lamin A/C proteins were used as loading controls for cytoplasm and nuclear fractions, respectively.

***Mass spectrometry***

MK2 was immunoprecipitated from WT and p38α KO breast cancer fibroblasts (4 mg and 6 mg respectively) in triplicates using MK2-Trap_A beads (160 µl/sample). As a control, the same lysates were immunoprecipitated in duplicates using binding agarose beads (160 µl/sample). After O/N incubation, beads were eluted with 400 µl of Glycine







pH 2.5 for 1 min at RT and centrifuged at 1000 rpm for 2 min. The supernatants were collected into new Eppendorf tubes and neutralized with 40 µl of 1 M Tris base pH 10.4. Samples were processed by the IRB Mass Spectrometry Facility. Briefly, around 90 µg of sample were reduced with DTT, carbamidomethylated and digested with trypsin (2%) following FASP protocol (Wiśniewski et al., 2009). Then, the digested peptides were diluted in 1% formic acid (FA). Samples were loaded onto a 30 µm × 10 cm nanoViper, C18 (Thermo Scientific) at a flow rate of 15 µl/min using a Dionex Ultimate 3000 chromatographic system (Thermo Scientific). Peptides were separated using a C18 analytical column (Acclaim PepMap® RSLC 75 µm × 15 cm, nanoViper, C18, 2 µm, 100Å, Thermo Scientific) with a 160 min run, comprising three consecutive steps with linear gradients from 3 to 35% B in 120 min, from 35 to 50% B in 5 min, and from 50% to 85% B in 2 min, followed by isocratic elution at 85 % B in 5 min and stabilization to initial conditions (A= 0.1% FA in water, B= 0.1% FA in CH3CN). The column outlet was directly connected to an Advion TriVersa NanoMate (Advion) fitted on an Orbitrap Fusion Lumos™ Tribrid (Thermo Scientific). The mass spectrometer was operated in a data-dependent acquisition (DDA) mode. Survey MS scans were acquired in the orbitrap with the resolution (defined at 200 m/z) set to 120,000. The lock mass was user-defined at 445.12 m/z in each Orbitrap scan. The top speed (most intense) ions per scan were fragmented and detected in the linear ion trap. The ion count target value was 400,000 for the survey scan and 10,000 for the MS/MS scan. Target ions already selected for MS/MS were dynamically excluded for 15 s. Spray voltage in the NanoMate source was set to 1.60 kV. RF Lens were tuned to 30%. Minimal signal required to trigger MS to MS/MS switch was set to 5000 and activation Q was 0.250. The spectrometer was working in positive polarity mode and singly charge state precursors were rejected for fragmentation.

A database search was performed with Proteome Discoverer software v2.1 using Sequest HT search engine, SwissProt Mouse isoforms release 2016_09. Contaminants database and user protein MK2 were manually introduced. Search was run against targeted and decoy database to determine the false discovery rate (FDR). Search parameters included Trypsin enzyme, allowing for two missed cleavage sites, carbamidomethyl in cysteine as static modification; methionine oxidation and acetylation in N-terminal as dynamic modifications. Peptide mass tolerance was 10 ppm and the MS/MS tolerance were 0.6 Da. Peptides with a q-value lower than 0.1 and a FDR < 1% were considered as positive identifications with a high confidence level. Finally, the Percolator FDR node was used to estimate the number of falsely identified proteins among all the identified proteins.

***Bioinformatic predictions of putative p38α interactors***

Bioinformatic predictions for putative p38α interactors were performed by Dr. Laura Isus and Dr. Richa Mudgal (Structural Bioinformatics and Network Biology Group

at IRB Barcelona). The first strategy used to select novel p38α interactor candidates was done following previous publications (Sardon et al., 2010). Briefly, they considered the presence of at least one SP/TP site, consensus motifs for docking motifs, Ser/Thr phosphorylation data from (Weintz et al., 2010), conservation of phosphorylation sites in vertebrates and sub-cellular localization according to the Gene Ontology (The Gene Ontology, 2010). The second strategy considered the p38α docking site alignment by using Clustal Omega. Then, the human proteome was scanned for p38α motif occurrences using Find Individual Motif Occurrences (FIMO) Software tool or HMMER search.

***Statistical analysis***

Data are expressed as mean ± SEM. Statistical analysis was performed by using a two-tailed Student's t-test for the comparison of two groups or ANOVA using Bonferroni post-hoc correction for multiple groups using GraphPad Prism Software 6.01 (GraphPad Software, Inc., La Jolla CA). p-values are expressed as *P ≤ 0.05, **P ≤ 0.01 and ***P ≤ 0.001.

# Results

## Identification of p38α protein interactors

To identify new p38α protein interactors, we performed a bioinformatics analysis in collaboration with Drs. Laura Isus and Patrick Aloy (IRB). To this end, we used three different approaches and considered information available in databases, the presence of D-motifs, and the modelling of docking peptides.

### *First approach:* Based on databases and putative docking motifs (D-motifs)

First, the *in-silico* analysis mined the information on p38α partners available in databases (Stark et al., 2011) (Ceol et al., 2010) (Aranda et al., 2010) (Prasad et al., 2009) (Bandyopadhyay et al., 2010). In addition, the analysis included a filtering strategy based on the presence of at least one putative docking sequence in the set of proteins found. Since the D-motif of some p38α substrates has been experimentally identified (Biondi & Nebreda, 2003) (Sharrocks et al., 2000) (Cargnello & Roux, 2011), we searched for D-motif occurrences in a list of 48 sequences with known p38α substrates and defined a set of four putative docking motifs (**Table 15**).

**Table 15 | Summary of the D-motif pattern-matching search in the set of known substrate sequences.**

| D-motif ID | D-motif pattern |
|---|---|
| 1 | K..[RK]….L.L |
| 2 | [KR].(4,5)[ILV].[ILV] |
| 3 | L..RR |
| 4 | [ILV](1,2).[RK](4,5) |

In total, 190 proteins from various studies were identified as putative p38α interactors (**Supplementary Table 1A** and **1B**). Proteins in the list, described in the literature by means of pull-down assays, immunoprecipitation, yeast two-hybrid (Y2H) screenings or other protein binding assays, were classified as physical interactors. On the other hand, proteins identified by kinase assays or other enzymatic studies were classified as functional interactors. Around 150 proteins were found to be physical interactors and 40 functional interactors (**Figure 13**).

Among the putative interactors, our screening identified known p38α binding proteins such as MK2 and PTPN7, thereby giving confidence to our filtering strategy. To validate our analysis, we selected up to 10 proteins (according to plasmid availability) and tested their interaction with p38α using pull-down assays (**Table 16**). The selected proteins were cloned in a GST-expression vector, purified, and incubated with 293T cell lysates.

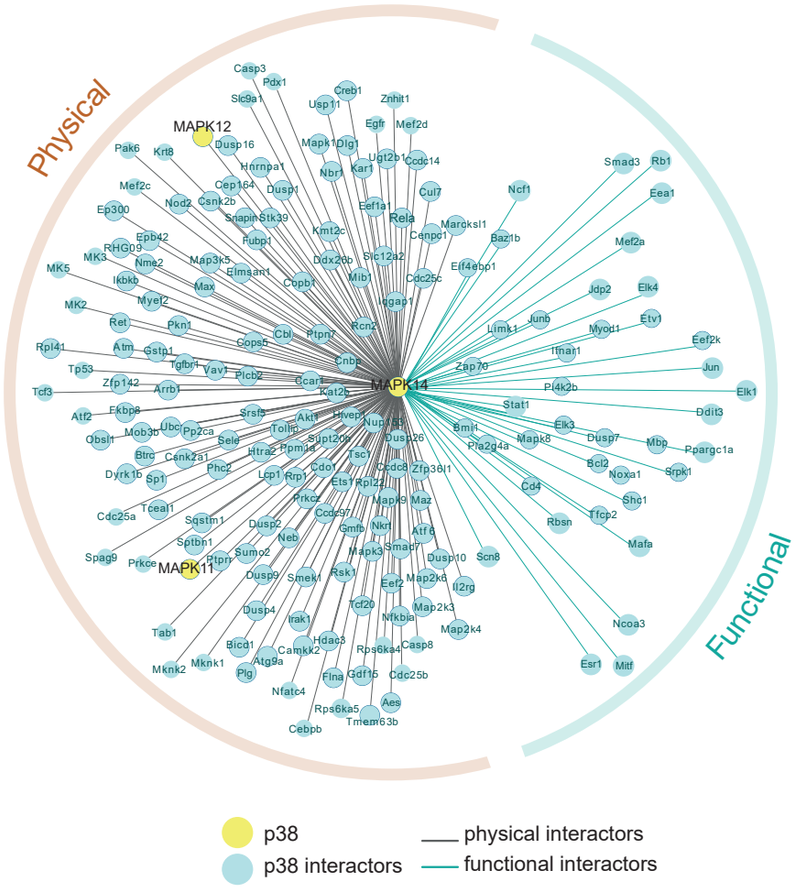


**Figure 13. Summary of the D-motif pattern-matching search in the set of known substrate sequences.**

**Table 16 | GST-expression constructs**

| Protein candidate | Interaction | D-motif (*) | Reference |
|---|---|---|---|
| CAMKK2 | Physical | 2 | (Huttlin et al., 2015) |
| CDO1 | Physical | 2 | (Takaesu et al., 2006) |
| COPS5 | Physical | 2 | (Wang et al., 2008) |
| FKBP8 | Physical | 2 | (Stelzl et al., 2005) |
| HNRNPA1 | Functional | 2 | (Noguchi et al., 2009) |
| HTRA2 | Functional | 2 | (Plun-Favreau et al., 2007) |
| NCF1 | Functional | 2,3 | (Qian et al., 2009) |
| PPM1A | Physical/Functional | 2 | (Takekawa et al., 1998) |
| PTPN7 | Physical | 2,3 | (Saxena et al., 1999) |
| MK2 | Physical/Functional | 2,3,4 | (Kotlyarov et al., 2002) |







GST-proteins were pulled down and their binding to endogenous p38α was analyzed using western blotting. GST-GFP protein was used as negative control, whereas GST-MK2 and GST-PTPN7 were used as positive controls. Apart from the positive controls, none of the preselected candidates interacted with p38α in the pull-down assay (**Figure 14A**).

Since some protein-protein interactions are mediated by post-translational modifications (PTMs) (Duan & Walther, 2015), we co-expressed p38α together with four proteins of interest in mammalian cells to facilitate a proper context for the PTM to happen. In this case, we tested their interaction using co-immunoprecipitation (**Figure 14B**). Likewise, we observed no interaction between p38α and the other proteins, except for MK2, thereby indicating that none of the selected candidates bound to p38α in a stable manner, neither *in vitro* nor *in vivo*.

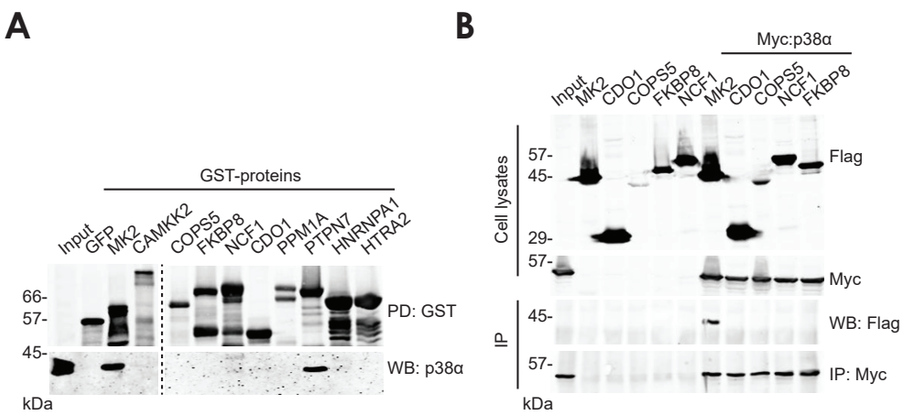


**Figure 13. Validation of preselected candidates.** (**A**) Pull down of GST-proteins (PD) incubated with 293T cell lysates. Binding of endogenous p38α was analyzed by western blotting (WB). Predicted molecular weights: GST-GFP: 53 kDa, GST-MK2: 68 kDa, GST-CAMKK2: 94k Da, GST-COPS5 64k Da, GST-FKBP8 (truncated): 50 kDa, GST-NCF1: 71kDa, GST-CDO1: 49 kDa, GST-PPM1A: 68 kDa, GST-PTPN7: 66 kDa, GST-hnRNPA1: 64 kDa and GST-HTRA2 (134-458 aa): 62k Da. (**B**) Immunoprecipitation of Flag-proteins (IP) expressed in 293T cells either alone or together with Myc-p38α Interaction with p38α was analyzed by western blot (WB). Predicted molecular weights: Flag-MK2: 46 kDa, Flag-CDO1: 24 kDa, Flag-COPS5: 38 kDa, Flag-FKBP8: 39 kDa and NCF1: 49 kDa, 6xMyc-p38α 49 kDa.

The methods used for the identification of p38α binding partners were based on the detection of stable interactions. Both pull-down and co-immunoprecipitation assays detect proteins that interact in a stable manner and that are typically subunits of complexes that carry out structural or functional roles. However, in most cases, p38α is thought to phosphorylate proteins by means of short, reversible and transient interactions.

To evaluate whether the preselected candidates were able to interact transiently with p38α, we used the Proximity Ligation Assay (PLA). This technique shows a highly specific and selective immunofluorescent signal when two proteins of interest co-localize and interact, even if transiently. To address this, Flag-tagged protein candidates, togeth-

er with Myc-p38α were co-transfected into U2OS cells and analyzed by both immunofluorescence and PLA (**Figure 15A**). Interestingly, three out of four proteins analyzed gave a similar PLA signal to that of the positive control MK2, thus confirming their transient interaction with p38α (**Figure 15A, 15B**).

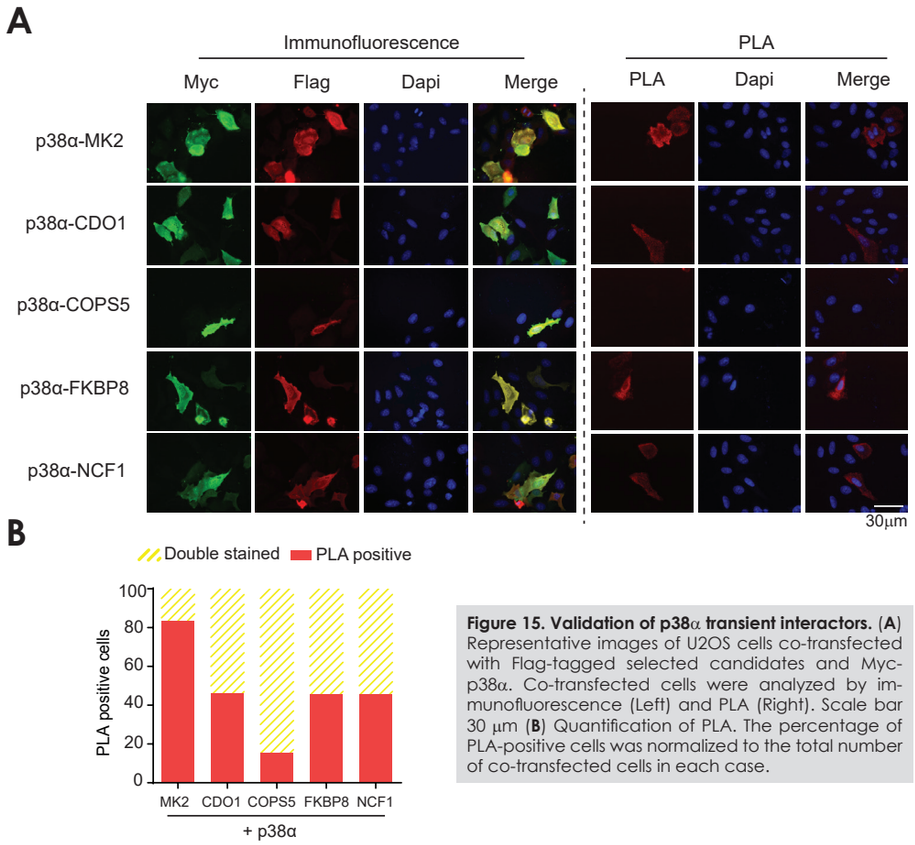


**Figure 15. Validation of p38α transient interactors.** (**A**) Representative images of U2OS cells co-transfected with Flag-tagged selected candidates and Myc-p38α. Co-transfected cells were analyzed by immunofluorescence (Left) and PLA (Right). Scale bar 30 μm (**B**) Quantification of PLA. The percentage of PLA-positive cells was normalized to the total number of co-transfected cells in each case.

In summary, we identified CDO1, FKBP8 and NCF1 proteins as putative transient interactors for p38α. CDO1 and NCF1 are described in the literature as p38α partners involved in specific cell processes (Takaesu et al., 2006) (Qian et al., 2009) whereas FKBP8 has been reported to be a yet non-validated interactor of p38α detected in a Y2H screening (Stelzl et al., 2005). Since transient interactions were successfully identified, we addressed whether the selected candidates were indeed substrates for p38α. To this end, recombinant GST-protein candidates were incubated *in vitro* with activated p38α and their phosphorylation was determined by kinase assays. Only substrates already characterized (MK2, ATF2, PTPN7 and NCF1) were phosphorylated by p38α whereas the rest of the proteins were not (**Figure 16A**). The phosphorylation detected in the case of CAMKK2 was also observed in the absence of p38α thereby suggesting that





it was due to CAMKK2 autophosphorylation (**Figure 16B**).

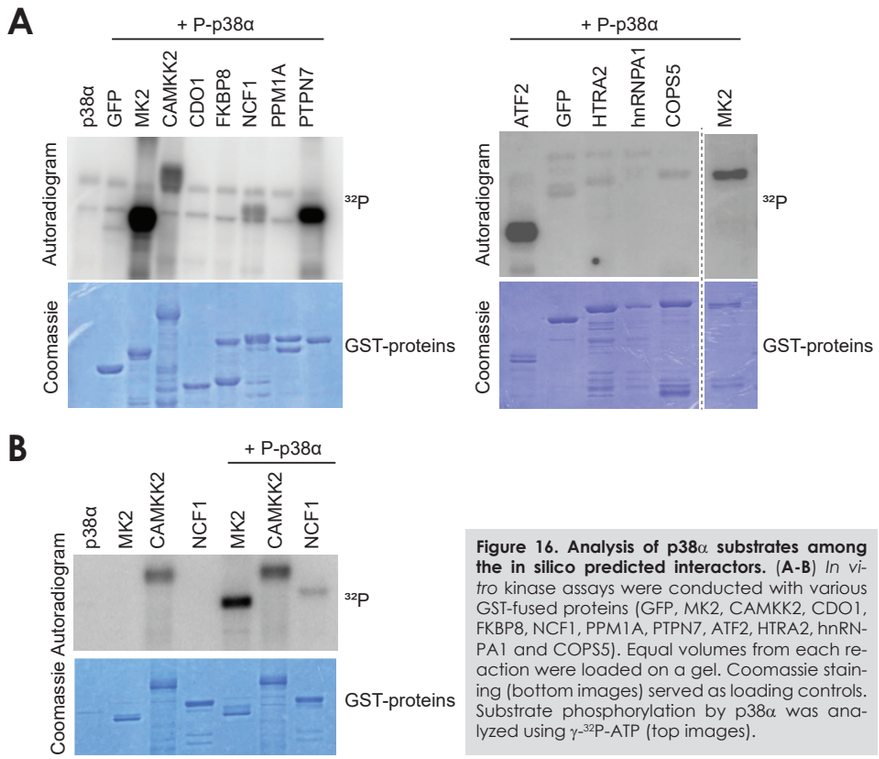


**Figure 16. Analysis of p38α substrates among the in silico predicted interactors.** (**A-B**) *In vitro* kinase assays were conducted with various GST-fused proteins (GFP, MK2, CAMKK2, CDO1, FKBP8, NCF1, PPM1A, PTPN7, ATF2, HTRA2, hnRNPA1 and COPS5). Equal volumes from each reaction were loaded on a gel. Coomassie staining (bottom images) served as loading controls. Substrate phosphorylation by p38α was analyzed using $\gamma$-$^{32}$P-ATP (top images).

Although CDO1, FKBP8 and NCF1 were found to be putative transient interactors in the PLA experiments, only the known substrate NCF1 was phosphorylated by p38α in kinase assays.

### *Second approach:* **Recharacterization of D-motifs**

Despite a large number of putative interactors reported for p38α, only the known partners characterized as docking interactors (MK2 or PTPN7) or substrates (MK2, PTPN7, ATF2 and NCF1) were identified. We therefore decided to change our strategy.
Since a main goal was the identification of new scaffolding partners for p38α, we redefined the possible docking sequences in order to reduce ambiguity using a more accurate methodology. A total of 15 docking sequences were manually retrieved from published data (Tanoue et al., 2000), filtering only for those associated with p38α. Docking sequences were classified on the basis of the type of docking proteins, such as activators (MKKPs), phosphatases (MKPs and PTPs) and substrates (MAPKAPKs) (**Table 17**) and were then aligned to the classified groups using Clustal Omega or M-Coffee alignment tools (**Supplementary Figure 1**). We searched the human proteome for p38α mo-

tif occurrences using the previously aligned sequences from each group as input. FIMO and hmmsearch softwares were used to scan the human proteome for the occurrences of a given motif described by position-specific scoring matrix (PSSM). FIMO software computed a log-likelihood ratio score for each position in the desired sequence database. Established dynamic programming methods converted this score to a p-value and then applied false discovery rate to estimate a q-value for each position in the given sequence. The scan revealed five proteins as new putative interactors for p38α two of which (GRK5 and ZBED6) were selected for *in vitro* validation (**Supplementary Table 2**). The interaction between the new protein candidates and p38α was analyzed by pull-down assays. Only the positive control MK2 interacted strongly with p38α whereas the two selected proteins failed to bind to p38α (**Figure 17**).

**Table 17 | List of MAP kinase docking sites.** Proteins were classified on the basis of the type of docking protein (MAPKK, MAPKAPK, PTP and MKP). Each protein contains a characterized D-motif for p38A. Table adapted from (Tanoue et al., 2000).

| Type of docking protein | Specific type of docking protein | D-motif | MAPK |
|---|---|---|---|
| MAPKK | MKK3 | KGKSKRKKDLRI | p38 |
| | MKK6 | SKGKKRNPGLKIP | p38 |
| | MKK4 | QGKRKALKLNF | JNK, p38 |
| MAPKAPK | MNK1 | KSRLARRRALAQAGRSRD | ERK,p38 |
| | MSK1 | KAPLAKRRKMKKTSTSTE | ERK,p38 |
| | MK2 | NPLLLKRRKKARALEAAA | p38 |
| | MK3 | NRLLNKRRKKQAGSSSAS | p38 |
| | PRAK | NNPILRKRKLLGTKPKDS | p38 |
| PTP | EC-PTP | GLQERRGSNVSLTLDM | ERK, p38 |
| | PTPN7 | RLQERRGSNVALMLDV | ERK, p38 |
| MKP | MKP1 | RFSTIVRRRAKGAKGAG | ERK,p38,JNK |
| | MKP2 | RCNTIVRRRAKGSVSLE | ERK,p38,JNK |
| | PAC1 | PWNALLRRRARARGPP | ERK,p38,JNK |
| | hVH5 | SKLVKRRLQQGKVTI | p38,JNK |
| | MKP5 | CADKISRRRLQQGKITV | p38,JNK |

Despite the new classification of the docking sequences into different categories and the high confidence predictions, we were not able to identify new docking interactors for p38α as stable as MK2. Taken together, these results suggest that *in silico* analysis using the docking sequence alone is not sufficient for the identification of stable partners for p38α with potential scaffolding functions.







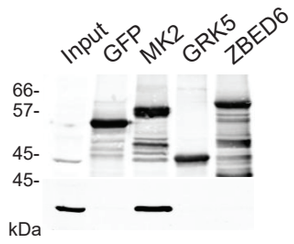


**Figure 17. Validation of selected candidates with redefined D-motifs.** Pull-down assay of GST-proteins (PD) incubated with 293T cell lysates. Endogenous p38α binding was analyzed by western blot (WB). Predicted molecular weight of proteins: GST-GFP: 53 kDa, GST-MK2: 68 kDa, GST-GRK5 (1-200): 40 kDa and GST-ZBED6 (1-384): 60 kDa.

## *Third approach:* **Modeling the MK2 docking peptide**

One of the best characterized interactors for p38α is its substrate MK2. Several studies have defined the crystal structure of the purified p38α and MK2 complex (ter Haar et al., 2007) (White et al., 2007). Interestingly, MK2 docking to p38α represents a special docking class since MK2 binds in the opposite direction to other characterized docking peptides derived from MEF2A or MKK3 (White et al., 2007) (Gaestel, 2006). In addition to the known docking residues, MK2 uses its basic C-terminal region to form extensive interactions with the p38α hydrophobic docking groove. The approaches that we used above for the identification of p38α interacting partners were based on simple pattern matching of D-motifs, which gave false positives hits. Therefore, we decided to consider not only the linear docking sequences but also the effect of the amino acid composition and structural compatibility with the p38α docking groove. We used the described docking peptide of MK2 as a reference for the prediction of new structural interactions. Since the docking motif of MK2 binds to p38α from the C' to the N' terminal direction, the Human Proteome Database was scanned for reverse motif hits with the following sequence:

-[LIVMP] – X – [LIV] –X – X – [LIVMFP] - X(6) - [LIVMP] – X-X- [RK][RK] –X-X-X

Up to 863 motifs from 833 proteins were identified. These hits were filtered on the basis of structural accessibility, predicted cellular localization, and presence of potential SP/TP sites. Finally, complexes of docking peptides with p38α were modeled using FoldX software to measure the interaction energy of protein complexes. We considered three available protein complexes with reverse motifs (2OKR, 2ONL and 2OZA), all of them were MK2 docking motifs and corresponded to the same docking peptide. However, they showed deviations in the p38α structure and, therefore, they were all used for modeling (**Table 18**).

Up to 78 proteins were found to be potential p38α interactors with docking peptides similar to MK2. As expected, MK2 and MK3 docking motifs were ranked in the first positions of the list, whereas all other motifs showed lower score (**Supplementary Table 3**).

As a preliminary observation, we analyzed the protein interactions of all putative candidates using STRING database, which provides a critical assessment and integration of protein–protein interactions (Szklarczyk et al., 2015). In addition to MK2 and MK3, we observed four proteins (PTPRQ, PIK3CD, PRDM16 and SMG1) with a potential functional link with p38α (**Figure 18**). Since our third approach had considered the nature of the p38α structure for docking interactions, we hypothesized that the identified proteins (**Figure 18**) are good candidates for future validations.

**Table 18 | Human MK2 docking peptides (370-389 aa).** 2OKR, 2ONL and 2OZA are three different structures available in the Protein Data Bank (PDB) of the MK2 docking peptide and p38α. Red: Non-polar and hydrophobic amino acids. Blue: Positively charged (basic and non-acidic amino acids), polar and hydrophilic amino acids.

| No. | MAPK | D-motif | Peptide | PDB |
|---|---|---|---|---|
| 1 | p38α | MK2 (370-389) | IkIkkIedasnpLIIKRrkk | 2OKR |
| 2 | p38α | MK2 (370-389) | IkIkkIedasnpLIIKRrkk | 2ONL |
| 3 | p38α | MK2 (370-389) | IkIkkIedasnpLIIKRrkk | 2OZA |

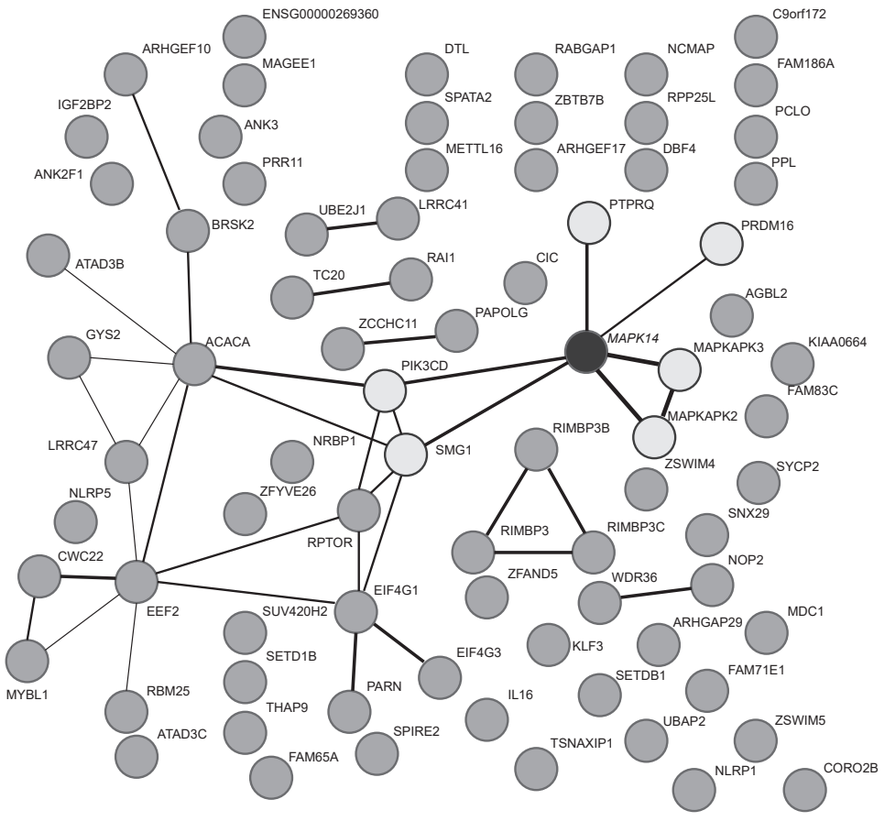








**Figure 18. p38α (MAPK14) interacting network with new predicted candidates.** PTPRQ, PIK3CD, PRDM16 and SMG1 (light grey) have a potential functional link with MAPK14 (black). Line thickness indicates the strength of data support. Edge confidence:
Low (0.15)
Medium (0.40)
High (0.70)
Very high (0.90)

In summary, our results demonstrate that the presence of canonical D-motifs that mediate the interaction of p38α with well-known partners is relatively common in proteins. However, we tested several candidates with potential D-motifs but found that only known interactors (such as MK2 or PTPN7) were able to interact with p38α in a stable and strong manner. Given these observations, other parameters must be examined in order to validate future predictions. We propose that consideration of the amino acid composition and structural accessibility of docking sequences should improve the recognition of stable p38α interactors.

## Characterization of the p38α:MK2 complex

Since one of the major goals was the identification of p38α kinase independent functions, we studied the scaffolding function of p38α in the context of MK2, which we found to be the most consistent stable interactor for p38α.

### Levels of endogenous MK2 depend on p38α:MK2 complex formation *in vivo*

In addition to the characterization of the p38α:MK2 crystal structure, it has been reported that MK2 protein levels are reduced in p38α-deficient cells, and vice versa, in MK2-null cells the levels of p38α are also diminished, thereby suggesting that p38α and MK2 mutually regulate their protein expression levels (Kotlyarov et al., 2002) (Sudo et al., 2005). We extended these observations, showing that MK2 protein levels were reduced in various tissues from p38α knock-out (KO) compared to wild-type (WT) mice (**Figure 19**).

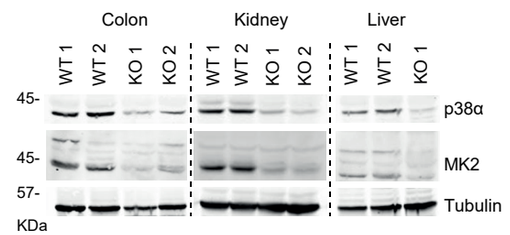


**Figure 19. Reduced MK2 protein levels in p38α KO mouse tissues.** Lysates from WT and p38α KO mouse tissues were analyzed by immunoblotting with the indicated antibodies.

Next, we measured the levels of MK2 in mesenchymal cell lines from several mouse tissues, including tumors. Mesenchymal stem cells were already available in our laboratory (Batlle et al. submitted), and breast cancer and colon fibroblasts were isolated using flow cytometry. Cells from PyMT-induced mammary tumors were first classified as CD45$^-$ and EpCAM$^-$ to exclude hematopoietic and epithelial cells and were then sorted using specific fibroblastic markers such as PDGFRα (**Figure 20A**). To extract colon fibroblasts, colon samples were treated with proteases to separate epithelial from mesenchymal cells and then characterized by CD45$^-$, CD31$^-$, PDGFRα$^+$ and PDGFRβ$^+$ markers (**Figure 20B**).

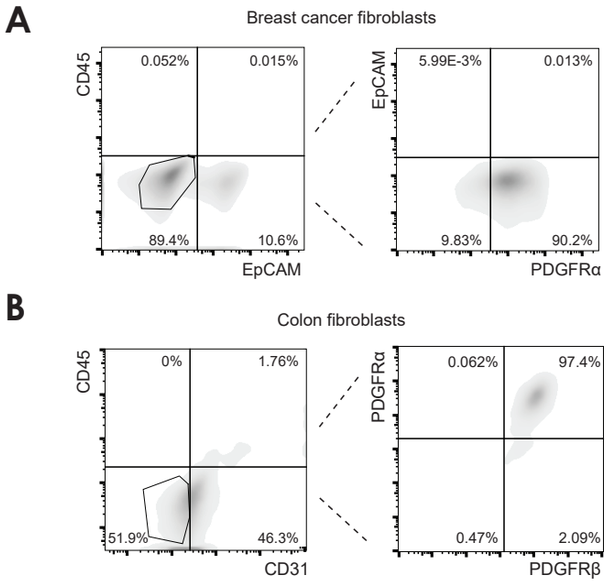


**Figure 20. Characterization of fibroblast cell lines.** (**A-B**) Cells were immortalized, stained with the indicated antibodies and analyzed in FACS Aria 2.0. Left panel: whole cell population. Right panel: cells from the selected gate (1st quadrant). (**A**) Breast cancer fibroblasts were isolated from tumors of PyMT, p38α$^{lox/lox}$, UBC-Cre-ERT2 mice. (**B**) Colon fibroblasts were obtained from colon pieces of p38α$^{lox/lox}$, UBC-Cre-ERT2 mice.

In addition, we used MK2 KO mouse embryonic fibroblasts (MEFs) provided by Dr. Mattias Gaestel. MK2 KO MEFs showed reduced levels of p38α protein, which were restored upon the re-expression of MK2 (**Figure 21A**). In agreement, all types of immortalized p38α KO cells showed reduced MK2 protein levels, and the re-expression of p38α protein resulted in the accumulation of MK2 (**Figure 21B**). Interestingly, MK2 mRNA levels were similar between WT and p38α KO cells (**Figure 21C**), thereby suggesting that the expression of the two kinases is regulated at the protein level. Since p38α is involved in the modulation of protein synthesis via the phosphorylation of the eukaryotic initiation factor 4E (eIF4E) (Shveygert et al., 2010), we analyzed global protein synthesis by measuring the O-propargyl-puromycin (OP-puro) incorporated into





nascent proteins from WT and p38α KO cells. A comparable protein synthesis rate was observed in both contexts (**Figure 21D**). This observation suggests that the reduced MK2 protein levels were not due to a general defect in protein synthesis.

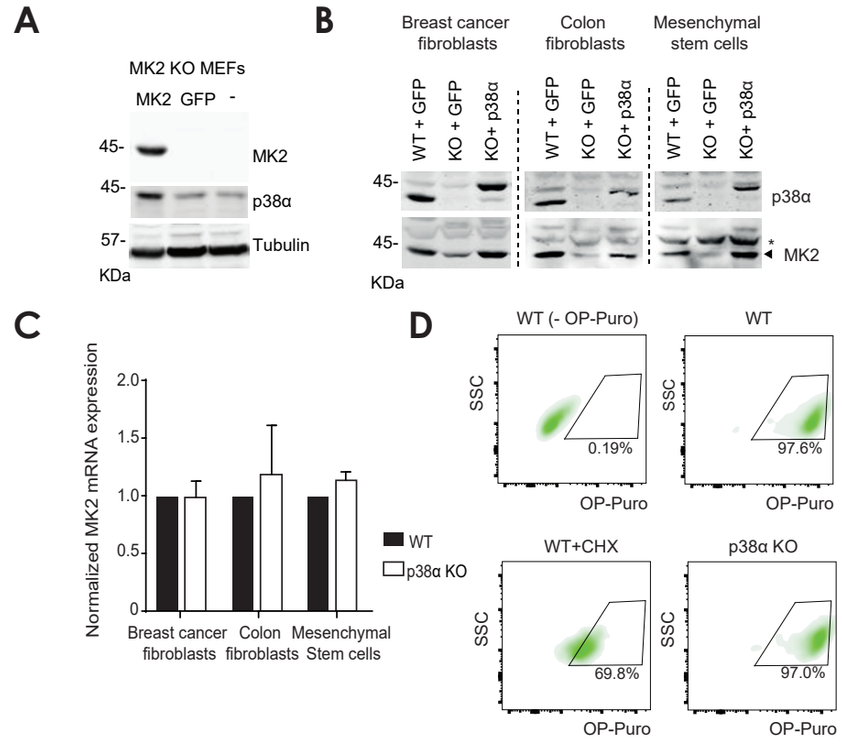


**Figure 21. p38α and MK2 regulate their protein expression levels.** (**A**) Lysates from MK2 KO MEFs re-expressing MK2 or GFP, as indicated. p38α and MK2 proteins were analyzed by western blotting. (**B**) Lysates from the indicated WT and p38α KO cells and also p38α KO cells re-expressing p38α or GFP were analyzed by immunoblotting with p38α and MK2 antibodies. The asterisk indicates a non-specific band. (**C**) MK2 mRNA levels were analyzed by qRT-PCR in the indicated WT and p38α KO cells and are referred to the expression level in the WT cells, which was given a value of 1. Data are mean ± SEM, n=2. (**D**) Analysis of protein synthesis in WT and p38α KO breast cancer fibroblasts. FACS analysis of OP-Puro signal (30 min pulse). Non-stained cells (-OP-Puro) and cells treated with protein synthesis inhibitor cycloheximide (50 μm, CHX) were used as negative control. Gates show % of OP-Puro positive cells.

Since previous studies on the interaction between p38α and MK2 were done with overexpressed or recombinant proteins, we examined whether endogenous p38α and MK2 proteins form a complex *in vivo*. To this end, first we fractionated lysates from WT and p38α KO cells on sucrose gradients and found that most endogenous MK2 co-fractionated with endogenous p38α in WT cells, whereas in the absence of p38α, MK2 was found mostly in a fraction with a lower molecular weight (**Figure 22A**). This observation supports the notion that MK2 normally forms a complex that probably involves p38α. The presence of a p38α:MK2 complex in cells was confirmed by immunoprecipi-

tation of endogenous MK2 using high-affinity nanobodies. Both in cell lines and mouse tissues, p38α co-immunoprecipitated with MK2, thereby indicating that the endogenous proteins indeed form a complex (**Figure 22B and 22C**).

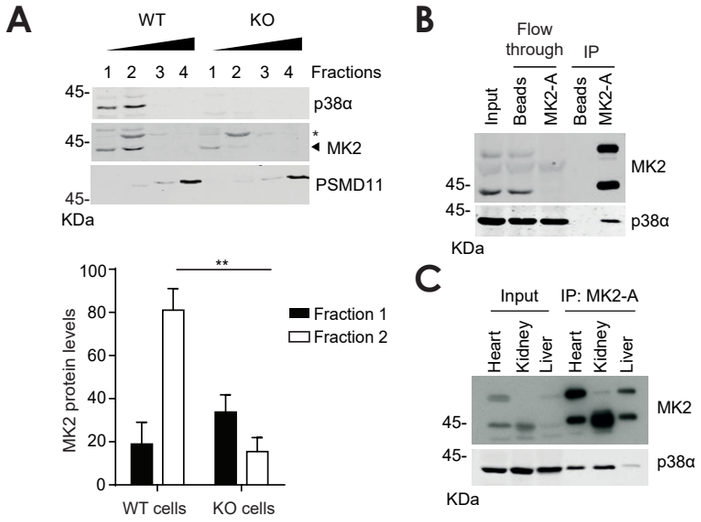


**Figure 22. Endogenous p38α and MK2 form a complex.** (**A**) Lysates from WT and p38α KO breast cancer fibroblasts were separated on 20-28% sucrose gradients. Triangles show the percentage of sucrose. Collected fractions were analyzed by immunoblotting using p38α and MK2 antibodies. The asterisk indicates a non-specific band. The 26S proteasome component PSMD11(Rpn6) was used as a control for high molecular weight complexes. The histogram shows the quantifications of the MK2 levels in fractions 1 and 2, which are normalized to the total amount of MK2 in WT cells. Data are mean ± SEM, n=3. (**B-C**) Lysates from breast cancer fibroblasts (**B**) and mouse tissues (**C**) were immunoprecipitated with MK2-Trap_A (MK2-A) or agarose beads (Beads), and then were analyzed by immunoblotting with p38α and MK2 antibodies.

To further characterize the interaction between p38α and MK2, we used various p38α mutants that either have impaired kinase activity or are unable to interact with other proteins (Chang et al., 2002)(Diskin et al., 2004)(Li et al., 2008)(Mittelstadt et al.,2009) (Peregrin et al., 2006)(Tanoue et al., 2000)(Tanoue et al., 2001) (**Table 19** and **Figure 23A**). We addressed whether particular p38α domains were required for the formation of the p38α:MK2 complex by studying the ability of the p38α mutants to bind to MK2 in pull-down assays and to phosphorylate MK2 *in vitro*. As expected, the p38α docking mutants were unable to bind to MK2 in pull-down assays (**Figure 23B**), and kinase-dead p38α proteins (KM and TY) failed to phosphorylate MK2 (**Figure 23C**). Surprisingly, only the p38α-CD mutant was impaired in MK2 binding and phosphorylation (**Figures 23B** and **23C**), suggesting that binding through the CD region is necessary for a functional p38α:MK2 complex.

**Table 19 | p38α mutants.**

| Name | Mutation | Reference |
|---|---|---|
| CD | D313/315/316N | (Tanoue et al., 2000) |
| ED | E160/E161T | (Tanoue et al., 2001) |
| IA, QA | I116A, Q120A | (Chang et al., 2002) |
| DF | D176A/F327S | (Diskin et al., 2004) |
| TA, TD | T123A, T123D | (Peregrin et al., 2006) |
| DG | D145G | (Li et al., 2008) |
| KM, TY | K53M, T180A/Y182F | (Mittelstadt et al., 2009) |







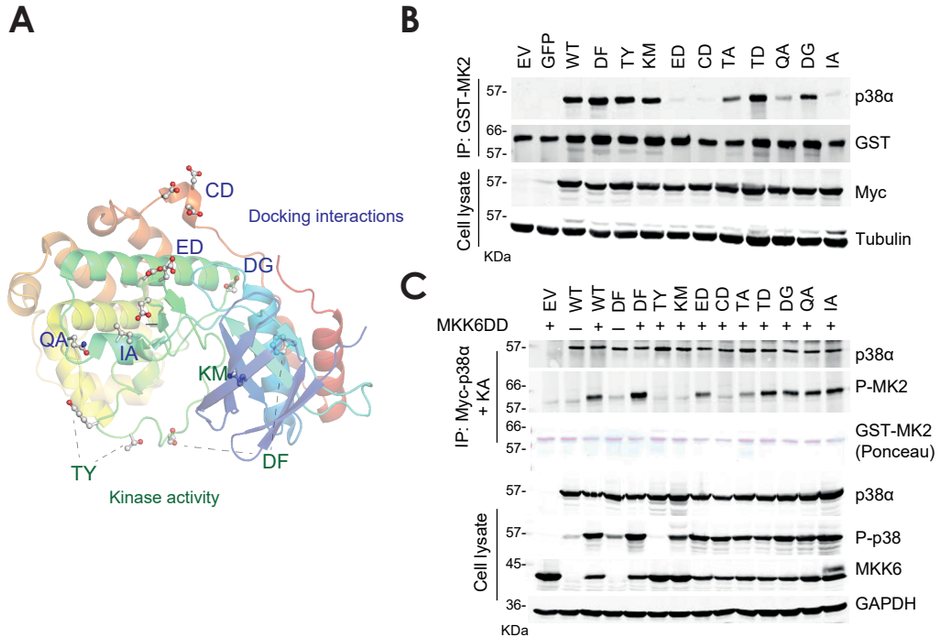


**Figure 23. p38α-CD mutant is impaired in MK2 binding and phosphorylation.** (**A**) Schematic representation of the p38α structure, indicating the mutations that affect kinase activity (green) or docking residues (blue). The figure was created using PyMOL v2. (**B**) Myc-tagged p38α mutants were overexpressed in 293T cells, and total lysates were incubated with recombinant GST-MK2 protein (5 μg), which was pulled down with glutathione beads and analyzed by immunoblotting. (**C**) 293T cells were transfected with the indicated Myc-tagged p38α mutants, together with constitutively active MKK6 (MKK6DD). Total lysates were immunoprecipitated with Myc-coupled agarose beads, and p38α activity was analyzed in kinase assays using GST-MK2 as a substrate. Immunoblotting with antibodies for p38α and phospho-MK2 was used to measure p38α levels and kinase activity, respectively. Total lysates were also directly analyzed by immunoblotting.

To study the contribution of p38α:MK2 binding to the reduced MK2 protein levels observed, we re-expressed p38α WT or various mutants in p38α KO cells. Interestingly, MK2 protein levels were recovered by p38α WT or the kinase-dead mutants (KM or TY) but not by the CD mutant (**Figure 24**). These observations suggest that the interaction through the CD domain of p38α is essential for the recovery of MK2 protein levels and therefore for the formation of a stable p38α:MK2 complex.

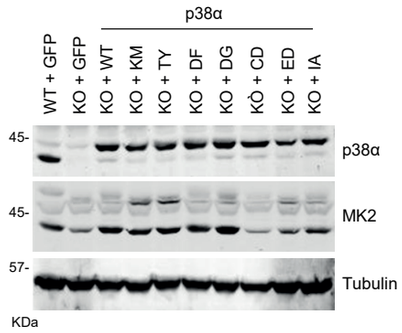


**Figure 24. MK2 protein levels depend on p38α-CD domain.** WT and p38α KO breast cancer fibroblasts were infected with retroviruses that express the indicated p38α WT or mutated forms, or with a control vector (GFP), and lysates were analyzed by immunoblotting.

Despite the presence of functional kinase residues, the CD mutant was the only docking mutant found with impaired MK2 phosphorylation. To evaluate whether the CD domain is both necessary and sufficient for the formation of a functional p38α:MK2 complex, we searched the p38α protein sequence for additional residues with potential roles in MK2 binding and subsequent activation. Using molecular modeling analysis in collaboration with Drs. Antonija Kuzmanic and Modesto Orozco (IRB), we identified up to four p38α amino acids potentially implicated in both MK2 binding and phosphorylation (**Table 20**). Mutations of the R49 and R136 residues were predicted to interfere with MK2 docking ability, whereas changes in the E178 and P322 sites were predicted to alter p38α activity (**Figure 25A**). Using *in vitro* pull-down and kinase assays, we analyzed the capacity of these new p38α mutants to bind or to phosphorylate MK2, respectively. Interestingly, we observed that the R136Q mutant showed impaired binding to and phosphorylation of MK2 to the same extent as the CD mutant, whereas these functions were not affected in the rest of the mutants (**Figure 25B** and **25C**). These observations suggested that, besides the CD domain, other residues, like R136, are involved in the regulation of p38α:MK2 complex formation and function.

**Table 20 | Predictions for new p38α residues potentially involved in MK2 interaction and phosphorylation.** The molecular modeling was performed using PyMOL_v2 software.

| Mutation | Predicted effect |
|---|---|
| R49Q | Interacts with the ED site, as well as the D112 at the end of the hinge. It could interfere with the binding to substrates and ATP. |
| R136Q | Interacts with the L16 loop and with the D313, D315, D316 residues. It is predicted to interfere with the binding of the docking motif. |
| E178A | Interacts with R173, R67 and R70, which are important for the phospho-T180 coordination. This mutation is predicted to affect kinase activity. |
| P322R | Loss of this proline causes the A-loop to become less flexible. Addition of an arginine can stabilize the A-loop. It is predicted to affect kinase activity. |





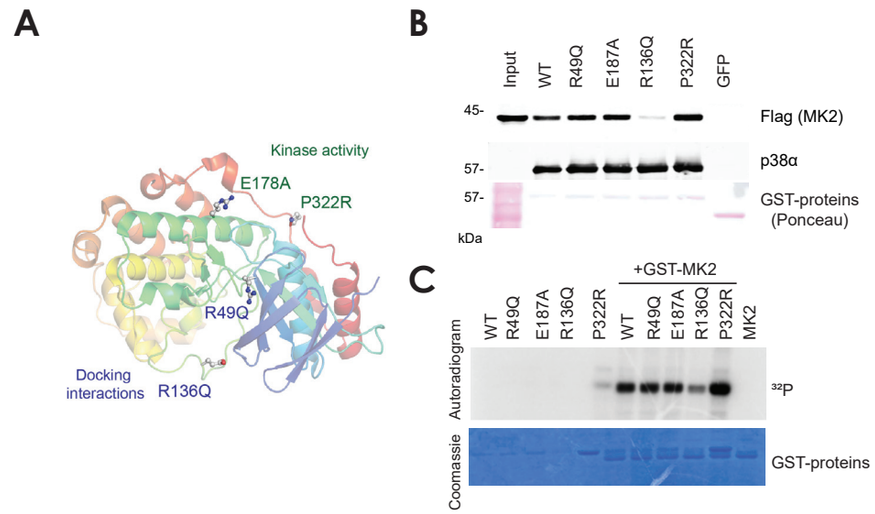


**Figure 25. p38α R136Q mutant impairs MK2-binding and phosphorylation.** (**A**) Schematic representation of the p38α structure, indicating mutations that affect kinase activity (green) or docking residues (blue). The figure was created using PyMOL v2. (**B**) Flag-MK2 was overexpressed in 293T cells, and total lysates were incubated with recombinant GST-p38α mutants (5 μg), which were pulled down and MK2 binding was analyzed by immunoblotting using anti-Flag antibody. (**C**) Recombinant GST-p38α mutants were incubated with GST-MK2 protein and ATP. GST-p38α mutants alone were also analyzed to rule out autophosphorylation. Coomassie staining (bottom image) served as loading control. Phosphorylation by p38α was analyzed using $\gamma$-$^{32}$P-ATP (top image).

In summary, our results indicate that endogenous p38α and MK2 proteins form a complex mediated by docking interactions that involve not only the p38α CD domain but also other docking residues such as the R136 amino acid. Moreover, the absence of either p38α or MK2 in cells or the lack of p38α:MK2 interaction by mutation of the CD site leads to reduced protein levels of the interacting partner. Since neither mRNA expression levels nor global protein synthesis were affected, we suggest that the two proteins depend on each other for their mutual stabilization.

## Phosphorylation of p38α and MK2 triggers complex dissociation

Surface plasmon resonance studies have shown that phosphorylation reduces the binding affinity between purified p38α and MK2 proteins (Lukas et al., 2004). Moreover, in fission yeast, phosphorylation also reduces the binding affinity between Sty1 (p38α) and Srk1 (MK2), with concomitant Skr1 degradation (Lopez-Aviles et al., 2008). To address how phosphorylation affects the endogenous p38α:MK2 complex in mammalian cells, we first examined MK2 protein levels in response to stimuli that activate the p38α pathway. Interestingly, all the stimuli tested induced the downregulation of MK2, concomitantly with its phosphorylation (**Figure 26A**- **26C**).

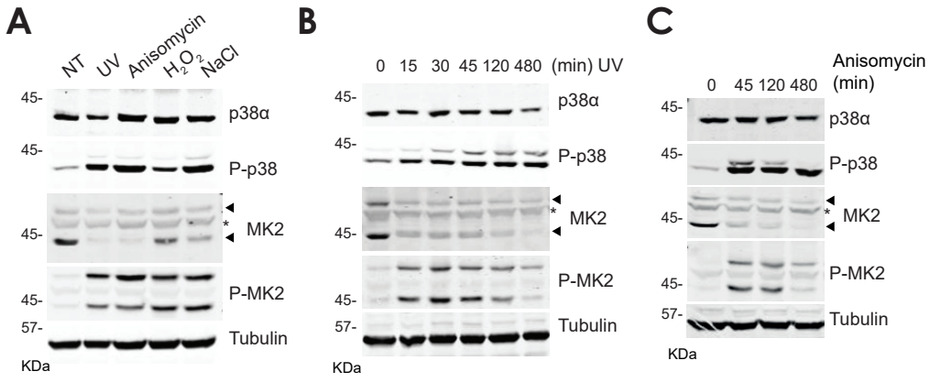


**Figure 26. MK2 downregulation upon p38α pathway activation.** (**A**) Breast cancer fibroblasts were stimulated with UV irradiation (30J/m²), Anisomycin (30μM), $H_2O_2$ (100 μM) or NaCl (200 mM) for 4 h to induce p38α activation. Lysates were analyzed by immunoblotting. (**B-C**) Breast cancer fibroblasts were stimulated either with UV light (30J/m²) (**B**) or Anisomycin (20 μM) (**C**) for the indicated times, and lysates were analyzed by immunoblotting. The asterisk indicates a non-specific band.

In addition, p38α KO cells were reconstituted with either p38α WT or the kinase-dead mutants (KM and TY) and then stimulated with UV light. Activation of the p38α pathway resulted in decreased MK2 protein levels in cells expressing WT p38α but not in those expressing kinase-dead mutants (**Figure 27**). This result supports the notion that phosphorylation of both p38α and MK2 is required for MK2 downregulation, probably due to impaired binding.

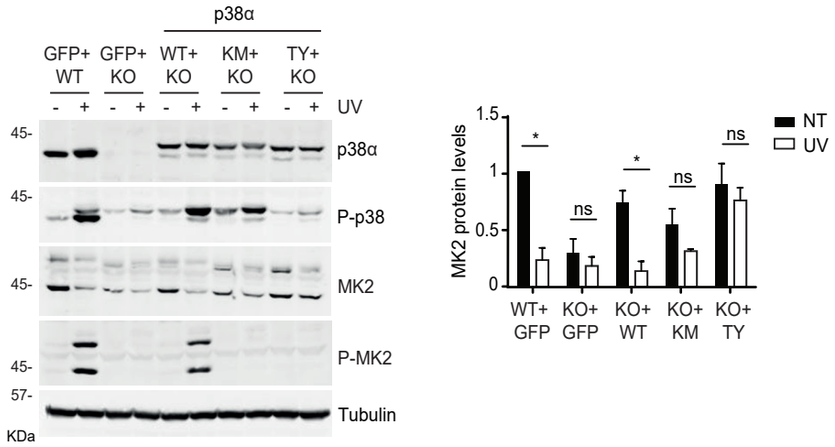


**Figure 27. MK2 downregulation depends on p38α and MK2 phosphorylation.** WT and p38α KO breast cancer fibroblasts were infected with retroviruses that express p38α WT or the kinase-dead mutants KD and TY, or with a control vector (GFP), and then were left untreated or stimulated with UV irradiation (30 J/m²) for 1 h. Lysates were analyzed by immunoblotting. The histogram shows the quantification of the MK2 protein levels that were normalized to non-treated WT cells. Data are mean ± SEM, n=3.





To further study the effect of pathway activation on the interaction between p38α and MK2, cells were stimulated with UV irradiation for different times, and lysates were then analyzed in sucrose gradients. In non-stimulated cells, we observed that p38α and MK2 co-localized in the same fraction. However, upon UV irradiation, concomitantly with the downregulation of MK2 levels, part of the p38α protein shifted to a lower molecular weight fraction (**Figure 28A**). Furthermore, endogenous MK2 immunoprecipitation confirmed that p38α:MK2 binding was reduced upon UV stimulation (**Figure 28B**), thereby suggesting that activation of the p38α pathway leads to the separation of the p38α:MK2 complex.

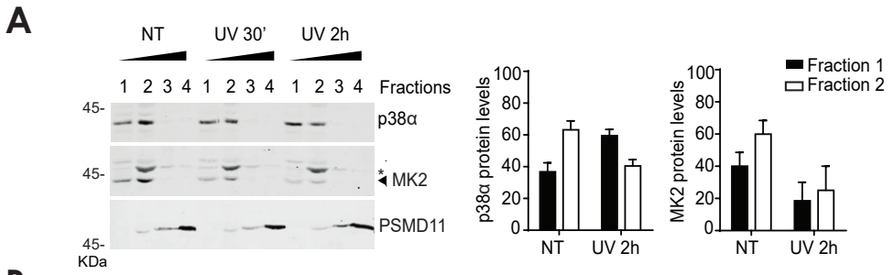


**Figure 28. p38α:MK2 complex separation upon p38α pathway activation.** (**A**) Breast cancer fibroblasts were stimulated with UV irradiation (30 J/m²) for the indicated times and lysates were separated on 20-28% sucrose gradients. Collected fractions were analyzed by immunoblotting using p38α and MK2 antibodies. The 26S proteasome component PSMD11 was used as a control for high molecular weight complexes. The asterisk indicates a non-specific band. The histograms show the p38α and MK2 levels in fractions 1 and 2, which are normalized to the total p38α and MK2 amounts in untreated cells. Data are mean ± SEM, n=2. (**B**) Breast cancer fibroblasts were stimulated with UV irradiation (30 J/m²) and the lysates were immunoprecipitated with MK2-Trap_A (MK2) or agarose beads (Beads) and were analyzed by immunoblotting. Band intensities were analyzed using the ImageJ software and the p38α/MK2 ratio was calculated.

## MK2 alone has reduced protein stability

Since p38α pathway activation resulted in lower MK2 protein levels, we evaluated the stability of the MK2 protein in the context of phosphorylated p38α by blocking protein synthesis with cycloheximide (CHX). Considering that short exposure to CHX induces p38α activation (Oksvold et al., 2012) and consequently MK2 phosphorylation, we used a chemical inhibitor of p38 MAPK (BIRB) to prevent MK2 phosphorylation and facilitate the interaction between the two proteins. We found that the MK2 half-life was shorter in cells treated with CHX alone than in those treated with CHX plus the p38 inhibitor (**Figure 29A**). Similarly, MK2 also showed a shorter half-life in p38α-deficient cells compared to WT cells. In this case, cells were treated equally with CHX and p38 MAPK inhibitor to avoid MK2 phosphorylation by other p38 MAPK family members

(**Figure 29B**). These results suggest that the reduced MK2 protein levels found in p38α KO cells and in WT cells upon p38α pathway activation are due to an increased degradation of the MK2 protein. Taken together, our data highlight the importance of the p38α:MK2 complex formation in the regulation of MK2 protein stability.

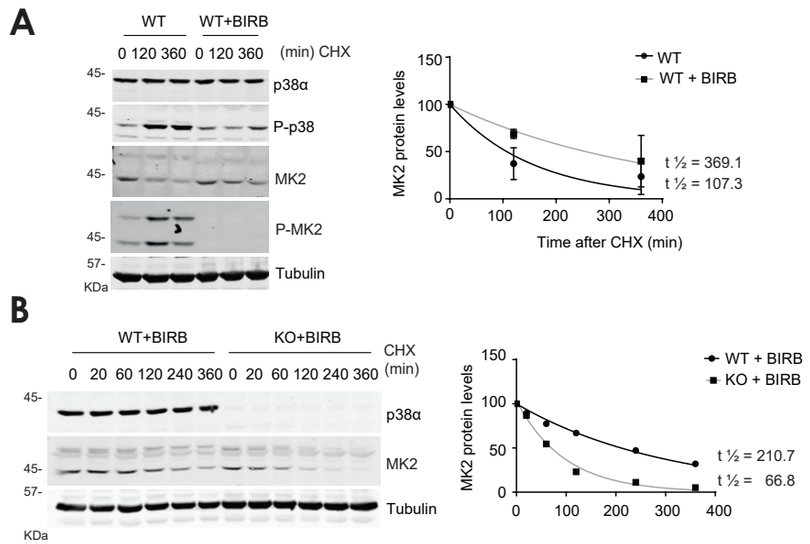


**Figure 29. MK2 is less stable upon separation from p38α.** (**A**) WT breast cancer fibroblasts were treated with BIRB796 (BIRB, 10 μM) or vehicle (DMSO) together with cycloheximide (CHX, 50 μg/ml) for the indicated times, and lysates were analyzed by immunoblotting. The graph shows MK2 protein levels normalized against the initial levels (0 min), which were given the value of 100%. MK2 half-life ($t^{1/2}$)was calculated as 107.3 min and 369.1 min for WT and WT+BIRB, respectively. Data are mean ± SEM, n= 2. (**B**) WT and p38α KO breast cancer fibroblasts were treated with BIRB and CHX as above for the indicated times. Lysates were analyzed by immunoblotting. The graph shows MK2 protein levels normalized against the initial levels (0 min), which were given the value of 100%. The MK2 half-life ($t^{1/2}$) was estimated as 210.7 min and 66.8 min for WT+BIRB and KO+BIRB, respectively.

## Dissociation of the p38α:MK2 complex leads to MK2 degradation by the 26S proteasome

In eukaryotic cells, protein degradation is usually regulated by two processes, namely autophagy and the UPS. Autophagy is a non-selective degradation process that delivers cytoplasmic components to the lysosome. In contrast, the UPS specifically targets ubiquitinated proteins for proteasome degradation (Dikic, 2017).

To address how MK2 is degraded upon p38α:MK2 complex separation, we used autophagy and proteasome inhibitors. Interestingly, both in p38α KO cells and in UV-stimulated WT cells, MK2 protein degradation was impaired by inhibition of the proteasome system but not of autophagy (**Figures 30A** and **30B**). To confirm that autophagy and proteasome inhibitors were working as expected, we analyzed the accumulation of LC3II and p53 proteins, respectively. Similarly, we observed impaired MK2 protein degradation by inhibition of the proteasome in UV-stimulated U2OS cells (**Figure 30C**). This observation suggests that MK2 degradation by the proteasome upon p38α activation is conserved in various cell systems.

In addition, immunoprecipitation assays using UV-stimulated cells treated with proteasome inhibitor revealed that the MK2 protein that accumulates upon proteasome blockade failed to interact with p38α (**Figure 30D**). This result confirms that phosphorylation impairs the binding between p38α and MK2 proteins.

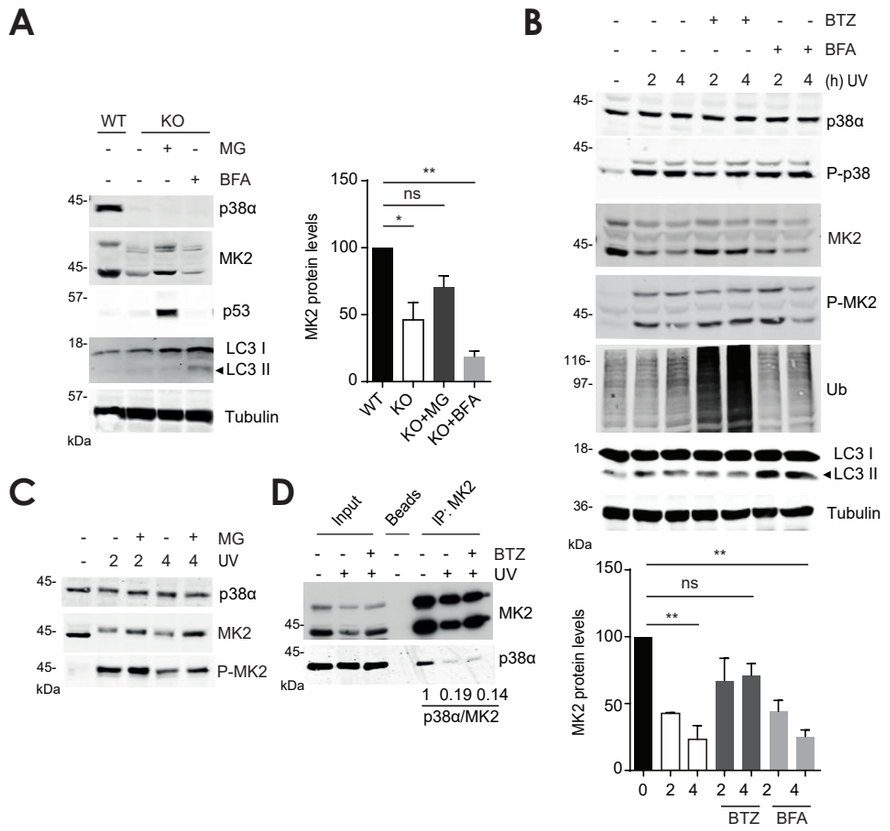


**Figure 30. MK2 protein levels are regulated by the proteasome.** (**A**) WT and p38α KO breast cancer fibroblasts were treated with MG132 (MG, 20 μM) or Bafilomycin A1 (BAF, 400 nM) for 16 h, and lysates were analyzed by immunoblotting. p53 and LC3II proteins were used as markers for proteasome and autophagy inhibition, respectively. The histogram shows the quantification of MK2 protein levels, which were normalized to the untreated WT cells. Statistical significance was calculated between WT and KO groups. Data are mean ± SEM, n=3. (**B**) Breast cancer fibroblasts were treated with Bortezomib (BTZ, 100 nM) or Bafilomycin A1 (BFA, 400 nM) and stimulated with UV irradiation (30 J/m$^2$) for the indicated times. Lysates were analyzed by immunoblotting. Ubiquitinated (Ub) and LC3II proteins were used as markers for proteasome or autophagy inhibition, respectively. The histogram shows the quantification of MK2 levels relative to non-treated cells (time 0). Statistical significance was calculated between non-stimulated and UV-stimulated groups. Data are mean ± SEM, n=3. (**C**) U2OS cells were pre-treated with MG132 (MG, 20 μM) and then stimulated with UV light (30 J/m$^2$) irradiation for 2 and 4 h. Lysates were analyzed by immunoblotting. (**D**) Breast cancer fibroblasts were pre-treated with Bortezomib (BTZ, 100 nM) for 2 h prior to stimulation with UV light (30 J/m$^2$) for 4 h. Lysates were immunoprecipitated with MK2-Trap_A (MK2) or agarose beads (Beads), and then were analyzed by immunoblotting. Band intensities were analyzed by ImageJ software and the p38α/MK2 ratio was calculated.

The proteasome is a multisubunit complex that is found in cells in two main forms, the 20S and 26S. Although most proteins rely on ubiquitination for proteasomal degradation, it has been proposed that some proteins can be degraded by the 20S proteasome in a ubiquitin-independent manner. To further dissect the proteasome-mediated degradation of MK2, we used inhibitors of the 20S (MG and BTZ) or 19S proteasome subunits (AP and OPA) (Paramore & Frantz, 2003)(Song et al., 2017)(Wang et al., 2014) in UV-treated cells. Interestingly, we observed an accumulation of MK2 protein levels with all the inhibitors (**Figure 31A**), indicating that MK2 is degraded by the 26S proteasome complex. We confirmed the specificity of the compounds used by analyzing the enhanced levels of ubiquitinated proteins and p53 (**Figure 31A** and **31B**). Overall, our results suggest that the MK2 protein is degraded by the 26S proteasome when it is not bound to p38α.

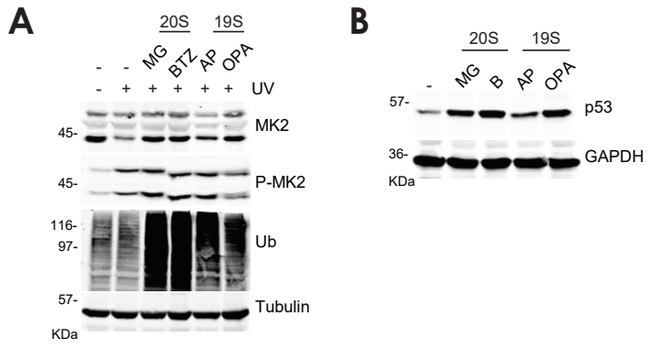


**Figure 31. MK2 is degraded by the 26S proteasome.** (**A**) Breast cancer fibroblasts were pre-incubated with the proteasome inhibitors MG132 (MG, 20 μM), Bortezomib (BTZ, 100 nM), b-AP15 (AP, 3 μM) and O-phenanthroline (OPA, 200 μM) for 2 h and then were irradiated with UV light (30 J/m$^2$) for 4 h. Lysates were analyzed by immunoblotting. Ubiquitinated (Ub) proteins were used as a control for proteasome inhibition. (**B**) Breast cancer fibroblasts were pre-incubated with the proteasome inhibitors MG132 (MG, 20 μM), Bortezomib (BTZ, 100 nM), b-AP15 (AP, 3 μM) and O-phenanthroline (OPA, 200 μM) for 6 h. Lysates were analyzed by immunoblotting with p53 antibodies to confirm proteasome inhibition.

## MK2 degradation requires neither its N-terminus nor the D-motif lysines

For proper proteasomal degradation, multiple ubiquitin molecules attach to lysine residues of proteins by ubiquitin-activating, -conjugating and -ligating enzymes (E1, E2, E3 respectively). However, in some cases, E3 transfers ubiquitin molecules into other amino acids or at the N-terminal amine group of the target protein (McDowell & Philpott, 2013) (Kim et al., 2014). Since our data indicate that MK2 is degraded by the proteasome, we first analyzed lysines potentially involved in the MK2 ubiquitination reaction using an automated method for recognition of the ubiquitination sites in proteins. Only 1 out of 29 lysines was found to be a potential target site for MK2 ubiquitination (Qiu et al., 2015). The predicted lysine K360 is located in the MK2 C-terminus and belongs to







the MK2 D-motif. Interestingly, MK2 is degraded upon p38α:MK2 complex separation and therefore upon D-motif dissociation. Consequently, the unbound D-motif could be accessible to ubiquitination. To validate this prediction, we studied the stability of a MK2 mutant (D-(R)) with all the lysines in the D-motif changed to arginine (K360R included) (**Figure 32A**). MK2 KO MEFs were reconstituted with MK2 WT or the D-motif mutant (D-(R)) and then were stimulated with UV irradiation in the presence or absence of the proteasome inhibitor. We found that the D-(R) mutant was degraded as the MK2 WT in UV-treated cells, suggesting that lysines present in the D-motif were not involved in the ubiquitination of MK2 upon UV stimulation (**Figure 32B**). To evaluate the role of the N-terminus in MK2 degradation, a N-terminally truncated version of MK2 (MK2 N-term) was generated (**Figure 32C**). MK2 KO MEFs were reconstituted with MK2 WT or the mutant (MK2 N-term), and then irradiated with UV light in the presence or absence of the proteasome inhibitor. The MK2 N-term mutant was degraded after UV stimulation as the WT MK2 (**Figure 32D**), suggesting that the N-terminal P-region is not involved in the MK2 degradation process.

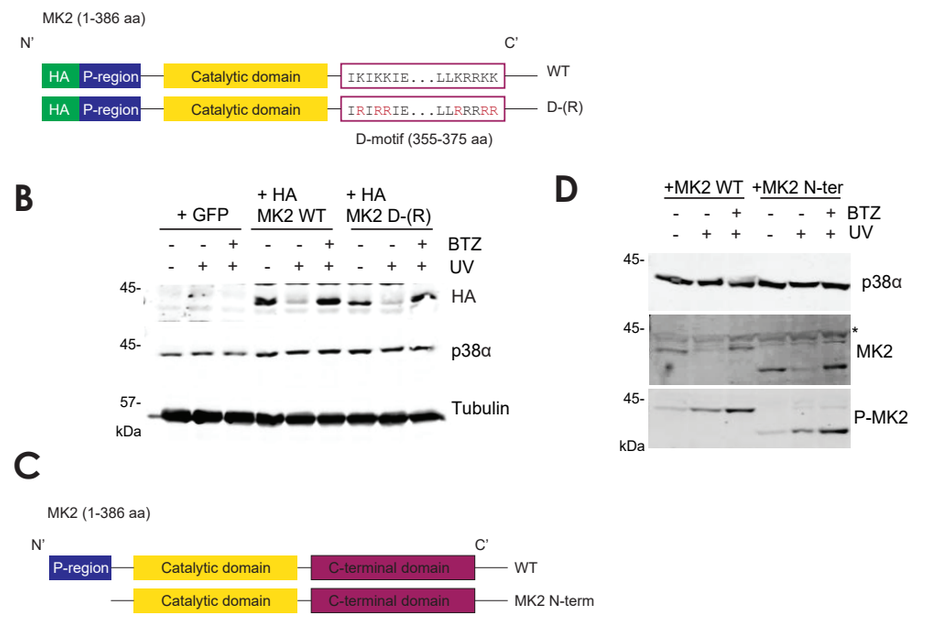


**Figure 32. MK2 D-motif containing lysines are not involved in MK2 degradation.** (**A**) Schematic representation of HA-MK2 WT and D-(R) mutant. Mouse MK2 D-motif is indicated. Blue indicates the proline-rich region (P-region) and red the lysine residues mutated to arginine. (**B**) MK2 KO MEFs infected with GFP, WT or D-(R) mutant were treated with Bortezamib (BTZ, 100 nM) for 2 h and irradiated with UV light (30 J/m$^2$) for 4 h. Lysates were analyzed by immunoblotting. (**C**) Schematic representation of MK2 WT and the N-terminally truncated form (MK2 N-term). (**D**) MK2 KO MEFs reconstituted with MK2 WT or MK2 N-term were pretreated with BTZ (100 nM) for 2 h and irradiated with UV light (30 J/m$^2$) for 4 h. Cell extracts were analyzed by immunoblotting. The asterisk indicates a non-specific band.

## MK2 is degraded by the proteasome in a Hsp27- independent manner

Upon stress stimuli, the phosphorylated Hsp27 protein enhances the degradation of several proteins through the proteasome pathway (Parcellier et al., 2003) (Parcellier et al., 2006). Since Hsp27 is one of the best characterized substrates for MK2 (Rouse et al., 1994), we analyzed the possible role of Hsp27 in MK2 degradation. Cells were infected with non-targeting shRNA (shNT) or shRNAs against Hsp27 (shHsp27_1 and shHsp27_2) and then were stimulated with UV irradiation to activate the p38α pathway and trigger MK2 degradation. Although the shRNAs varied in their efficiency to downregulate MK2, no differences were observed in terms of MK2 degradation upon UV stimuli (**Figure 33**). This result suggests that Hsp27 is not important for MK2 degradation.

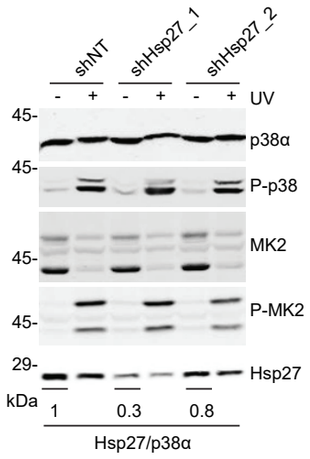


**Figure 33. Hsp27 downregulation does not impair MK2 degradation.** Breast cancer fibroblasts were infected with Non-targeting (shNT) or Hsp27 (shHsp27_1, shHsp27_2) shRNAs. Cells were stimulated with UV light (30 J/m$^2$) for 4 h. Lysates were analyzed by immunoblotting. Band intensity was analyzed with ImageJ software to calculate the Hsp27/p38α ratio.

## MDM2 ubiquitin ligase plays a role in MK2 degradation

An integrated bioinformatics platform that predicts the proteome-wide E3-substrate interaction network was recently reported (Li et al., 2017). We used this tool to predict MK2 interactions with putative E3 enzymes that might be involved in MK2 degradation. Interestingly, the analysis identified MK2 as a high confidence substrate for the SMURF1, STUB1 and MDM2 E3-ubiquitin ligases (**Figure 34A** and **Supplementary Table 4**). Since the bioinformatics analysis was based on the human proteome, we use human U2OS cells to validate the potential role of SMURF1, STUB1 and MDM2 in MK2 degradation. First, the E3 candidates were downregulated using specific siRNAs against the E3 ligase (siMDM2, siSMURF1 and siSTUB1). We measured the efficiency of the siRNAs by comparing the E3 mRNA levels from control (siControl) and E3-downregulated cells (**Figure 34B**). Then, cells were irradiated with UV followed by







immunoblotting analysis. Interestingly, MK2 protein levels accumulated in UV-treated cells deficient for MDM2 but not for the other E3 ligases (**Figure 34C**), thereby suggesting that MDM2 might regulate MK2 proteasomal degradation.

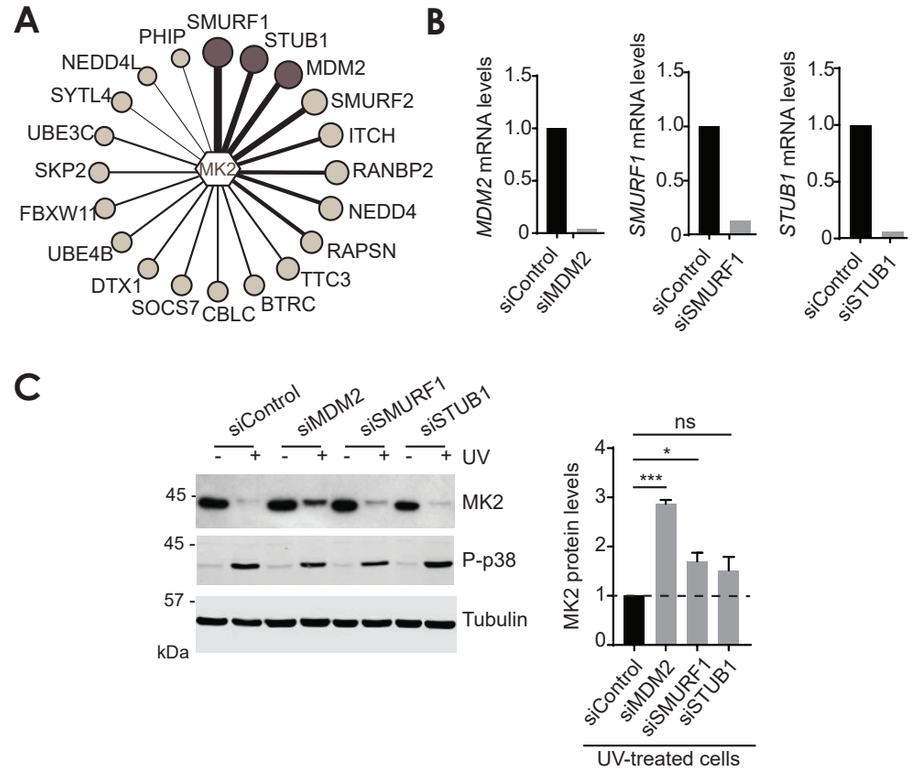


**Figure 34. Predicted E3-MK2 network.** (**A**) Network view of the E3 ligases predicted to target MK2. The panel is adapted from the webserver (http://ubibrowser.ncpsb.org) described in (Y. Li et al., 2017). E3-MK2 interactions with a high confidence score are shown darker. (**B**) U2OS cells were transfected with siRNA control or against MDM2, SMURF1 and STUB1. mRNA xpression levels were determined by qRT-PCR and were referred to the expression levels of siControl cells. (**C**) U2OS cells were transfected as in (**B**), stimulated with UV (30 J/m$^2$) and analyzed 4 h later. Lysates were analyzed by immunoblotting. The histogram shows the quantification of MK2 protein levels relative to siControl cells treated with UV light. Data are mean ± SEM, n=3.

## MK2 protein levels are restored after transient activation of the p38α pathway through *de novo* gene expression

Since the presence of MK2 is important to maintain p38α protein stability (Kotlyarov et al., 2002)(Ronkina et al., 2007), we questioned whether MK2 protein levels are eventually restored after p38α pathway activation.

To this end, we used LPS and TGFβ stimuli, which induce transient activation of p38α to evaluate the recovery of MK2 protein levels in two cell systems. First, bone marrow-derived macrophages (BMDMs) were differentiated to mature macrophages, as

previously described (Bailon et al., 2010), and then treated with LPS for up to 6 h. At early time points, we observed phosphorylation of both p38α and MK2 with concomitantly MK2 downregulation. Interestingly, both MK2 protein and mRNA levels were increased after 4-6 h of LPS treatment (**Figures 35A** and **35B**). To confirm a proper response in LPS-treated BMDMs, the expression of the LPS-induced cytokines TNFα CXCL2 and IL6 was also analyzed (**Figure 35C**).

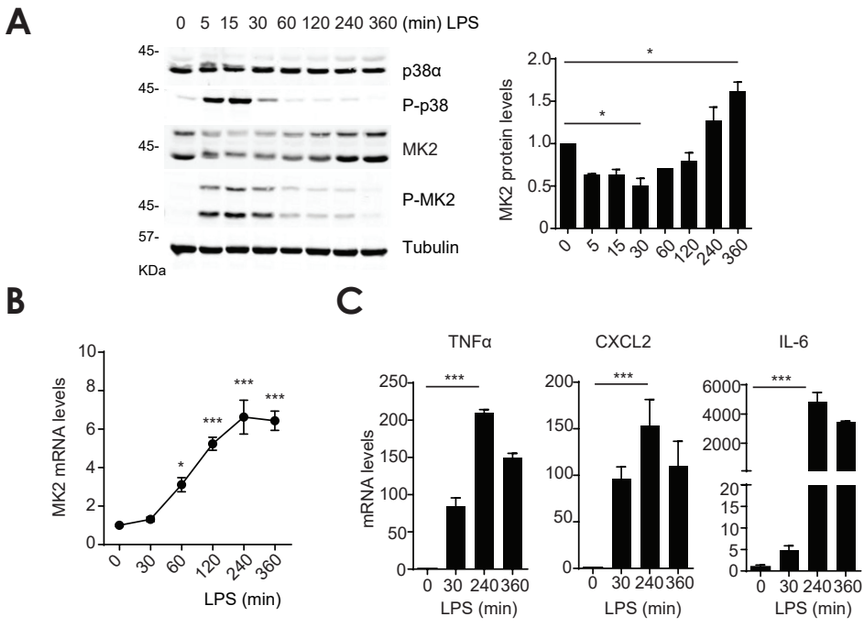


**Figure 35. MK2 protein and mRNA accumulate upon LPS stimulation.** (**A**) BMDMs were starved for 17 h and then stimulated with LPS (10 ng/ml) for the indicated times. Lysates were analyzed by immunoblotting. The histograms show the quantification of MK2 protein levels relative to non-treated cells (time 0). Statistical significance was calculated between non-treated and LPS-treated cells. Data are mean ± SEM, n=3. (**B**) RNA was extracted from BMDMs that were treated as in (**A**). MK2 mRNA levels were determined by qRT-PCR and were referred to the expression level in the non-treated cells (time 0), which was given the value of 1. Statistical significance was calculated between non-treated and LPS-treated cells. Data are mean ± SEM, n=5. (**C**) BMDM were treated as in (**A**) and RNA samples were collected at the indicated times. TNFα, CXCL2 and IL6 mRNA levels were determined by qRT-PCR and were referred to the expression level in the non-treated cells (time 0), which was given a value of 1. Statistical significance was calculated between non-treated and LPS-treated cells (240 minutes). Data are mean ± SEM, n=3.

Similar increases in MK2 protein and mRNA levels were observed in breast cancer fibroblasts treated with TGF-β (**Figures 36A** and **36B**), thus indicating a conserved response in different types of transiently stimulated cells. Overall, the results in the two cell types suggest that, after transient stimulation of the p38α pathway, MK2 protein levels are restored, which correlates with enhanced levels of MK2 mRNA.

Since p38α and MK2 phosphorylation seems to be the main cause of MK2 degradation, we evaluated the effect of p38α and MK2 inhibition on the restoration of MK2 protein levels. As expected, p38α inhibition impaired MK2 phosphorylation, whereas the MK2





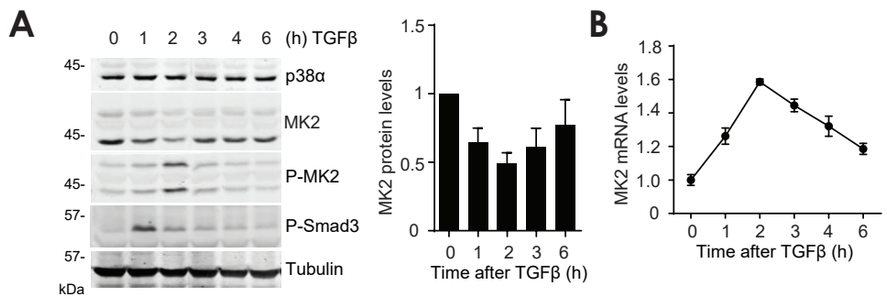


**Figure 36. MK2 protein and mRNA levels are restored upon TGFβ stimulation.** (**A**) Breast cancer fibroblasts were treated with TGFβ (5 ng/μl) for the indicated times, and lysates were analyzed by immunoblotting. Phospho-Smad3 antibodies were used to confirm TGFβ stimulation. The histogram shows the quantification of MK2 protein levels relative to non-treated cells (time 0). Data are mean ± SEM, n=2. (**B**) Lysates from cells treated with TGFβ (5 ng/μl) were used to measure MK2 mRNA levels by qRT-PCR. Values are referred to the expression level in the non-treated cells, which was given a value of 1. n=1 with three technical replicates.

inhibitor did not hinder this process (**Figure 37A**). The efficacy of the MK2 inhibitor was confirmed by measuring the TNFα mRNA expression levels induced by LPS, which are known to depend on both p38α and MK2 activity (Kotlyarov et al., 1999) (**Figure 37B**). Interestingly, 30 min after LPS stimulation, the reduced MK2 protein levels were maintained in BMDMs treated with the MK2 inhibitor, whereas BMDMs treated with the p38 inhibitor showed higher MK2 protein levels (**Figure 37A**). Moreover, the MK2 inhibitor did not affect the increase in MK2 mRNA levels observed at later times after LPS stimulation, whereas the p38 inhibitor significantly impaired this increase (**Figure 37C**). These results suggest that MK2 mRNA accumulation is regulated in a p38α dependent manner but independently of MK2 activity. To characterize the mechanism of MK2 mRNA accumulation in p38α and MK2-inhibited BMDMs treated with LPS, we analyzed the MK2 mRNA stability by blocking gene transcription with Actinomycin D (**Figure 37D**). Interestingly, p38α or MK2 inhibition did not significantly affect the MK2 mRNA half-life, thereby suggesting that the increased MK2 mRNA levels observed upon LPS treatment were probably due to enhanced MK2 gene transcription.

Taken together, these results indicate that MK2 protein levels are restored upon transient activation of p38α due to an increase in *de novo* MK2 gene transcription triggered by p38α activity.

### Sustained activation of the p38α pathway determines the fate of p38α and MK2 proteins

In addition to the stimuli that induce the transient activation of p38α, several extracellular agents, such as osmotic or oxidative stress, can trigger more sustained activation. This is usually associated with severe stress, upon which cells need to acquire a status that prepares them for damage repair or often for cell death.

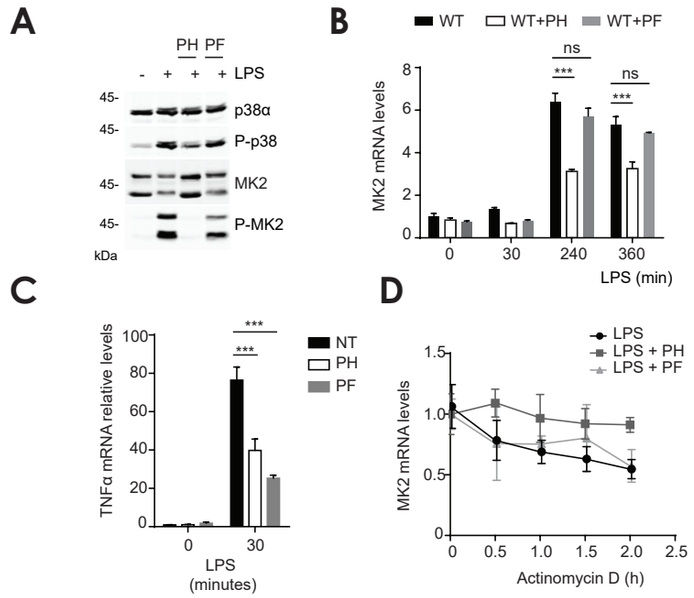


**Figure 37. MK2 protein levels are restored through** *de novo* **gene expression and in a p38α-dependent manner.** (**A**) BMDMs were starved for 17 h and then pre-treated with the p38 inhibitor PH-797804 (PH, 2 μM), the MK2 inhibitor PF-3644022 (PF, 10 μM) or vehicle (DMSO) for 2 h prior to stimulation with LPS for 15 min. Lysates were analyzed by immunoblotting. (**B-C**) BMDMs were treated with p38α and MK2 inhibitors as in (**A**) and were then stimulated with LPS for the indicated times. TNFα and MK2 mRNA levels were determined by qRT-PCR and were referred to the expression level in the non-treated cells (time 0), which was given the value of 1. Statistical significance was calculated between WT and WT+PH or WT+PF cells. Data are mean ± SEM, n= 3. (**D**) BMDMs were treated with p38α and MK2 inhibitors as in (**A**) and then stimulated with LPS for 4 h. Then, actinomycin D (5 μg/ml) was added and RNA samples were collected at indicated times. MK2 mRNA levels were determined by qRT-PCR and were referred to the expression level in the non-treated cells (time 0), which was given a value of 1. No significant differences were found between samples. Statistical analysis was calculated between WT and WT+PH or WT+PF cells. Data are mean ± SEM, n= 4.

It has recently been reported that sustained p38α and MK2 activation eventually leads to reduced cell viability, an observation that emphasizes the importance of negative feedback loops for proper cell homeostasis (Trempolec et al., 2017). To evaluate how sustained p38α activation affects the fate of MK2 protein, we expressed a constitutively active form of the p38α activator MKK6 (MKK6DD). As expected, MKK6DD induction led to p38α and MK2 activation, as well as MK2 downregulation. Strikingly, MK2 protein levels were not restored and, consequently, we found a progressive reduction in p38α protein levels (**Figure 38**). This observation indicates that long-term phosphorylation would prevent complex formation and thereby affect the stability of both proteins.

To demonstrate that the reduced protein levels were a consequence of complex separation, we took advantage of a p38α substrate selective inhibitor, CMPD1, that binds to p38α affecting the docking groove residues and therefore MK2 activation (Davidson et al., 2004). Since CMPD1 is predicted to perturb p38α docking sites, we analyzed the capacity of this compound to disrupt the p38α:MK2 complex in cells.





Interestingly, immunoprecipitation assays showed impaired binding of MK2 to p38α in CMPD1-treated cells compared with non-treated cells (**Figure 39A**). Consistently, MK2 and p38α protein levels were downregulated upon long-term treatment with CMPD1 but restored after removing the compound (**Figure 39B**). Importantly, CMPD1 administration did not activate the p38α pathway (**Figure 39C**), thereby suggesting that the reduced protein levels observed were due mainly to the interference with MK2-p38α binding *per se*, without affecting their phosphorylation.

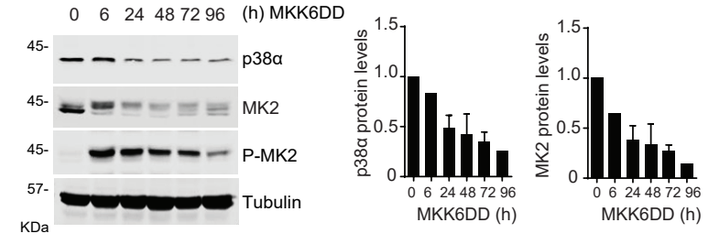


**Figure 38. Sustained activation of p38α leads to p38α and MK2 downregulation.** U2OS cells bearing a Tetracycline-inducible MKK6DD construct were incubated with Tetracycline (1 μg/ml) and were collected at the indicated times after MKK6DD induction. Lysates were analyzed by immunoblotting. The histograms show the quantification of p38α and MK2 protein levels relative to non-treated cells (time 0). Data are mean ± SEM, n=2.

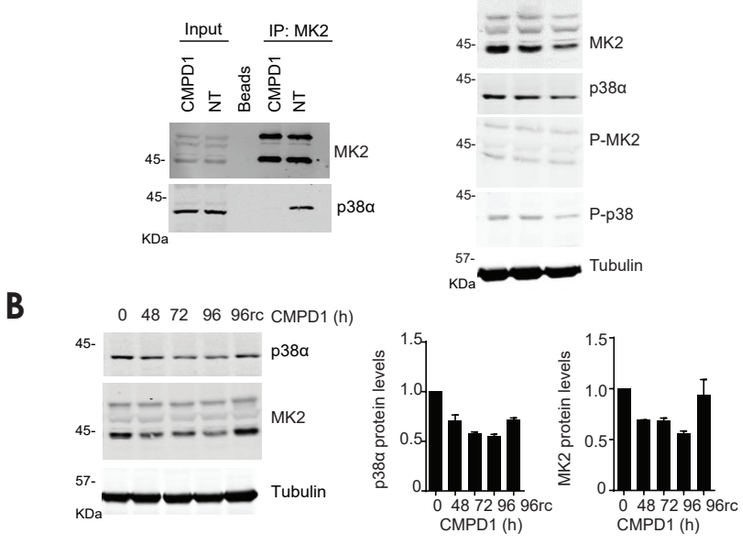


**Figure 39. Separation of the p38α:MK2 complex by CMPD1 leads to the downregulation of both proteins.** (**A**) Breast cancer fibroblasts were treated with CMPD1 (10 μM) or DMSO for 3 days. Lysates were immunoprecipitated with MK2-Trap_A (MK2) or agarose beads (Beads), and then were analyzed by immunoblotting. (**B-C**) Breast cancer fibroblasts were treated with CMPD1 for the indicated times. 96rc (96 rescue) refers to cells that after 72 h of incubation with CMPD1 were incubated in normal media for 24 h. Samples were analyzed by immunoblotting using the indicated antibodies.
The histograms show the quantification of p38α and MK2 protein levels relative to non-treated cells (time 0). Data are mean ± SEM, n=2.

Overall, our results strongly suggest that the re-expression of MK2 protein following p38α and MK2 transient activation constitutes a regulatory feedback loop, which allows to reassemble the protein complex, maintaining the stability of both proteins and allowing the recovery of the stand-by cellular status. Otherwise, if the activation persists, phosphorylation of p38α and MK2 avoids complex formation, leading to the downregulation of both proteins and compromising the homeostasis of the cell.

### MK2 subcellular localization depends on the p38α:MK2 complex formation

Next, we addressed whether our proposed mechanism of p38α and MK2 protein regulation through complex dynamics could account for some functions attributed to p38α and MK2 signaling that are still not well understood. In particular, the modulation of p38α and MK2 subcellular localization is controversial. Some authors claim that p38α and MK2 are located inside the nucleus of resting cells, whereas others propose that both proteins reside in the nucleus and cytoplasm (Ben-Levy et al., 1998)(Gaestel, 2006) (Gong et al., 2010). Although MK2 contains a nuclear export signal (NES) and a nuclear localization signal (NLS) in its C-terminal domain, it is unknown whether these regions are functional.

To evaluate the distribution of p38α and MK2 proteins inside the cell and the importance of the MK2-NES or MK2-NLS in this localization, cells were infected with non-targeting shRNA (shNT) or shRNAs against MK2 (shMK2_1 and shMK2_2) and subjected to subcellular fractionation assays. We found that p38α and MK2 colocalized mostly in the cytoplasm. Interestingly, the localization of p38α did not change upon MK2 downregulation (**Figure 40A**), thereby suggesting that neither the MK2-NES nor the MK2-NLS were implicated in the p38α subcellular distribution. Immunofluorescence analysis in 293T cells confirmed that both kinases co-localized mainly in the cytoplasm. Interestingly, whereas p38α expressed alone was also found in the cytoplasm, MK2 expressed alone appeared mainly in the nucleus (**Figure 40B**). This result suggests that in the absence of p38α the MK2-NLS is exposed, thus leading to MK2 nuclear localization.

### In search of partners interacting with the p38α:MK2 complex

Analysis of the proteomes of many organisms highlights the importance of multiprotein complexes for the implementation of cellular functions (Hartwell et al., 1999). Our results indicate that, under resting conditions, p38α and MK2 proteins form a complex that maintains their stability and proper subcellular distribution. Given that a wide range of proteins are organized in macromolecular assemblies, we investigated the association of additional proteins with the p38α:MK2 complex in order to further







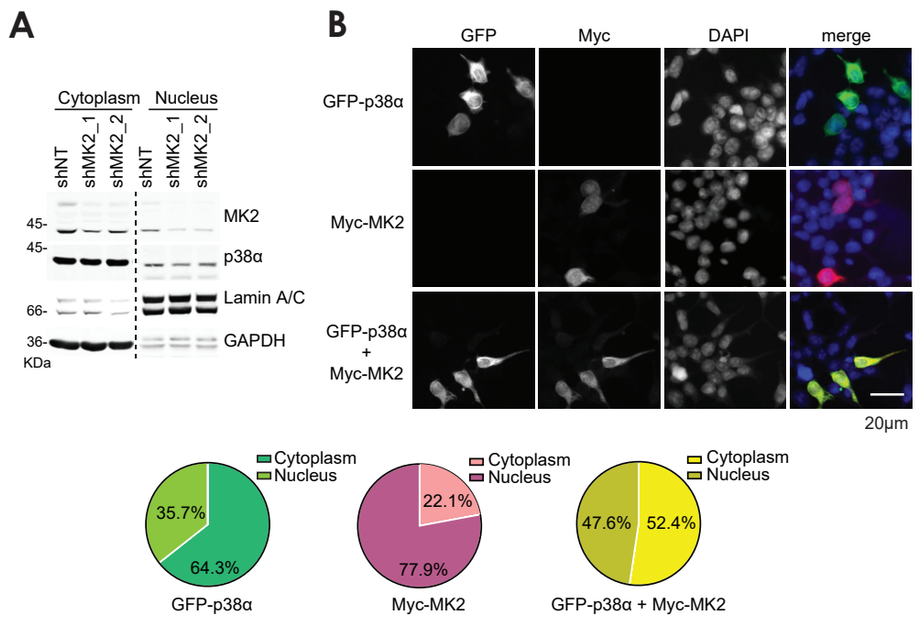


**Figure 40. MK2 association with p38α determines the MK2 subcellular localization.** (**A**) Breast cancer fibroblasts were infected with shRNAs either non-targeting (shNT) or against MK2 (shMK2_1, shMK2_2). Lysates were fractionated in cytoplasm and nucleus and were analyzed by immunoblotting. (**B**) Representative images of 293T cells transfected with GFP-p38α and Myc-MK2 alone or in combination. Pie charts show the percentage of stained cells found in the cytoplasm or nucleus compartments.

characterize the cellular functions of this assembly.

To identify proteins associated with the p38α:MK2 complex, endogenous MK2 from WT or p38α KO cells was immunoprecipitated and analyzed by mass spectrometry. Samples were reduced, digested and trypsinized following the FASP protocol (Wiśniewski et al., 2009) and were analyzed by label free quantification. Up to 41 proteins were found to be associated with MK2 (**Supplementary Table 5**). As expected, p38α was detected as a MK2 interactor, showing a high number of peptide spectrum matches (PSMs) in WT samples but undetectable PSMs in p38α KO samples. Curiously, most of the proteins identified showed a similar number of PSMs in WT and p38α KO samples (**Supplementary Table 5**), suggesting that most potential partners can bind to MK2 independently of p38α. To validate the interaction with MK2, some candidates were analyzed at endogenous or overexpressed levels according to the availability of antibodies (**Table 21**). p38α protein was used as a positive control in all cases.

First, MK2 immunoprecipitations from WT and p38α KO breast cancer fibroblasts were analyzed by immunoblotting using specific antibodies. Interestingly, Strip1 was found to interact with MK2 to the same extent as p38α (**Figure 41A**). However, the interaction between MK2 and Strip1 was found in both WT and p38α KO samples, indicating that these two proteins bind in a p38α-independent manner. Similar results

were observed in overexpressed 293T cells. Strikingly, besides p38α and Strip1, two more proteins (Bccip and Pcmtd1) were validated as MK2 interactors (**Figure 41B**). However, due to the lack of antibodies, the interaction between endogenous proteins could not be confirmed.

Overall, our results suggested that Strip1, Bccip and Pcmdt1 are new interacting partners for MK2, with Strip1 being a promising candidate as it binds to MK2 at endogenous levels. Since p38α is not required for the interaction of these partners, Strip1 could be associated to MK2 alone or to the p38α:MK2 complex via MK2 binding.

**Table 21 | Putative MK2 binding partners.** Endogenous (E) or overexpressed (O) proteins were used for the validation of MK2 interactors identified by mass spectrometry.

| Gene names | Protein name | Validation |
|---|---|---|
| Dnajb6 | DnaJ homolog subfamily B member 6 | E |
| Pcmt1 | Protein-L-isoaspartate(D-aspartate) O-methyltransferase | E |
| Mapk14 | p38α (mitogen-activated protein kinase 14) | E/ O |
| Pcmtd1 | Protein-L-isoaspartate O-methyltransferase domain-containing protein 1 | O |
| Sptbn1 | Spectrin beta chain, non-erythrocytic 1 | E |
| Strip1 | Striatin-interacting protein 1 | E/ O |
| Bccip | BRCA2 and CDKN1A-interacting protein | O |
| Mpp6 | MAGUK p55 subfamily member 6 | E/ O |

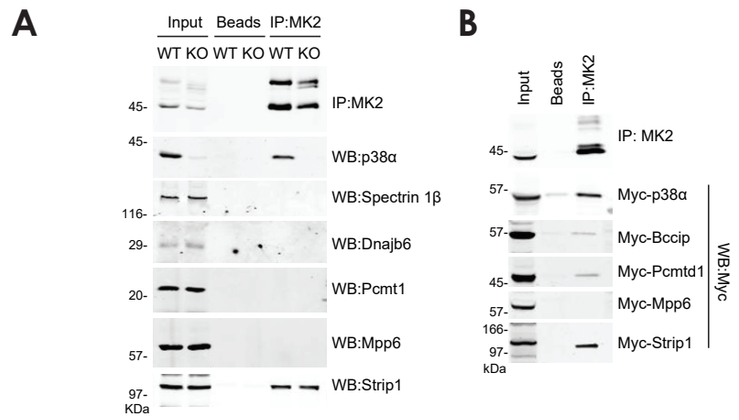


**Figure 41. Validation of putative MK2-interacting partners.** (**A**) WT and p38α KO breast cancer fibroblasts were immunoprecipitated with MK2-Trap_A (MK2) or agarose beads (Beads) and analyzed by immunoblotting with the indicated antibodies. (**B**) 293T cells were overexpressed with Myc-tagged protein candidates and immunoprecipitated using MK2-Trap_A (MK2) or agarose beads (Beads). Samples were then analyzed by immunoblot.

## Strip1, a MK2-binding partner with unknown functional implication

Strip1 is a core component of the mammalian striatin-interacting phosphatase and





kinase (STRIPAK) complexes that act through regulation of protein phosphatase 2A (PP2A). In addition to Strip1, members of the germinal center kinase (GCK) and Striatins (STRN) are partners of this macromolecular assembly (Hwang & Pallas, 2014). There is evidence supporting the notion that STRIPAK complexes participate in the regulation of MAPK signaling through direct activation of MAPKKKs (Dan, Watanabe, & Kusumi, 2001). However, little is known about the relationship between Strip1 and MK2 proteins.

According to our data, MK2 is tightly regulated by p38α:MK2 complex dynamics. Upon stimuli, the p38α:MK2 complex separates, leading to MK2 degradation by the proteasome. In parallel, p38α triggers the upregulation of MK2 mRNA so that the cell can recover MK2 protein levels. Since Strip1 was found to interact with MK2, we evaluated the role of Strip1 in MK2 regulation by analyzing the MK2 levels in Strip1-downregulated cells. First, breast cancer fibroblasts were transfected with control siRNA (siCntrl) or siRNA against Strip1 (siStrip1) and were stimulated with UV irradiation for 4 hours. As expected, UV stimuli activated the p38α pathway and induced MK2 downregulation in control cells. However, Strip1-downregulated cells showed similar MK2 degradation (**Figure 42A**). Likewise, BMDMs were electroporated with the siRNAs and then were treated with LPS, but MK2 was similarly downregulated in both control and Strip1-downregulated cells. Moreover, the levels of MK2 protein and mRNA were also restored in both siCntrl and siStrip1 cells (**Figure 42B**). These results suggest that Strip1 does not play a critical role in the regulation of the p38α:MK2 complex dynamics.

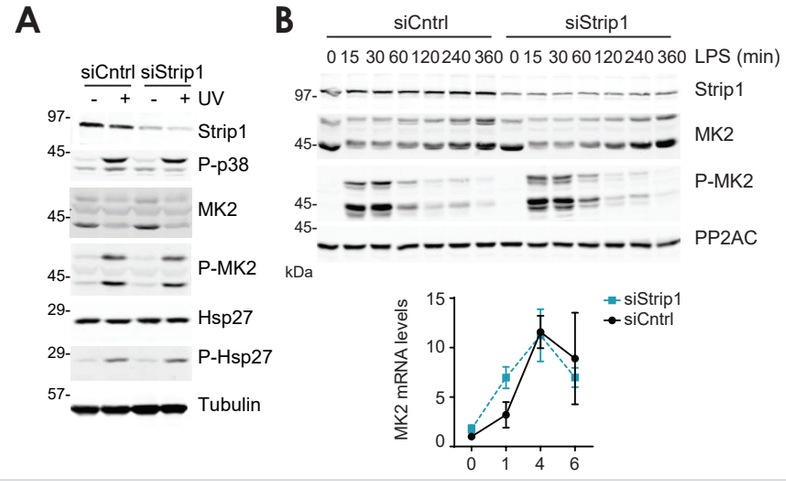


**Figure 42. Strip1 is not involved in the regulation of the p38α:MK2 complex dynamics.** (**A**) Breast cancer fibroblasts were transfected with siRNAs against Luciferase (siCntrl) or Strip1 (siStrip1). Cells were then stimulated with UV light (30 J/m$^2$) for 4 h and lysates were analyzed by immunoblotting. (**B**) BMDMs were electroporated with siCntrl or siStrip1. Cells were then starved for 17 h and stimulated with LPS (10 ng/ml) for the indicated times. Lysates were analyzed by immunoblotting. RNA samples were collected at the indicated times. MK2 mRNA levels were determined by qRT-PCR and were referred to the expression level in the non-treated cells (time 0), which was given a value of 1. No significant differences were found between samples. Statistical analysis was calculated between siCntrl and siStrip1 cells. Data are mean ± SEM, n= 3.

One of the best characterized functions of MK2 is the regulation of proinflammatory cytokine expression upon LPS stimulation. MK2 regulates the stability and translation of mRNAs through phosphorylation of TTP. TTP recognizes adenosine and uridine (AU)-rich elements (ARE), which are located in the 3' untranslated region of mRNAs, eventually leading to transcript decay (Brooks & Blackshear, 2013). Phosphorylation by MK2 increases TTP interaction with 14-3-3 proteins, thus interfering with TTP binding to target mRNAs (Gaestel, 2006) and enhancing gene expression. Of note, TTP dephosphorylation through the PP2A phosphatase plays a key role in this process (Sun et al., 2007). Since Strip1 is a member of STRIPAK complex, which contains PP2A and was found to be a putative binding partner of MK2, we examined the role of Strip1 in MK2/TTP-mediated cytokine expression. Given that TNFα, IL6 and CXCL2 are regulated by the MK2/TTP axis (Gaestel, 2006) (Brooks & Blackshear, 2013), we analyzed the expression of these mRNAs upon Strip1 downregulation. Despite the promising correlations, our results showed no differences between control and Strip1-downregulated cells (**Figure 43**), thereby suggesting that Strip1 is not implicated in the MK2/TTP regulation of cytokine expression. Further work will be needed to characterize the potential role of Strip1 in other MK2-mediated functions.

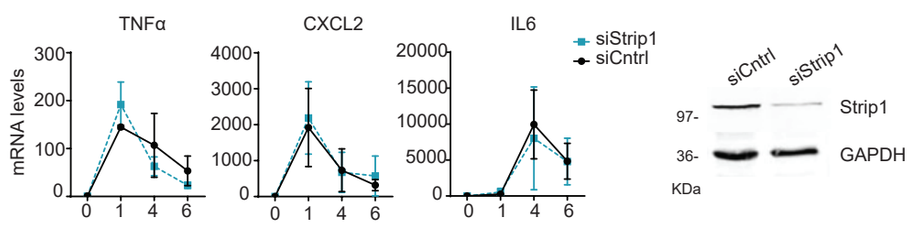


**Figure 43. Strip1 is not involved in MK2-regulated cytokine expression.** BMDMs were electroporated with siRNAs against Luciferase (siCntrl) or Strip1 (siStrip1), starved for 17 h and stimulated with LPS (10 ng/ml) for the indicated times. Lysates were analyzed by qRT-PCR (Right). Data are mean ± SEM, n= 3. Strip1 downregulation was analyzed by immunoblotting (Left).

## Analysis of p38α- kinase independent functions *in vivo*

As a kinase, p38α has been characterized mainly by its capacity to regulate a range of cell responses by phosphorylating many substrates. In addition to our results showing the regulation of the p38α:MK2 complex by a p38α-scaffolding function, some reports have previously proposed that p38α regulates particular functions in a kinase-independent manner (Fan et al., 2005) (Chou et al.,2001). These reports support that p38α docking interactions regulate cellular functions. To further study the contribution of p38α scaffolding functions *in vivo*, we generated mice expressing kinase-dead p38α (p38α KD) by mutating Lysine 53 (K53M), which is essential for ATP binding of p38α





(See methods ***Generation of p38α kinase dead mice***).

### Characterization of p38α KD mice

One of the first phenotypes observed in mice lacking p38α was embryonic lethality due to placenta defects (Adams et al., 2000). We found that $p38\alpha^{KD/KD}$ embryos were embryonic lethal, thereby indicating that p38α activity was required for placental morphogenesis (**Figure 44A**). To confirm that p38α activity was disrupted biochemically, MEFs from $p38\alpha^{KI/KI}$ embryos were immortalized and treated with Tat-Cre protein to induce p38α KD expression. Cells were then stimulated with UV irradiation to induce p38α kinase activation and were analyzed by immunoblotting. The levels of phosphorylated Hsp27, a substrate of MK2, were lower in Tat-Cre treated MEFs compared to non-treated cells (**Figure 44B**), consistent with the idea that p38α kinase activity was impaired in those cells.

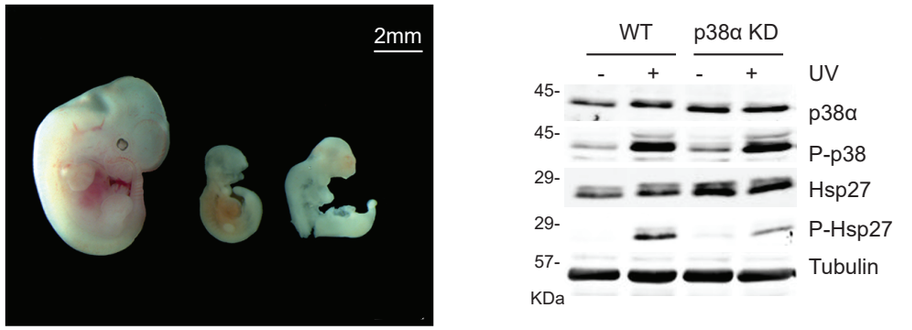


**Figure 44. Validation of p38α KD-expressing mice.** (**A**) Wild-type and $p38\alpha^{KI/KI}$ Sox2-Cre E11.5 embryos are shown. Scale bar 2 mm. (**B**) Immortalized $p38\alpha^{KI/KI}$ MEFs were treated with Tat-Cre (60 µg) and stimulated with UV light (30 J/m²) for 1 h. Lysates were analyzed by immunoblot with the indicated antibodies.

### p38α regulates breast tumor progression in a kinase-dependent and -independent manner

Since p38α KD mice were embryonic lethal, we turned our attention to the role of potential p38α scaffolding functions in a tumor context, using an inducible CRE recombinase. Our group recently demonstrated the importance of p38α for PyMT-induced mammary tumor progression. While PyMT WT mice showed continuous tumor growth, p38α KO littermates showed reduced tumor sizes as a result of less proliferation and impaired DNA replication (Cánovas et al., 2018). Interestingly, another study has proposed that p38α regulates the mitotic progression of some cancer cell lines in a kinase-independent manner (Fan et al., 2005).
To address the kinase-independent roles of p38α in breast tumorigenesis, we generat-

ed mice with PyMT, UBC-Cre-ERT2 (UbCre) and p38α$^{KI/KI}$ alleles. Moreover, we used mice with PyMT, UBC-Cre-ERT2 (UbCre) and p38α$^{lox/lox}$ as controls (Cánovas et al., 2018). Once the mammary tumors were formed, p38α$^{KI/KI}$;UbCre and p38α$^{lox/lox}$;UbCre mice were treated with 4-OHT to induce Cre activation and either expression of p38α KD (p38α$^{KI/KI}$) or p38α deletion (p38α$^{lox/lox}$). As expected, a progressive regression in the size of mammary tumors upon induction of the p38α KO was observed (**Figure 45A**) (Cánovas et al., 2018). Interestingly, when p38α KD expression was induced, tumor size shrank less than in p38α KO mice (**Figure 45A**). To confirm that p38α signaling was abrogated in p38α KD tumors, we analyzed p38α activity by detecting the phosphorylated levels of downstream substrates. As expected, the p38α pathway was activated in WT tumors but not in p38α KD tumors (**Figure 45B**). In agreement with the reduced tumor size, we observed decreased cell proliferation, as determined by Ki67 and phospho-H3 staining, in p38α KD tumors compared to WT tumors (**Figure 45C**). However, this decrease was not as pronounced as reported in p38α KO tumors (Cánovas et al., 2018). These results suggest that PyMT-induced tumor progression is mediated by a p38α-scaffolding function, although it also clearly requires p38α activity.

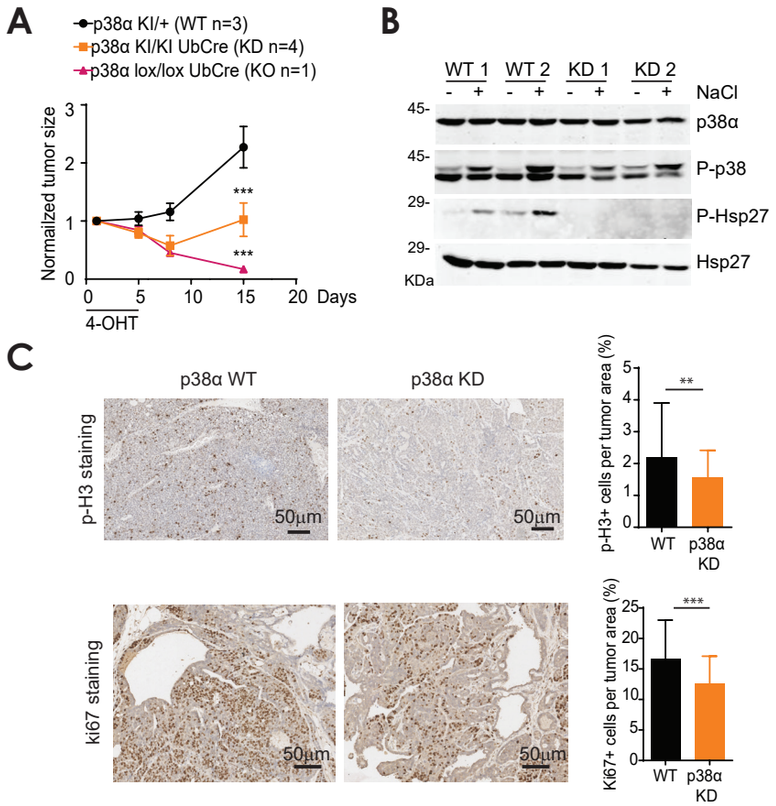






**Figure 45. p38α KD mice showed impaired tumor progression but to a lower extent than p38α KO mice.** (**A**) Mammary tumor growth in MMTV-PyMT mice. Measurements were normalized to the initial tumor size. Statistical significance was performed between either p38α$^{KI/KI}$ UbCre or p38α$^{lox/lox}$ UbCre and p38α$^{KI/+}$. (**B**) Tumors from p38α$^{KI/KI}$ and p38α$^{KI/KI}$ UbCre mice were isolated and treated or not with NaCl (300 mM) for 15 min to activate the p38α pathway, as indicated. Lysates were analyzed by immunoblotting. (**C**) Representative Ki67 and phospho-H3 stainings in tumors at day 15. Scale bars, 50 μm. Histograms show the quantification of Ki67$^+$ and phospho-H3$^+$ areas (WT, n=3; KD, n=3); at least ten fields per tumor were analyzed. Statistical significance was calculated between WT and p38α KD or p38α KO samples.

To further characterize the contribution of p38α catalytic activity in tumor progression, we isolated epithelial cancer cells from the mammary tumors. We initially obtained primary cultures from p38α$^{KI/KI}$ and p38α$^{KI/KI}$ UbCre tumors and confirmed their epithelial origin (**Figure 46A**). Moreover, we corroborated that 4-OHT efficiently induced Cre activation and impaired p38α kinase in cells (**Figure 46B**). We then used tumor-derived cancer cell lines (p38α$^{KI/KI}$, p38α$^{KI/KI}$;UbCre and p38α$^{lox/lox}$;UbCre) to analyze cell proliferation by 5-Bromo-2'-deoxyuridine (BrdU) incorporation. We observed that 4-OHT treatment did not affect the proliferation rate of p38α$^{KI/KI}$ control cells. Interestingly, p38α$^{KI/KI}$;UbCre cells treated with 4-OHT showed reduced proliferation but to a lower extent than p38α$^{lox/lox}$;UbCre cells (**Figure 46C**). This result phenocopied the *in vivo* effect, thus supporting the notion that p38α contributes to cell proliferation in both a kinase-dependent and -independent manner.

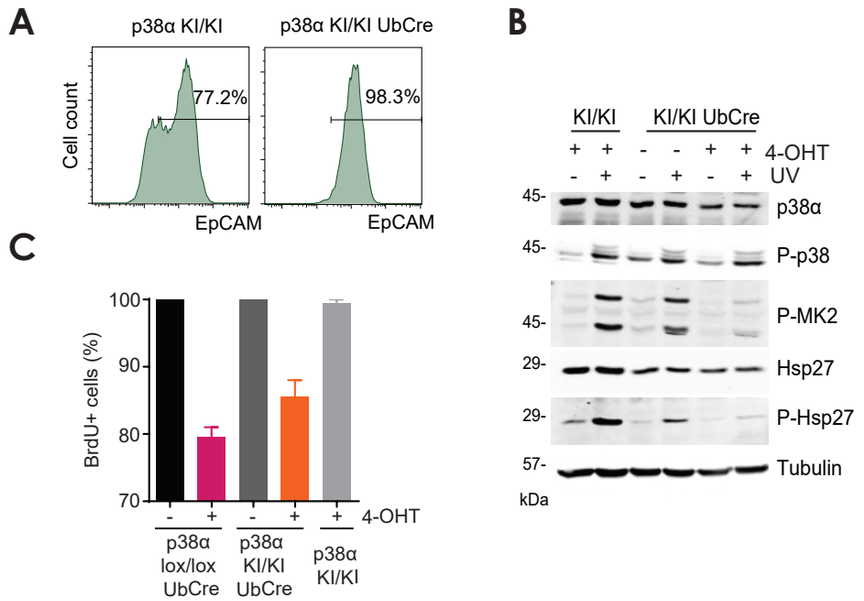


**Figure 46. p38α KD cancer cells showed reduced proliferation but to a lower extent than p38α KO cells.** (**A**) Cells from p38α$^{KI/KI}$ PyMT and p38α$^{KI/KI}$ UbCre PyMT mice were isolated, immortalized and evaluated for epithelial status using the indicated antibodies and a Galios Flow cytometer. (**B**) Cells were treated with 4-OHT and stimulated with UV light (30 J/m$^2$). Lysates were analyzed by immunoblotting. (**C**) BrdU uptake. Histograms represent the quantification of two independent experiments. Data are mean ± SEM, n= 2.

Given that p38α regulates the p38α:MK2 complex by docking interactions, we validated the presence of MK2 protein in p38α KD mouse tissues. In agreement with previous data, the levels of MK2 were maintained in p38α WT and KD animals but were downregulated in the absence of p38α (**Figure 47**). These observations suggest that the p38α:MK2 complex would be stable in p38α KD mice. The fact that MK2 protein is present in p38α KD mice but not in p38α KO mice could have implications for the observed phenotypes.

Although the molecular determinants that control mammary tumor progression in a p38α- kinase independent manner remain to be elucidated, we have established *in vivo* and *in vitro* models to further explore this phenotype.

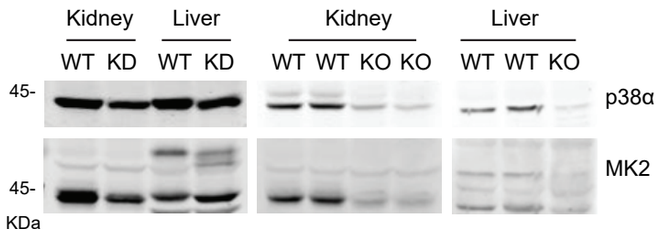


**Figure 47. Tissues from p38α KD mice showed maintained MK2 protein levels.** Tissue lysates from WT, p38α KD and p38α KO mice were analyzed by immunoblotting with the indicated antibodies.

# Discussion

Protein kinases mediate cellular functions via phosphorylation of multiple substrates. Besides the catalytically active kinase domains, protein kinases often have the ability to recognize a specific set of unique protein partners, including substrates and regulators. Therefore, the scaffolding roles of protein kinases contribute to orchestrate efficient and specific phosphotransfer reactions. However, studies over recent decades have indicated that scaffolding functions not only support phosphorylation but also regulate key cell functions *per se* (Good et al., 2011). The non-catalytic functions of kinases are involved in the allosteric regulation of enzymes, in the assembly of signaling components, and in the regulation of transcription by binding to transcription factors or directly to DNA (Kung & Jura, 2016). Despite increasing interest in the phosphorylation-independent roles of kinases, there is still a large number of protein kinases with uncharacterized phosphorylation-independent functions.
Here we have studied kinase-independent functions of p38α by looking for new interacting partners, characterizing its association with MK2, and generating a p38α-kinase dead mouse model.

## Docking determinants for the recognition of p38α interactors

A key mechanism through which non-catalytic functions are achieved is through protein-protein interactions (Langeberg & Scott, 2015). For example, ERK2 regulates the activity of the dual-specificity phosphatase MKP3 through direct binding. Upon interaction, ERK2 triggers a conformational change in the MKP3 catalytic domain leading to ERK2 dephosphorylation. Interestingly, an ERK2 kinase dead mutant activates MKP3 to the same extent as the ERK2 WT protein (Camps et al., 1998). Another example is the prevention of N-Myc degradation by its binding to Aurora A kinase. N-Myc is degraded through its interaction with the SCF ubiquitin ligase, but the binding to Aurora A prevents its degradation even in the presence of Aurora A inhibitors (Otto et al., 2009). These two examples highlight the importance of protein-protein interactions for the functions of protein kinases.
p38α is thought to use mainly transient enzyme-substrate interactions to phosphorylate downstream partners. However, in some cases, this kinase also interacts with substrates and regulators through auxiliary docking surfaces. The most important docking site of p38α consists of a hydrophobic docking groove and a negatively charged CD region (Tanoue & Nishida, 2003). Target proteins use positively charged short linear motifs (D-motifs) to recognize and interact with the p38α docking regions. Since one of the goals of our study was the identification of new scaffolding partners for p38α, we started by selecting proteins whose structures contain linear D-motifs and then analyzed their interaction with p38α. Curiously, only known interactors (MK2 and PTPN7) were

found to bind to p38α in a stable manner (**Figure 14**). Using PLA experiments, we have also identified CDO1, FKBP8 and NCF1 as putative transient interactors, but only the known substrate NCF1 was found to be directly phosphorylated by p38α in kinase assays (**Figure 16**). Since PLA is based mainly on the identification of co-localizing proteins, we propose that CDO1 and FKBP8 proteins interact with p38α in an indirect manner. In fact, it has been described that CDO1 interacts directly with the scaffold protein JLP (JNK-associated leucine zipper protein), and with p38α and p38β proteins via JLP(Takaesu et al., 2006). This indirect interaction between CDO1 and p38α through JLP might explain why CDO1 is not phosphorylated in the kinase assay. In a second screening, we considered 15 motifs that belong to distinct MAPK partners (**Table 17**). We re-defined D-motifs on the basis of the type of docking motifs present in the MAPK groups; however, we were still unable to identify new strong interactors for p38α.

To date, attempts to predict MAPK-binding proteins have used the generic consensus of D-motifs as established more than a decade ago (Sharrocks et al., 2000) (Tanoue & Nishida, 2003). However, despite using extensive alignments and predictions, the success rate was low due to high sequence degeneration in the linear motif. In fact, peptides containing classical D-motifs from specific MAPK-protein partners have been reported to bind non-specifically to p38, JNK and ERK, thereby indicating the limitations of considering simple D-motif mediated interactions (Garai et al., 2012). Accordingly, the following requirements for MAPK binding have been proposed. On the one hand, to ensure proper binding, several MAPK partners that contain classical D-motifs often need other structures, such as the residues that flank the phospho-acceptor site (DEF pockets or FxF motifs) (Tzarum et al., 2013). On the other hand, MAPKAPK substrates recognize their upstream kinases (p38, ERK or both) using reverse D-motifs (RevD-motifs) which comprise different H-bond staples that affect MAPKAPK conformation and binding (Garai et al., 2012). Overall, these studies suggest that besides the simple pattern matching of D-motifs, other features, such as the structural compatibility to the p38α docking groove, should be used to define new p38α interactors in a more reliable manner. In fact, a recent study used a similar approach to identify novel MAPK docking partners. D-motifs were classified using a coherent structural model and analyzed by FoldX structural-based scoring, and the new hits identified were validated using a kinase assay and low affinity protein-protein interaction methods (Zeke et al., 2015).

Since we were interested in identifying new p38α scaffolding functions and MK2 is a well-known partner of p38α, we used the MK2 RevD-motif structure to score the human proteome. Interestingly, PTPRQ, PIK3CD, PRDM16 and SMG1 proteins were identified as high confident interactors for p38α (**Figure 18**). Given that putative homologs were found to interact with p38α in other species (Kim et al., 2012) (Aronova et al., 2007) (Costanzo et al., 2016) (Kusari et al., 2004) we propose that these proteins are potential interactors for p38α and as such interesting candidates for further validation.







Overall, we hypothesize that the strategy based on the MK2 RevD-motif structure will increase stringency in the consensus sequence, as we considered both the length and the amino acid composition of the D-motif intervening regions.

## Importance of docking interactions in the p38α: MK2 complex

Given that we wanted to study the scaffolding function of p38α through RevD-motif binding, we chose the MK2 substrate as a model.

As aforementioned, MK2 recognizes the p38α docking groove through its RevD-motif located in the C-terminal part of the protein (White et al., 2007). In addition to the consensus MK2 RevD-motif, other MK2 residues have been found to be evolutionarily conserved in most vertebrate homologs (Garai et al., 2012), thereby suggesting that other residues can fine-tune the conformation of the intervening regions between anchor points, hence increasing binding specificity. Accordingly, our results identified R136 as an additional residue of p38α implicated in the binding to MK2 *in vitro* (**Figure 25**). This finding suggests that residues other than the established p38α docking motif also participate in the formation of tight interactions between the two kinases.

The complexity of the docking surface leads us to speculate that the interaction between p38α and MK2 has evolved to ensure proper functioning. Firstly, as the C-terminal region of MK2 is partially unstructured (Underwood et al., 2003), the binding to p38α might cause a disordered-to-ordered transition in MK2 which may be assisted by features located on both the p38α docking groove and the MK2 RevD-motif. Secondly, structural studies have shown that the MK2 RevD-motif bound to phosphorylated p38α, acts as a positive allosteric modulator of the kinase reaction enhancing ATP loading, substrate binding and phosphorylation (Tokunaga et al., 2014). In this regard, the formation of the p38α:MK2 complex would maximize the efficiency of the reaction, allowing a rapid and full activation in response to stimuli.

## p38α pathway activity is controlled by the dynamics of the p38α:MK2 complex

The concept that p38α and MK2 act as an enzyme-substrate complex is well known. The reduced levels of either p38α or MK2 in cells that are deficient in the other interacting partner suggest that the two proteins need each other for their own stabilization (Ben-Levy et al., 1998)(Kotlyarov et al., 2002)(Sudo et al., 2005)(White et al., 2007) (Lopez-Aviles et al., 2008). However, most of these studies used purified or overexpressed proteins and the behavior of endogenous proteins was not addressed. Our results indicate that endogenous p38α and MK2 are downregulated in the absence of their complex

partner, or when interfering with docking-mediated interactions.

Structural studies proposed that the high affinity between p38α and MK2 combined with the disposition of the monomers in the complex would make the interface of the heterodimer inaccessible to substrates (Lukas et al., 2004)(ter Haar et al., 2007). However, stress signals are known to induce the activation of the two kinases, and the phosphorylation of their respective substrates. This issue has been addressed by controversial studies. On one hand, some reports propose that the enzyme-substrate assembly remains stable even after p38α and MK2 phosphorylation and phosphorylation of substrates depends on the protein assembly (Ben-Levy et al., 1998)(A. Kotlyarov et al., 2002). On the other hand, studies done in fission yeast or with purified recombinant mammalian proteins indicate that phosphorylation decreases the affinity of the two kinases (Lukas et al., 2004) (Lopez-Aviles et al., 2008). Herein, we confirm that phosphorylation of endogenous p38α and MK2 leads to complex separation in mammalian cells, thus making the two protein kinases available for other targets.

At the molecular level, p38α activation requires both dual phosphorylation of the TGY-motif in the activation loop and ATP binding. The activation loop phosphorylation has been perceived as the trigger for the conformational change necessary for ATP binding (Kuzmanic et al., 2017). The structural changes associated with p38α activation together with the phosphorylation of MK2 probably contribute to the release of MK2 from p38α.

There is good evidence implicating the p38α pathway in the regulation of many cellular processes, including inflammation, proliferation and cell death. Accordingly, aberrant activation of this signaling pathway has been linked to many diseases (Cuenda & Rousseau, 2007)(Yasuda et al., 2011). Therefore, the extent of pathway activation must be strictly controlled in order to ensure cell homeostasis. Protein phosphatases are responsible for returning active kinases to their basal state. Thus, the intensity and duration of the activation of a signaling pathway would be regulated by the abundance and activity of relevant phosphatases (Bhalla et al., 2002). Genes encoding about 530 kinases and 180 phosphatases have been identified in the human genome, thus indicating that most phosphatases target several kinases, sometimes a large number of them. Moreover, additional mechanisms such as protein degradation can also control the extent of signaling pathway activation (Hershko et al., 2000). The inactivation of p38α by several types of phosphatases has been broadly studied (Caunt & Keyse, 2013)(Cuadrado & Nebreda, 2010), but very little is known about MK2 dephosphorylation. Our results indicate that MK2 undergoes protein degradation relatively soon after activation (**Figure 26** and **Figure 30**), thereby suggesting that activity of MK2 is regulated mainly by proteolysis and probably phosphatases do not play a major role.

The degradation of proteins is usually achieved by autophagy or by the UPS. The UPS relies on protein ubiquitination mediated by E3 ubiquitin ligases, which provide substrate specificity. More than 600 different E3 ligase have been described in humans







(Morreale & Walden, 2016), however, many are poorly characterized, particularly with respect to the individual substrates that they can target. Our results implicate the E3 ligase MDM2 in the MK2 degradation process (**Figure 34**). MDM2 is mainly known to ubiquitinate p53 controlling its expression levels (Haupt et al., 1997). The stabilization of p53 by certain types of stresses such us UV involve MDM2 phosphorylation, which then auto-ubiquitinates and is degraded by the proteasome (Stommel & Wahl, 2004). The ability of MDM2 to ubiquitinate itself in these conditions indicates that it retains the E3 ligase activity per se. Moreover, stabilized p53 induces transcription of the MDM2 gene (Kruse & Gu, 2009), suggesting that the MDM2 levels are restored in UV-stimulated cells, and MDM2 could target other proteins. In fact, MDM2 has been reported to regulate the degradation of other proteins besides p53, such as HUWE1, NUMB or IRF-2 (Kurokawa et al., 2013)(Pettersson et al., 2009)(Sczaniecka et al., 2012). Interestingly, MK2 can phosphorylate MDM2 modulating the extent and the duration of the p53 response (Weber et al., 2005). However, our results show that MK2 inhibition does not affect MK2 degradation, suggesting that MDM2 phosphorylation by MK2 is unlikely to be involved in the process. Further investigations are needed to elucidate how MDM2 regulates MK2 degradation.

The activity of the p38α signaling pathway is tightly controlled by multiple mechanisms, including several feedback loops. For example, p38α can negatively regulate upstream activators such as MKK6 at the expression level (Ambrosino et al., 2003) or TAK1 through the phosphorylation levels of its regulator TAB1 (Cheung et al., 2003), and can also induce the expression of phosphatases such as MKP1 (Hu et al., 2007). Our data suggest a new mechanism of regulation based on the dynamics of the p38α:MK2 complex.

Thus, in homeostatic conditions, MK2 is bound to p38α, which ensures proper activation of p38α and facilitating the concomitant activation of MK2, as both kinases are known to co-regulate several cellular processes such as cell cycle regulation and mRNA stability (Gaestel, 2015). In response to weak stimuli that induce transient pathway activation, p38α and MK2 are phosphorylated, reducing their binding affinity and leading to complex separation. Once dissociated, the two active kinases can phosphorylate their relevant substrates, which will in turn mediate the pathway functions. However, the phosphorylated MK2 protein unbound to p38α has low stability and is targeted by the MDM2 ubiquitin ligase for its degradation by the 26S proteasome, thereby ensuring a limited activation. The inactivation of p38α, occurs mainly by de-phosphorylation. Before its inactivation, p38α triggers the upregulation of MK2 mRNA, probably at the transcriptional level, and the cell recovers the levels of MK2 protein, which bind to the unphosphorylated p38α forming a heterodimer again (**Figure 48A**). However, under persistent stimuli, p38α and MK2 remain phosphorylated and unbound longer, thereby reducing their protein stability and thus impairing complex formation and the restoration of the basal state (**Figure 48B**).

We speculate that this mechanism could be interpreted by the cell as a sign of irreversible damage, thus facilitating the occurrence of cell death.

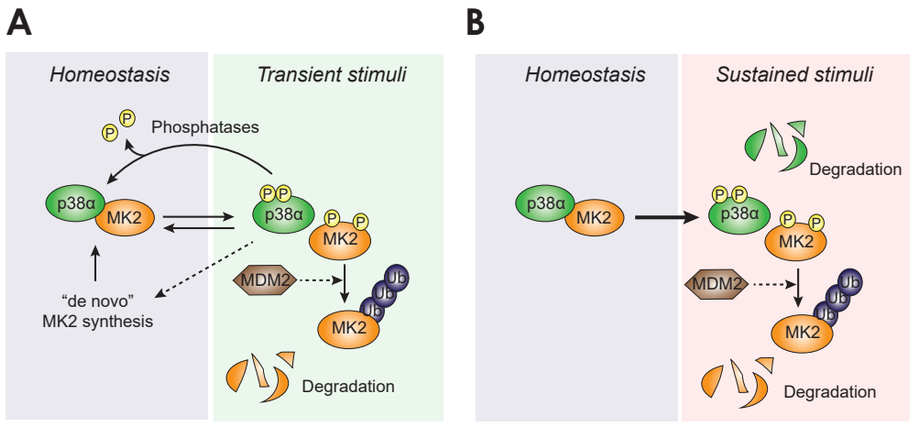


**Figure 48. Proposed model for p38α:MK2 complex dynamics.** In homeostasis, p38α and MK2 proteins form a complex mediated by docking interactions. (**A**) After stimulation by agents such as LPS that transiently activate p38α, the two proteins become phosphorylated and separate from each other, leading to MK2 ubiquitination and degradation by the 26S proteasome. MDM2 controls MK2 degradation. At later times, there is de novo MK2 re-expression in a p38α dependent manner. In parallel, p38α is dephosphorylated by phosphatases and both proteins would form a complex again. (**B**) Stimuli that induce persistent p38α activation result in sustained phosphorylation of both p38α and MK2, which remain unbound and are eventually degraded. Therefore, the complex is unable to form to recover the steady state.

Taking into account this model, new strategies can be used to design p38α-specific inhibitors. In fact, instead of competing with ATP binding, several molecules have been reported to target the p38α docking groove, thus interfering with docking-dependent substrates such as MK2 (Davidson et al., 2004) (Willemen et al., 2014) (Shah et al., 2017). For example, CMPD1 uses this mode of action, preventing the formation of the p38α:MK2 complex and inhibiting MK2 phosphorylation. However, long term treatment with CMPD1 maintains p38α and MK2 unbound, resulting in the downregulation of both proteins (**Figure 39**). This observation would indicate that, by triggering p38α downregulation, CMPD1 loses its proposed specificity of selectively inhibiting MK2. In agreement, it has been described that CMPD1-induced cytotoxic activity in glioblastoma cells is independent of MK2 (Gurgis et al., 2015). This observation would suggest that p38α downregulation is a side effect of this compound.
Recently, a new p38α inhibitor (CDD-450) was reported to selectively bind to and inhibit the p38α:MK2 complex. CDD-450 targets the unique binding surfaces formed between p38α and MK2, stabilizing the complex and preventing MK2 activation (Wang et al., 2018). This approach emphasizes the importance of the dynamics of the complex conformation for proper activation of the signaling pathway. Interestingly, CDD-450 does not impair the activation of other p38α substrates such as ATF2, suggesting that other proteins can be phosphorylated either by monomeric p38α or by the p38α in the







complex using transient interactions through the phosphoacceptor site.
In addition to MK2, other proteins, such as MEF2A and MKK3, are known to interact with p38α through docking interactions (Chang et al., 2002)(Tanoue et al., 2001). Moreover, in certain situations, p38α can be activated by an alternative pathway that leads to autophosphorylation induced by TAB1 binding (Ashwell, 2006). Given that docking interactions are a common mechanism for the binding of different MAPK partners, the existence of other p38α protein complexes should be considered. Since our results show a faster degradation of MK2 than of p38α upon complex separation, we hypothesize that p38α interacts with other proteins that help to stabilize it and avoid its degradation. Alternatively, maybe de-phosphorylation helps to stabilize the p38α protein.

In summary, we propose that complex formation between MK2 and p38α plays an important role in the regulation of this signaling pathway, which not only helps to synchronize the timely activation of the two kinases but also provides a mechanism through which cells can interpret the strength of the stimuli and modulate the extent of pathway activity output.

## Functional relevance of p38α:MK2 complex dynamics

Our model allows a better understanding of different functions attributed to p38α and MK2 signaling. For example, the modulation of their subcellular localization is controversial (Ben-Levy et al., 1998)(Gaestel, 2006)(Gong et al., 2010). It was proposed that activation of MK2 leads to the exposure of its nuclear export signal (NES) and that the p38α:MK2 complex translocates from the nucleus to the cytosol (Ben-Levy et al., 1998) (Gaestel, 2006). However, other studies claim that p38α shuttles from the cytoplasm to the nucleus in response to several stimuli, in a p38α phosphorylation-dependent but MK2-independent manner, while nuclear export depends on p38α dephosphorylation using phosphorylated MK2 as a carrier (Gong et al., 2010). Our model indicates that both proteins need to be unphosphorylated to form a complex, thereby suggesting that they should be initially located in the same subcellular compartment. In fact, we observed that under basal conditions both proteins are in the cytoplasm (**Figure 40**). Interestingly, a different localization pattern is observed when the two kinases are expressed alone (**Figure 40**). p38α is still found in the cytoplasm, whereas MK2 shuttles into the nucleus. We hypothesize that the formation of the p38α:MK2 complex buries the C-terminal region of MK2 containing the MK2-NLS and MK2-NES sequences, and therefore controlling the MK2 subcellular localization. Although the localization of p38α and MK2 in response to stimuli still needs to be evaluated, we propose that, upon activation these two kinases dissociate from each other resulting in MK2 degradation.

This dissociation would facilitate the shuttling of p38α to the nucleus by other proteins such as exportins or microtubule- and dynein-associated molecules (Gong et al., 2010). After stimulation, the two kinases would return to their basal state, allowing the formation of a stable complex again (**Figure 49**).

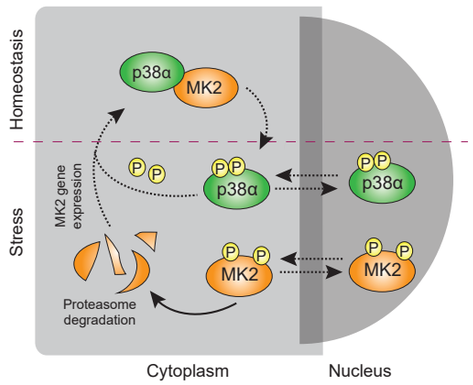


**Figure 49. Proposed model for the p38α:MK2 shuttling.** At resting conditions both kinases are bound together in the cytoplasm. Upon stimuli they separate to each other and can in turn translocate to de nucleus. MK2 phosphorylation leads to MK2 degradation. After stimulation both proteins will form a complex again.

In addition to its participation in regulating their subcellular localization, the p38α:MK2 complex may be involved in other processes. It is now becoming clear that protein-protein-protein interactions induce conformational changes that allow catalytic activity of enzymes or expose new structural surfaces that are important for cell signaling (Langeberg & Scott, 2015). In fact, it has been proposed that p38α and MK2 associate with RIPK1 in cytoplasmic complexes that mediate RIPK1 kinase-dependent cytotoxicity (Menon et al., 2017). This proposal suggests that the p38α:MK2 assembly could regulate other protein partners via scaffolding. Our data based on mass spectrometry analysis (**Supplementary Table 5**) identified Strip1 as a bona-fide MK2 interactor at endogenous levels (**Figure 41**). However, Strip1 apparently interacts with MK2 in a p38α independent manner, suggesting that the formation of the p38α:MK2 complex is not necessary for the interaction of Strip1 with MK2. Although the relevance of Strip1 for MK2-mediated functions remains to be determined, we hypothesize that Strip1 modulates some MK2 functions. Strip1 was recently shown to regulate cell migration in both mouse embryo development and in cancer cells (Bazzi et al., 2017) (Madsen et al., 2014). Since the p38α pathway also contributes to the regulation of cell migration through several mechanisms, including MK2-dependent phosphorylation of Hsp27, it would be pertinent to addres whether the interaction between Strip1 and MK2 regulates cell migration.







## Generation of p38α kinase dead mice

Besides the regulation of the p38α:MK2 complex, other p38α-kinase independent functions have been identified. Specifically, one study suggests that p38α regulates mitotic progression in a kinase-independent manner (Fan et al., 2005). To further investigate new p38α functions independent of its kinase activity, we generated a p38α KD mouse model. Interestingly, our group has recently reported that the absence of p38α impairs cancer cell proliferation and enhanced cell death halting mammary tumor progression (Cánovas et al., 2018). The use of chemical inhibitors indicated the contribution of the p38α kinase activity in this phenotype, however, our data shows that tumor progression is also partially impaired by the expression of kinase dead p38α, thus suggesting that mammary cancer cell proliferation is regulated by p38α both in kinase-dependent and independent manners. In agreement with our observations, MK2 protein levels are not downregulated in p38α KD animals (**Figure 47**), suggesting that p38α forms a stable complex with MK2 in p38α KD mouse tissues *in vivo*. The presence of p38α and MK2 in p38α KD mice (but not in p38α KO mice) may explain the differences observed in cancer cell proliferation between p38α KD and p38α KO tumors. Interestingly, mass spectrometry analysis and preliminary results in overexpressed 293T cells identified Bccip protein as a MK2 interactor (**Supplementary Table 5** and **Figure 41**). Bccip was found to be a BRCA2 and p21-interacting protein, and it has been identified as an important cofactor for BRCA2 in breast tumor progression (Liu et al., 2001). Specifically, depletion of Bccip in cancer cell lines leads to disoriented mitotic spindles, chromosome congression defects and delayed mitotic progression (Huhn et al., 2017). Accordingly, similar phenotypes were observed in tumors lacking the p38α protein (Cánovas et al., 2018). Since MK2 is stable in p38α KD mice but not in p38αKO animals, it is possible that p38α-mediated MK2 stabilization regulates Bccip-dependent cell functions to some extent. This hypothesis would contribute to the identification of a new p38α-kinase independent function through MK2 stability and consequently through the regulation of Bccip protein.

Overall, our results support the notion that p38α scaffolding domains are involved in breast tumor progression. Although more research is required to identify the underlying mechanisms, we have established new mouse and cell models that are expected to facilitate the characterization of these functions.

# Conclusions

- The D-motif sequence alone is not sufficient to identify stable interactors of p38α.

- p38α and MK2 form a stable complex *in vivo*, which is mediated by docking interactions through the p38α-CD domain and other residues such as Arg136.

- Phosphorylation of p38α and MK2 triggers complex separation.

- Dissociation of the p38α:MK2 complex upon p38α activation leads to MK2 degradation by the proteasome.

- The extent and duration of p38α activation determines the fate of p38α and MK2 proteins.

- The regulation of mammary tumor growth by p38α may involve a kinase-independent function.

# Supplementary Material

**Supplementary Table 1 | A. p38α putative physical interactors from information available in databases.** PMID number refers to the manuscript ID. Detection methods: AC: Affinity chromatography, PD: Pull down, TAP: Tandem affinity purification, Y2H: Yeast two hybrid, ES: Enzymatic study, KA: Kinase assay, IP: Immunoprecipitation, PLA: Proximity ligation assay, PA: Phosphatase assay and EID: Experimental interaction detection.

| Physical Interactor | PMID | Detection Method | Physical Interactor | PMID | Detection Method | Physical Interactor | PMID | Detection Method |
|---|---|---|---|---|---|---|---|---|
| Atf6 | 21131360 | AC | Marcksl1 | 23602568 | TAP | Supt20h | 20936779, 19893488, 16751104, 21988832 | IP, Y2H |
| Atm | 17172861 | AC | Max | 7479834, 25241761 | PLA | Flna | 20936779 | Y2H |
| Btrc | 20797629, 23532963 | AC | Maz | 23602568 | TAP | Tcf3 | 15719023 | AC |
| Cbl | 9434624, 19635790 | AC | Neb | 23602568 | TAP | Ubc | 21139048, 21890473, 24816145, 22053931, 21963094 | AC |
| Ccdc8 | 23602568, 23455922 | TAP | Nfatc4 | 11997522, 25241761 | PLA | Ugt2b1 | 21988832 | Y2H |
| Cebpb | 21847090 | AC | Nfkbia | 20797629 | AC | Usp11 | 23602568 | TAP |
| Cnbp | 23602568 | TAP | Obsl1 | 23602568, 23455922 | TAP | Vav1 | 9064344 | AC |
| Creb1 | 23532963, 11377386 | AC | Pak6 | 21900206 | Y2H | Atf2 | 11259586, 9305639, 14499342, 9155018, 9707433, 17380123, 9235954, 7535770, 15569672, 12110590, 10708586, 10581204, | KA, PD |
| Csnk2b | 20797629 | AC | Pdx1 | 23331010 | AC | Krt8 | 9211903, 11788583 | EID |
| Cul7 | 23455922 | TAP | Phc2 | 21675959 | AC | Mknk1 | 11157753, 23602568, 23455922, 9155018, 20936779 | IP, EID, Y2H, TAP |
| Dlg1 | 17187070 | AC | Prkcz | 15665819 | IP | Mef2c | 9069290, 20936779, 10805738 | Y2H, EID |
| Dusp2 | 16288922 | PD | Ptprr | 23932588, 10601328 | PD, PA | Mapkapk2 | 23602568, 9768359, 8846784, 11042204, 7592979, 21675959, 23455922, 25241761, 10581204, 17255097, 21988832 | Y2H, PLA, PD, TAP EID |
| Dusp9 | 21908610 | Y2H, PD | Rela | 21900206 | Y2H | Camkk2 | 20562859 | IP |
| Eef2 | 23602568 | TAP | Ret | 16153436 | | Sp1 | 18419748 | AC |
| Ep300 | 17982102, 21444723 | AC, ES PD | Map2k4 | 12788955, 7716521 | EID, PD | Egfr | 7535770, 23397142 | ES, PLA |
| Ets1 | 22521293 | IP | Rrp1b | 23602568 | TAP | Tgfbr1 | 18758450 | AC |
| Hdac3 | 21444723 | AC | Sele | 9006914 | AC | Pkn1 | 12761180 | IP |
| Ikbkb | 20797629 | AC | Slc9a1 | 11604491 | IP | Mapk1 | 17255949, 21675959, 12697810, 22521293 | IP, CA, PLA |
| Iqgap1 | 23602568 | TAP | Sqstm1 | 10708586 | AC | Mapk3 | 11238443, 21675959, 12697810, 23397142 | IP, CA, PD, PLA |

| Physical Interactor | PMID | Detection Method | Physical Interactor | PMID | Detection Method | Physical Interactor | PMID | Detection Method |
|---|---|---|---|---|---|---|---|---|
| Map2k3 | 7839144, 23602568, 12384504, 12589052, 17255949, 9841871, 20213747, 7750576, 8622669 | TAP, KA, ES, IP | Ccdc97 | 20936779 | Y2H | Eef1a1 | 18624398 | Y2H |
| Map2k6 | 8626699, 16342939, 8622669, 17255949, 17255097, 10347227, 7750576 | EID, KA ES, IP | Ddx26b | 20936779 | Y2H | Epb42 | 18624398 | Y2H |
| Tab1 | 11847341, 12829618, 16648477, 25241761, 12429732, 21900206 | IP, Y2H, PLA | Elmsan1 | 20936779 | Y2H | Gdf15 | 18624398 | Y2H |
| Dusp16 | 11489891, 11359773, 14586399, 12794087, 20936779 | IP,Y2H, EID | Hivep1 | 20936779 | Y2H | Rpl22 | 18624398 | Y2H |
| Dusp1 | 20936779, 25241761, 20347885 | PA, Y2H, EID | Kmt2c | 20936779 | Y2H | Rpl41 | 18624398 | Y2H |
| Dusp10 | 10597297, 20936779, 10391943 | EID | Mef2d | 20936779 | Y2H | Snapin | 18624398 | Y2H |
| Cdc25c | 11333986, 9278512 | EID, ES, PD, | Mknk2 | 23602568, 20936779, 25241761 | Y2H, TAP, PLA | Srsf5 | 18624398 | Y2H |
| Cdc25b | 15629715, 11333986 | ES, EID, PD | Mob3b | 20936779 | Y2H | Arhgap9 | 17284314 | circular dichroism |
| Mapkapk5 | 11157753, 20936779 | IP,Y2H | Nktr | 20936779 | Y2H | Nup153 | 17255949 | PD |
| Rps6ka5 | 11157753, 20936779 | IP, Y2H | Smek1 | 20936779 | Y2H | Cdo1 | 17074887 | IP |
| Rps6ka4 | 10806207, 11157753, 23602568, 9792677 | EID, Y2H, IP, TAP | Sptbn1 | 20936779 | Y2H | Mapkap1 | 17054722 | IP, PD |
| Tp53 | 10581258, 17172861, 21675959, 20213747 | AC, KA, ES | Tcf20 | 20936779 | Y2H | Dusp26 | 16924234 | PD, PA |
| Mapkapk3 | 11157753, 23602568, 8626550, 25241761, 10581204, 23455922 | PD, TAP, PLA, IP, Y2H, PLA, KA, TAP | Zfp142 | 20936779 | Y2H | Arrb1 | 16709866 | IP |
| Ptpn7 | 10415025, 25241761, 10206983 | IP, PLA | Nbr1 | 20616007 | IP | Map3k5 | 16709866 | IP |
| Bicd1 | 21988832 | Y2H | Tsc1 | 20368287 | Y2H, PD | Gstp1 | 16636664 | IP |
| Cep164 | 21988832 | Y2H | Atg9a | 19893488 | IP | Zfp36l1 | 16189514 | Y2H, PD |
| Plg | 21988832 | Y2H | Hnrnpa1 | 19349988 | IP | Fkbp8 | 16169070 | Y2H |
| Tmem63b | 21988832 | Y2H | Nod2 | 19349988 | IP | Ppp2ca | 15569672 | IP |
| Aes | 20936779 | Y2H | Cenpc | 18624398 | Y2H | Irak1 | 15388348 | IP |
| Myef2 | 15111488 | AC | Ccar1 | 15102471 | Y2H | Copb1 | 15102471 | Y2H |
| Ccdc14 | 20936779 | Y2H | Cops5 | 18624398 | Y2H | Tollip | 15388348 | IP, Y2H |



| Physical Interactor | PMID | Detection Method | Physical Interactor | PMID | Detection Method |
|---|---|---|---|---|---|
| Kat2b | 21444723 | AC, ES PD | Sumo2 | 19471022 | AC |
| Mapk11 | 23602568, 21900206 | Y2H, TAP | Tceal1 | 23602568 | TAP |
| Il2rg | 15102471 | Y2H | Dyrk1b | 12384504 | IP |
| Lcp1 | 15102471 | Y2H | Plcb2 | 12054652 | IP |
| Mapk12 | 15102471 | Y2H | Dusp4 | 11387337, 16038800 | IP, PD |
| Mib1 | 15102471 | Y2H | Mapk9 | 15102471 | Y2H |
| Nme2 | 15102471 | Y2H | Prkce | 11139474 | IP |
| Rcn2 | 15102471 | Y2H | Akt1 | 23397142, 11042204 | AC, ES, PD |
| Casp3 | 14970175 | KA, IP | Htrc2 | 10644717, 17906618 | AC, ES, Y2H |
| Casp8 | 14970175 | KA, IP | Ppm1a | 23560844, 9707433 | IP, PA |
| Slc12a2 | 14563843 | IP | Gmfb | 8798479 | AC |
| Stk39 | 14563843 | IP | Csnk2a1 | 10747897 | AC, PD |
| Cdc25a | 12963847 | pull down | Znhit1 | 18624398, 17380123 | IP, KA, PD, Y2H |
| Fubp1 | 12819782 | AC, Y2H | | | |
| Kars | 12819782 | Y2H | | | |
| Smad7 | 17172861, 12589052 | AC, IP | | | |
| Spag9 | 12391307 | AC | | | |

**Supplementary Table 1 | B. p38α putative functional interactors from information available in databases.** PMID number refers to the manuscript ID. Detection methods: ES: Enzymatic study, KA: Kinase assay, IP: Immunoprecipitation and EID: Experimental interaction detection.

| Functional Interactor | PMID | Detection Method | Functional Interactor | PMID | Detection Method |
|---|---|---|---|---|---|
| Bcl2 | 11495898 | EID | Myod1 | 15719023 | EID |
| Bmi1 | 21675959 | ES | Plc2g4a | 9468497 | EID |
| Cd4 | 20530479 | ES | Ppargc1a | 11741533 | EID |
| Dusp7 | 9788880 | PA | Rbsn | 16138080 | EID |
| Eea1 | 16138080 | EID | Scn8a | 16014723 | EID |
| Eef2k | 12171600 | EID | Shc1 | 16251354 | ES |
| Eif4ebp1 | 11777913, 20090955 | EID, ES | Smad3 | 14512875 | EID |
| Elk3 | 11042694 | EID | Srpk1 | 23602568 | KA |
| Casp3 | 14970175 | KA, IP | Stat1 | 11226159 | EID |
| Esr1 | 12138194 | EID | Zap70 | 15736548, 15735649 | EID |
| Ifnar1 | 21695243 | KA | Elk4 | 9235954, 9130707 | EID |
| Jdp2 | 11602244, 12225289 | EID | Elk1 | 9155018, 8548291, 9130707 | EID |
| Junb | 8917518, 9889198 | EID | Limk1 | 16456544 | KA |
| Mafa | 11416124 | EID | Ncoa3 | 16456540, 16135815 | EID, KA |
| Mapk8 | 15778365 | EID | Ncf1 | 15629715 | EID |
| Mbp | 17906618, 10708586, 15728454 | EID | Mef2a | 9858528, 10330143, 10849446 | EID, ES |
| Noxa1 | 20110267 | KA | Pi4k2b | 16949365 | ES |
| Baz1b | 19776015 | ES | Tfcp2 | 15857981 | ES |
| Rb1 | 20871633, 17380128 | KA | Etv1 | 11551945 | ES |
| Mitf | 11792706 | EID | Jun | 24945502, 9155018 | ES |
| Ddit3 | 8650547 | ES | | | |

**Supplementary Figure 1 | MAPK sequence alignment using Clustal Omega or M-Coffee.** In Clustal Omega red indicates hydrophobic amino acids, blue indicates acidic aminoacid, magenta indicates basic amino acids and green shows polar amino acids with hydroxyl, sulfhydryl and amine groups. In M-Coffe alignment each residue has a color that indicates the agreement of the individual MSAs with respect to the alignment of that specific residue. Dark red indicates residues aligned in a similar fashion among all the individual MSAs; yellow, orange and red residues can be considered to be reliably aligned.

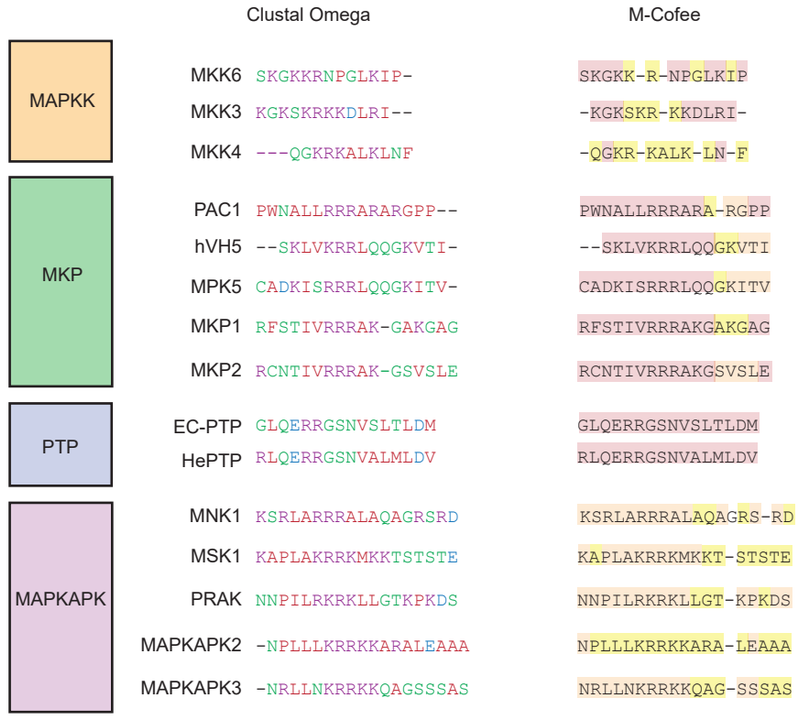






**Supplementary Table 2 | p38α interacting partners based on FIMO ranked output.** Significant motif occurrences have a p-value ≤ 0.05. Start and Stop parameters show the amino acid region of the matched sequence inside the protein. Bold indicates new putative docking interactors for p38α. The selected proteins for validation are indicated in bold red.

| Docking protein | Interactor candidate | start | stop | score | p-value | q-value | matched sequence |
|---|---|---|---|---|---|---|---|
| MAPKAPK | MK3 | 358 | 376 | 51,2551 | 1,73E-018 | 1,89E-011 | NNRLLNKRRKKQAGSSSAS |
| | MSK1 | 737 | 755 | 44,2449 | 5,70E-015 | 3,12E-008 | KAPLAKRRKMKKTSTSTET |
| | MK5 | 356 | 374 | 42,6633 | 1,73E-014 | 6,32E-008 | NNPILRKRKLLGTKPKDSV |
| | MK2 | 379 | 397 | 41,2041 | 4,31E-014 | 1,18E-007 | SNPLLLKRRKKARALEAAA |
| | MNK1 | 441 | 459 | 26,7959 | 6,65E-011 | 0,000146 | KSRLARRRALAQAGRGEDR |
| | **AHDC1** | 389 | 407 | 15,0918 | 7,86E-009 | 0,0143 | RPKILCRRRKAGRGRKADA |
| | **SHRM1** | 720 | 738 | 11,8367 | 2,60E-008 | 0,0406 | GSRLARVRRALARAASDSD |
| | **IQCA1** | 796 | 814 | 11,3265 | 3,08E-008 | 0,0421 | KTPLGKKRALAITGGSTEK |
| MAPKK | MKK6 | 4 | 17 | 36,6964 | 5,09E-013 | 5,61E-006 | SKGKKRNPGLKIPK |
| | MKK3 | 16 | 29 | 33,3661 | 8,26E-012 | 4,55E-005 | KGKSKRKKDLRISC |
| | **GRK5** | 23 | 37 | 22,6364 | 4,38E-009 | 0,0161 | RKGKSKKWKEILKFP |
| | MKK4 | 35 | 48 | 30,3929 | 6,96E-011 | 0,000256 | SSMQGKRKALKLNF |
| | **ZBED6** | 59 | 72 | 23,7679 | 3,63E-009 | 0,01 | PAKKKRKKGLRIKG |
| MKP | DUS8 | 50 | 67 | 47,8265 | 2,27E-016 | 2,49E-009 | CCSKLVKRRLQQGKVTIA |
| | DUS10 | 196 | 213 | 46,2857 | 8,99E-016 | 4,92E-009 | CADKISRRRLQQGKITVL |
| | DUS16 | 49 | 66 | 16,4694 | 7,30E-009 | 0,0266 | NCSKLMKRRLQQDKVLIT |
| PTP | PTN7 | 37 | 52 | 59,8137 | 1,07E-019 | 1,01E-012 | RLQERRGSNVALMLDV |
| | PTN5 | 238 | 253 | 59,5 | 2,76E-019 | 1,01E-012 | GLQERRGSNVSLTLDM |
| | PTPRR | 332 | 347 | 59,5 | 2,76E-019 | 1,01E-012 | GLQERRGSNVSLTLDM |

**Supplementary Table 3 | Modeling of motifs on p38α and scoring the structural compatibility.** The obtained sequences were ranked from best binding energies for p38α model (2OKR, 2ONL and 2OZA).

| Protein candi-date | Docking motif | Binding energy 2OKR | Binding energy 2ONL | Binding energy 2OZA |
|---|---|---|---|---|
| MAPK3 | DQVKIKDLKTSNNRLLNKRRKK-347-368 | -21,8743 | -22,0076 | -20,6469 |
| MAPK2 | EQIKIKKIEDASNPLLLKRRKK-368-389 | -21,1262 | -19,1279 | -19,5412 |
| ZSWM4 | LELGLQVMRMTLNVMTWRRREM-671-692 | -20,3523 | -19,9477 | -20,4595 |
| LRC47 | DCPKLKEINFRGNKLRDKRLEK-223-244 | -19,2423 | -17,5567 | -17,5643 |
| FA83C | GAPELGSLRPGDRALEDRRLSL-566-587 | -19,1068 | -13,0425 | -12,7359 |
| UBAP2 | ISVSVHQPQPKHIKLAKRRIPP-491-512 | -19,0696 | -19,0491 | -16,5511 |
| ACACA | HGMLINTPYVTKDLLQSKRFQA-1569-1590 | -18,9313 | -13,0184 | -15,856 |
| MET16 | VSLFLTAIENSWIHLRRKKRER-367-388 | -18,8183 | -16,7172 | -17,3167 |
| UB2J1 | SAVLIVILTLALAALIFRRIYL-287-308 | -18,796 | -16,7891 | -16,4803 |
| MYBA | TSPNIAKFSTPPAILRKKRKMR-433-454 | -18,6972 | -17,2124 | -17,0167 |
| KMT5C | SPLWLQWLPQPQPRVRPRKRRR-316-337 | -18,3828 | -16,9055 | -18,5248 |
| IF4G3 | RGVPLLNVGSRRSQPGQRREPR-692-713 | -18,3081 | -16,1128 | -18,6296 |
| CWC22 | KFPQIGELILKRLILNFRKGYR-225-246 | -18,1793 | -12,5357 | -13,0969 |
| SYCP2 | RFMEIESPHINENYIQSKREES-1228-1249 | -18,1649 | -16,5443 | -14,0447 |
| LRC41 | QNLTLQEITFSFCRLFEKRPAQ-668-689 | -17,9769 | -15,3809 | -20,2967 |
| RPTOR | PGVTLDLIEKIPGRLNDRRTPL-288-309 | -17,8719 | -15,4144 | -16,8526 |
| PAPOG | GQPHLNGMSNITKTVTPKRSHS-627-648 | -17,8372 | -15,0284 | -13,9248 |
| ZSWM5 | LELGLQVMRMTLSTLNWRRREM-866-887 | -17,7992 | -17,5714 | -19,6432 |
| PTPRQ | FDLQLAEVESTQVRITWKKPRQ-443-464 | -17,7586 | -11,8088 | -13,8319 |
| COR2B | KLVTLKGLIEPISMIVPRRSDS-342-363 | -17,3127 | -16,0407 | -13,5089 |
| SNX29 | ESMTISELRQATVAMMNRKDEL-463-484 | -17,3064 | -16,148 | -14,2632 |
| ZFY26 | PRLKVSKPSLSWKELRGRREVP-1325-1346 | -17,1423 | -17,208 | -15,3251 |
| WDR36 | LGLALDDFSISVLDIETRKIVR-595-616 | -16,9456 | -11,1907 | -10,276 |
| ZBT7B | PQVPLPPPPPPPPRPVARRSRK-182-203 | -16,887 | -14,6154 | -12,8214 |
| DBF4A | WGVKILHIDDIRYYIEQKKKEL-165-186 | -16,869 | -14,7052 | -14,8972 |
| NCMAP | VVIIIFTVVLILLKMYNRKMRT-39-60 | -16,8532 | -15,8484 | -16,0141 |
| MAGE1 | KLVQLFLLMDSTKLPIPKKGIL-751-772 | -16,5292 | -14,0533 | -11,9482 |
| ATD3B | RHILLYGPPGTGKTLFAKKLAL-346-367 | -16,4115 | -13,5778 | -14,0643 |
| ATD3C | RHILLYGPPGTGKTLFAKKLAL-171-192 | -16,4115 | -13,5778 | -14,0643 |
| F71E1 | FLPLLLRPLPSDGDIAMRRDRG-48-69 | -16,3927 | -13,9484 | -14,3661 |
| RP25L | APPGLGSMPSSSCGPRSRRRAR-138-159 | -16,3559 | -17,3906 | -17,6363 |
| ANKZ1 | VELTVGTLDLCESEVLPKRRRR-418-439 | -16,227 | -17,5566 | -17,3906 |
| TUT4 | CLIHIENIQGAHKHIKEKRHKK-309-330 | -16,1144 | -18,7912 | -19,1171 |
| IF2B2 | EIVNLFIPTQAVGAIIGKKGAH-428-449 | -16,001 | -14,0963 | -12,5836 |
| MDC1 | APPPLLSPLLPSIKPTVRKTRQ-1062-1083 | -15,9298 | -15,3958 | -9,96271 |
| THAP9 | DEVFLSKVSIFDISIARRKDLA-649-670 | -15,8977 | -12,1658 | -12,1969 |
| SET1B | LPPLLPAPLASCPPPMKRKPGR-1500-1521 | -15,7949 | -12,6178 | -9,00266 |
| TCF20 | RGLKLEAIVQKITSPNIRRSAS-1348-1369 | -15,6852 | -12,8987 | -15,9461 |
| YO001 | VYLNLSLPLKSVHRLSLKKSFG-129-150 | -15,6039 | -14,1985 | -13,0743 |

| Protein candi-date | Docking motif | Binding energy 2OKR | Binding energy 2ONL | Binding energy 2OZA |
|---|---|---|---|---|
| PRD16 | GLLALEPMPTFGKGLDLRRAAE-1182-1203 | -15,4267 | -1,00977 | -13,9123 |
| IL16 | FEILVRKPMSSKPKPPPRKYFK-585-606 | -14,8399 | -14,239 | -10,4905 |
| SMG1 | FSLLVEKLNKMEIPIAWRKIDI-2975-2996 | -14,6861 | -11,8989 | -11,8949 |
| CBPC2 | VNPRLREPQELFSILSTKRPLQ-156-177 | -14,36 | -16,8179 | -17,7821 |
| PCLO | PPPPLPPPTSPKPTILPKKKLT-2354-2375 | -14,3335 | -12,9515 | -6,26607 |
| RAI1 | RGLKLEAIVQKITSPSLKKFAC-1325-1346 | -14,3271 | -9,65419 | -12,2793 |
| ZFAN5 | KAPELPKPKKNRCFMCRKKVGL-142-163 | -14,294 | -15,0449 | -10,8336 |
| BRSK2 | KSMEVLSVTDGGSPVPARRAIE-381-402 | -14,1965 | -12,0796 | -12,7758 |
| NOP2 | QPPTVSPIRSSRPPPAKRKKSQ-781-802 | -13,9515 | -13,0432 | -8,56485 |
| F186A | KKPKVMVPPSSPQELEEKRYFV-2086-2107 | -13,9243 | -12,782 | -11,4976 |
| PEPL | EEISVKGPNGESSVIHDRKSGK-1696-1717 | -13,8336 | -8,88581 | -11,1645 |
| DTL | SSPPITPPASETKIMSPRKALI-511-532 | -13,5555 | -11,6032 | -11,4844 |
| EF2 | LEICLKDLEEDHACIPIKKSDP-554-575 | -13,4625 | -7,75117 | -10,3061 |
| TXIP1 | TQMELNNMKANFGDVVPRRDFE-241-262 | -13,1111 | -11,6311 | -13,8492 |
| SETB1 | DFLFLEMFCLDPYVLVDRKFQP-651-672 | -13,0248 | -12,4009 | -13,036 |
| PRR11 | PPPPLPPPPPPLAPVLLRKPSL-189-210 | -12,6669 | -10,546 | -8,03984 |
| CIC | AFLSIMSPEIQLPLPPGKRRTQ-151-172 | -12,6619 | -11,7429 | -13,9907 |
| RIM3A | ELIKLNWLLAKALWVLARRCYT-372-393 | -12,5065 | -12,7215 | -13,022 |
| RIM3B | ELIKLNWLLAKALWVLARRCYT-372-393 | -12,5065 | -12,7215 | -13,022 |
| RIM3C | ELIKLNWLLAKALWVLARRCYT-372-393 | -12,5065 | -12,7215 | -13,022 |
| NLRP1 | QLLLLQRPHPRSQDPLVKRSWP-280-301 | -12,3278 | -12,65 | -10,9965 |
| FA65A | PRPLVQQPEPLPIQVAFRRPET-404-425 | -11,9587 | -12,9519 | -11,8956 |
| SPAT2 | LRPDVWLLRNDAHSLYHKRSPP-353-374 | -11,6855 | -16,5035 | -7,0511 |
| PARN | RVMDIPYLNLEGPDLQPKRDHV-426-447 | -11,4731 | -10,469 | -8,44175 |
| NALP5 | SNLQIIGLWKWQYPVQIRKLLE-1151-1172 | -10,9042 | -8,23604 | -10,1249 |
| PK3CD | PAPQVQKPRAKPPPIPAKKPSS-292-313 | -10,8903 | -11,0669 | -6,21188 |
| KLF3 | SSMQVPVIESYEKPISQKKIKI-178-199 | -10,7404 | -6,5333 | -5,98824 |
| ANK3 | ITVPVYSVVNVLPEPALKKLPD-1820-1841 | -10,3772 | -9,84348 | -7,14908 |
| RBM25 | PTVLVPTVSMVGKHLGARKDHP-51-72 | -9,97386 | -11,7032 | -9,01823 |
| CI172 | GTPALPAPAPRSHGPTVRKFAK-828-849 | -9,8586 | -11,256 | -12,6912 |
| RHG29 | EELGLPDVNPMCQRPRLKRMQQ-1228-1249 | -9,77258 | -14,5996 | -13,6912 |
| NRBP | VPPSVKTPTPEPAEVETRKVVL-425-446 | -9,59147 | -5,60348 | -3,61307 |
| CLU | QCLKVLTMSGWNPPPGNRKMHG-213-234 | -9,35173 | 5,12331 | -7,69608 |
| ARHGH | AWPSVTEMRKLFGGPGSRRPSA-122-143 | -8,65843 | -12,9422 | -9,67026 |
| ARHGA | LQMALTELETLAEKLNERKRDA-591-612 | -8,4884 | -6,37087 | -9,16367 |
| IF4G1 | ASLLLEILGLLCKSMGPKKVGT-1373-1394 | -8,30425 | -9,70509 | -8,56517 |
| GYS2 | DRLNIKSPFSLSHVPHGKKKLH-677-698 | -7,66625 | -12,8816 | -8,63448 |
| SPIR2 | ARLWVQLMRELRRGVKLKKVQE-243-264 | -7,60181 | -12,809 | -12,4931 |
| RBGP1 | TKVRVCSPNERLFWPFSKRSTT-428-449 | -4,83029 | -12,9642 | -10,8336 |

**Supplementary Table 4 |Predicted E3-ligases for MK2. Information adapted from UbiBrowser database** (Only the first 40 proteins are shown). Labels are as follows: E3 (putative E3 ligase). EDP (Enriched domain pair), predicts the interaction domains between E3 and substrate. E3 motif indicates the E3 recognition of short linear sequence motifs inside the substrate. NL (Network loops) refers to the physical interaction network between the E3 and the substrate. EGP (Enriched GO pair) indicates functional association between the E3 and the substrate. CL (Confidence level).

| Rank | E3 | EDP | E3 Motif | NL | EGP | CL | Score |
|---|---|---|---|---|---|---|---|
| 1 | SMURF1 | • | • | • | • | HIGH | 0.802 |
| 2 | STUB1 | • | | • | • | HIGH | 0.775 |
| 3 | MDM2 | • | • | • | • | HIGH | 0.770 |
| 4 | SMURF2 | • | • | • | • | MIDDLE | 0.761 |
| 5 | ITCH | • | • | • | • | MIDDLE | 0.747 |
| 6 | RANBP2 | • | | • | • | MIDDLE | 0.736 |
| 7 | NEDD4 | • | | • | • | MIDDLE | 0.736 |
| 8 | RAPSN | • | | • | • | MIDDLE | 0.717 |
| 9 | TTC3 | • | • | | • | MIDDLE | 0.716 |
| 10 | BTRC | • | • | • | • | MIDDLE | 0.708 |
| 11 | CBLC | | | • | • | MIDDLE | 0.705 |
| 12 | SOCS7 | | | • | • | MIDDLE | 0.705 |
| 13 | DTX1 | | | • | • | MIDDLE | 0.702 |
| 14 | UBE4B | • | | • | • | MIDDLE | 0.701 |
| 15 | FBXW11 | • | | • | • | MIDDLE | 0.700 |
| 16 | SKP2 | • | • | • | | MIDDLE | 0.696 |
| 17 | UBE3C | • | • | | • | MIDDLE | 0.693 |
| 18 | SYTL4 | • | | • | • | MIDDLE | 0.688 |
| 19 | NEDD4L | • | • | • | • | MIDDLE | 0.688 |
| 21 | PHIP | | | • | • | MIDDLE | 0.683 |
| 22 | WWP1 | • | | • | • | MIDDLE | 0.681 |
| 23 | UBR5 | • | | • | • | MIDDLE | 0.680 |
| 24 | BIRC3 | • | | • | • | MIDDLE | 0.676 |
| 25 | HUWE1 | • | | • | • | MIDDLE | 0.676 |
| 26 | BIRC2 | • | | • | • | MIDDLE | 0.676 |
| 27 | APAF1 | • | | • | • | MIDDLE | 0.676 |
| 28 | CBL | | | • | • | MIDDLE | 0.674 |
| 29 | FANCG | • | | • | • | MIDDLE | 0.670 |
| 30 | HECW1 | • | | • | • | MIDDLE | 0.670 |
| 31 | ZEB2 | | | • | • | MIDDLE | 0.670 |
| 32 | SYVN1 | | • | • | • | MIDDLE | 0.669 |
| 33 | UBE3A | • | • | • | • | LOW | 0.662 |
| 34 | PELI2 | • | | • | • | LOW | 0.657 |
| 35 | WWP2 | • | | • | • | LOW | 0.657 |
| 36 | HERC1 | • | | • | • | LOW | 0.657 |
| 37 | PELI3 | • | | • | | LOW | 0.655 |
| 38 | CRYAB | | | • | • | LOW | 0.653 |
| 39 | BARD1 | | | • | • | LOW | 0.653 |
| 40 | MIB1 | | • | | • | LOW | 0.652 |







**Supplementary Table 5 |Raw data for MK2-IP mass spectrometry analysis**. It contains the three analyzed replicates for MK2-IP samples and two replicates for agarose beads (negative control). PSMs (peptides spectrum matches) indicate the number of peptides found.

| Gene names | KO (PSMs) | WT (PSMs) | KO Cneg (PSMs) | WT Cneg (PSMs) |
|---|---|---|---|---|
| Mfap1b | 2\|1\|0 | 0\|0\|0 | 0\|0 | 0\|0 |
| Dnajb6 | 2\|2\|2 | 2\|4\|0 | 0\|0 | 0\|0 |
| Dhcr7 | 0\|0\|1 | 0\|1\|1 | 0\|0 | 0\|0 |
| Hmgn1 | 1\|2\|3 | 0\|2\|0 | 0\|0 | 0\|0 |
| Pcmt1 | 4\|5\|8 | 1\|2\|2 | 1\|1 | 1\|0 |
| Cryab | 0\|0\|0 | 3\|2\|1 | 0\|0 | 0\|0 |
| Lta4h | 0\|0\|1 | 0\|1\|0 | 0\|0 | 0\|0 |
| Pdcd2 | 3\|2\|3 | 7\|9\|3 | 1\|2 | 2\|4 |
| Mapk14 | 0\|0\|1 | 15\|20\|17 | 0\|0 | 0\|0 |
| Mapkapk2 | 56\|69\|82 | 88\|86\|69 | 0\|0 | 0\|0 |
| Pcmtd1 | 6\|6\|8 | 12\|12\|4 | 0\|0 | 0\|0 |
| Vamp3;Vamp2 | 1\|1\|1 | 1\|1\|1 | 0\|0 | 0\|0 |
| Fbxo31 | 2\|7\|3 | 4\|1\|2 | 0\|0 | 0\|0 |
| Tmem109 | 0\|0\|0 | 1\|0\|0 | 0\|0 | 0\|0 |
| Ppp1r13l | 1\|0\|0 | 1\|0\|2 | 0\|0 | 0\|0 |
| Sptbn1 | 3\|2\|4 | 2\|1\|1 | 1\|1 | 0\|0 |
| Mylk | 0\|0\|0 | 2\|1\|0 | 0\|0 | 0\|0 |
| Ubr2 | 0\|0\|0 | 2\|1\|1 | 0\|0 | 0\|0 |
| Ubr5 | 2\|0\|1 | 1\|0\|0 | 0\|0 | 0\|0 |
| Pgrmc2 | 0\|1\|1 | 1\|3\|2 | 0\|0 | 0\|0 |
| Pcmtd2 | 1\|1\|2 | 2\|4\|2 | 0\|0 | 0\|1 |
| Rcn2 | 1\|1\|2 | 3\|0\|0 | 2\|0 | 0\|0 |
| Kank2 | 1\|0\|0 | 1\|1\|1 | 0\|1 | 1\|0 |
| Strip1 | 16\|20\|19 | 25\|24\|21 | 0\|0 | 0\|0 |
| Trim47 | 0\|0\|0 | 0\|3\|0 | 0\|1 | 0\|0 |
| Snap47 | 1\|0\|1 | 0\|0\|0 | 0\|0 | 0\|0 |
| Kctd5 | 2\|2\|1 | 1\|2\|0 | 0\|0 | 0\|0 |
| Ddx41 | 0\|3\|0 | 1\|2\|1 | 0\|0 | 0\|0 |
| Far1 | 1\|1\|0 | 0\|1\|0 | 0\|0 | 0\|0 |
| Sirt1 | 2\|1\|2 | 0\|0\|1 | 0\|0 | 0\|0 |
| Dnaja3 | 4\|4\|5 | 3\|3\|2 | 0\|0 | 2\|1 |
| Ranbp3 | 1\|0\|0 | 1\|1\|0 | 0\|1 | 0\|0 |
| Bccip | 10\|13\|9 | 12\|13\|5 | 1\|2 | 3\|4 |
| Ppp1r12a;Ppp1r12b | 0\|2\|0 | 0\|0\|0 | 0\|1 | 0\|0 |
| Osbpl3 | 1\|1\|1 | 1\|1\|0 | 0\|0 | 0\|0 |
| Strn3 | 2\|2\|3 | 2\|2\|0 | 0\|0 | 0\|0 |
| Clpx | 2\|1\|1 | 0\|0\|0 | 0\|0 | 0\|0 |
| Mpp6 | 12\|12\|16 | 3\|4\|4 | 0\|0 | 0\|0 |
| Ecsit | 2\|1\|1 | 2\|2\|0 | 0\|0 | 0\|0 |
| Ripk3 | 0\|0\|1 | 0\|2\|0 | 0\|0 | 0\|0 |
| Pts | 6\|7\|8 | 5\|5\|4 | 0\|0 | 0\|0 |
| Rnf7 | 1\|3\|2 | 2\|1\|2 | 1\|1 | 1\|2 |

# References

Adams, R. H., Porras, A., Alonso, G., Jones, M., Vintersten, K., Panelli, S., . . . Nebreda, A. R. (2000). Essential role of p38alpha MAP kinase in placental but not embryonic cardiovascular development. Mol Cell, 6(1), 109-116.

Adams, Ralf H., Porras, Almudena, Alonso, Gema, Jones, Margaret, Vintersten, Kristina, Panelli, Simona, . . . Nebreda, Angel R. (2000). Essential Role of p38α MAP Kinase in Placental but Not Embryonic Cardiovascular Development. Molecular Cell, 6(1), 109-116. doi: https://doi.org/10.1016/S1097-2765(05)00014-6

Alonso, G., Ambrosino, C., Jones, M., & Nebreda, A. R. (2000). Differential activation of p38 mitogen-activated protein kinase isoforms depending on signal strength. J Biol Chem, 275(51), 40641-40648. doi: 10.1074/jbc.M007835200

Ambrosino, C., Mace, G., Galban, S., Fritsch, C., Vintersten, K., Black, E., . . . Nebreda, A. R. (2003). Negative feedback regulation of MKK6 mRNA stability by p38alpha mitogen-activated protein kinase. Mol Cell Biol, 23(1), 370-381

Anderson, P. (2008). Post-transcriptional control of cytokine production. Nat Immunol, 9(4), 353-359. doi: 10.1038/ni1584

Aranda, B., Achuthan, P., Alam-Faruque, Y., Armean, I., Bridge, A., Derow, C., . . . Hermjakob, H. (2010). The IntAct molecular interaction database in 2010. Nucleic Acids Res, 38(Database issue), D525-531. doi: 10.1093/nar/gkp878

Aronova, S., Wedaman, K., Anderson, S., Yates, J., 3rd, & Powers, T. (2007). Probing the membrane environment of the TOR kinases reveals functional interactions between TORC1, actin, and membrane trafficking in Saccharomyces cerevisiae. Mol Biol Cell, 18(8), 2779-2794. doi: 10.1091/mbc.E07-03-0274

Asher, G., Reuven, N., & Shaul, Y. (2006). 20S proteasomes and protein degradation "by default". Bioessays, 28(8), 844-849. doi: 10.1002/bies.20447

Ashwell, Jonathan D. (2006). The many paths to p38 mitogen-activated protein kinase activation in the immune system. Nature Reviews Immunology, 6, 532. doi: 10.1038/nri1865

Bailon, E., Cueto-Sola, M., Utrilla, P., Rodriguez-Cabezas, M. E., Garrido-Mesa, N., Zarzuelo, A., . . . Comalada, M. (2010). Butyrate in vitro immune-modulatory effects might be mediated through a proliferation-related induction of apoptosis. Immunobiology, 215(11), 863-873. doi: 10.1016/j.imbio.2010.01.001

Bandyopadhyay, S., Chiang, C. Y., Srivastava, J., Gersten, M., White, S., Bell, R., . . . Ideker, T. (2010). A human MAP kinase interactome. Nat Methods, 7(10), 801-805.
Banks, Rosamonde E., Dunn, Michael J., Hochstrasser, Denis F., Sanchez, Jean-Charles, Blackstock, Walter, Pappin, Darryl J., & Selby, Peter J. (2000). Proteomics: new perspectives, new biomedical opportunities. The Lancet, 356(9243), 1749-1756. doi: https://doi.org/10.1016/S0140-6736(00)03214-1

Bazzi, Hisham, Soroka, Ekaterina, Alcorn, Heather L., & Anderson, Kathryn V. (2017). STRIP1, a core component of STRIPAK complexes, is essential for normal mesoderm migration in the mouse embryo. Proceedings of the National Academy of Sciences, 114(51), E10928-E10936. doi: 10.1073/pnas.1713535114

Beardmore, V. A., Hinton, H. J., Eftychi, C., Apostolaki, M., Armaka, M., Darragh, J., . . . Arthur, J. S. (2005). Generation and characterization of p38beta (MAPK11) gene-targeted mice. Mol Cell Biol, 25(23), 10454-10464. doi: 10.1128/mcb.25.23.10454-10464.2005
Bedford, Lynn, Paine, Simon, Sheppard, Paul W., Mayer, R. John, & Roelofs, Jeroen. (2010). Assembly, Structure and Function of the 26S proteasome. Trends in cell biology, 20(7), 391-401. doi: 10.1016/j.tcb.2010.03.007

Ben-Levy, R., Hooper, S., Wilson, R., Paterson, H. F., & Marshall, C. J. (1998). Nuclear export of the stress-activated protein kinase p38 mediated by its substrate MAPKAP kinase-2. Curr Biol, 8(19), 1049-1057.

Berndsen, Christopher E., & Wolberger, Cynthia. (2014). New insights into ubiquitin E3 ligase mechanism. Nature Structural &Amp; Molecular Biology, 21, 301. doi: 10.1038/nsmb.2780

Bhalla, U. S., Ram, P. T., & Iyengar, R. (2002). MAP kinase phosphatase as a locus of flexibility in a mitogen-activated protein kinase signaling network. Science, 297(5583), 1018-1023. doi: 10.1126/science.1068873

Biondi, Ricardo M., & Nebreda, Angel R. (2003). Signalling specificity of Ser/Thr protein kinases through docking-site-mediated interactions. Biochemical Journal, 372(Pt 1), 1-13. doi: 10.1042/BJ20021641

Brancho, Deborah, Tanaka, Nobuyuki, Jaeschke, Anja, Ventura, Juan-Jose, Kelkar, Nyaya, Tanaka, Yoshinori, . . . Davis, Roger J. (2003). Mechanism of p38 MAP kinase activation in vivo. Genes & Development, 17(16), 1969-1978. doi: 10.1101/gad.1107303





Brooks, Seth A., & Blackshear, Perry J. (2013). Tristetraprolin (TTP): Interactions with mRNA and proteins, and current thoughts on mechanisms of action. Biochimica et biophysica acta, 1829(0), 666-679. doi: 10.1016/j.bbagrm.2013.02.003

Brown, Matthew D., & Sacks, David B. (2009). Protein Scaffolds in MAP Kinase Signalling. Cellular signalling, 21(4), 462-469. doi: 10.1016/j.cellsig.2008.11.013

Budhidarmo, Rhesa, Nakatani, Yoshio, & Day, Catherine L. (2012). RINGs hold the key to ubiquitin transfer. Trends in Biochemical Sciences, 37(2), 58-65. doi: https://doi.org/10.1016/j.tibs.2011.11.001

Bulavin, D. V., Higashimoto, Y., Popoff, I. J., Gaarde, W. A., Basrur, V., Potapova, O., . . . Fornace, A. J., Jr. (2001). Initiation of a G2/M checkpoint after ultraviolet radiation requires p38 kinase. Nature, 411(6833), 102-107. doi: 10.1038/35075107

Burack, W. R., & Shaw, A. S. (2000). Signal transduction: hanging on a scaffold. Curr Opin Cell Biol, 12(2), 211-216.

Buxade, M., Parra-Palau, J. L., & Proud, C. G. (2008). The Mnks: MAP kinase-interacting kinases (MAP kinase signal-integrating kinases). Front Biosci, 13, 5359-5373.

Camps, M., Nichols, A., Gillieron, C., Antonsson, B., Muda, M., Chabert, C., . . . Arkinstall, S. (1998). Catalytic activation of the phosphatase MKP-3 by ERK2 mitogen-activated protein kinase. Science, 280(5367), 1262-1265.

Canovas, B., Igea, A., Sartori, A. A., Gomis, R. R., Paull, T. T., Isoda, M., . . . Nebreda, A. R. (2018). Targeting p38alpha Increases DNA Damage, Chromosome Instability, and the Anti-tumoral Response to Taxanes in Breast Cancer Cells. Cancer Cell, 33(6), 1094-1110 e1098. doi: 10.1016/j.ccell.2018.04.010

Cargnello, M., & Roux, P. P. (2011). Activation and function of the MAPKs and their substrates, the MAPK-activated protein kinases. Microbiol Mol Biol Rev, 75(1), 50-83. doi: 10.1128/mmbr.00031-10

Carman, C. V., Lisanti, M. P., & Benovic, J. L. (1999). Regulation of G protein-coupled receptor kinases by caveolin. J Biol Chem, 274(13), 8858-8864

Carriere, A., Ray, H., Blenis, J., & Roux, P. P. (2008). The RSK factors of activating the Ras/MAPK signaling cascade. Front Biosci, 13, 4258-4275

Casanovas, O., Miro, F., Estanyol, J. M., Itarte, E., Agell, N., & Bachs, O. (2000). Osmotic stress regulates the stability of cyclin D1 in a p38SAPK2-dependent manner. J Biol Chem, 275(45), 35091-35097. doi: 10.1074/jbc.M006324200

Caunt, C. J., & Keyse, S. M. (2013). Dual-specificity MAP kinase phosphatases (MKPs): shaping the outcome of MAP kinase signalling. FEBS J, 280(2), 489-504. doi: 10.1111/j.1742-4658.2012.08716.x

Ceol, A., Chatr Aryamontri, A., Licata, L., Peluso, D., Briganti, L., Perfetto, L., . . . Cesareni, G. (2010). MINT, the molecular interaction database: 2009 update. Nucleic Acids Res, 38(Database issue), D532-539. doi: 10.1093/nar/gkp983

Chang, C. I., Xu, B. E., Akella, R., Cobb, M. H., & Goldsmith, E. J. (2002). Crystal structures of MAP kinase p38 complexed to the docking sites on its nuclear substrate MEF2A and activator MKK3b. Mol Cell, 9(6), 1241-1249

Chen, D., Frezza, M., Schmitt, S., Kanwar, J., & Dou, Q. P. (2011). Bortezomib as the First Proteasome Inhibitor Anticancer Drug: Current Status and Future Perspectives. Current Cancer Drug Targets, 11(3), 239-253

Cheung, P. C., Campbell, D. G., Nebreda, A. R., & Cohen, P. (2003). Feedback control of the protein kinase TAK1 by SAPK2a/p38alpha. EMBO J, 22(21), 5793-5805. doi: 10.1093/emboj/cdg552

Chou, T. T., Trojanowski, J. Q., & Lee, V. M. (2001). p38 mitogen-activated protein kinase-independent induction of gadd45 expression in nerve growth factor-induced apoptosis in medulloblastomas. J Biol Chem, 276(44), 41120-41127. doi: 10.1074/jbc.M102832200

Clark, Andrew R., & Dean, Jonathan L. E. (2016). The control of inflammation via the phosphorylation and dephosphorylation of tristetraprolin: a tale of two phosphatases. Biochemical Society Transactions, 44(5), 1321

Cohen-Armon, M. (2007). PARP-1 activation in the ERK signaling pathway. Trends Pharmacol Sci, 28(11), 556-560. doi: 10.1016/j.tips.2007.08.005

Corrêa, Sônia A. L., & Eales, Katherine L. (2012). The Role of p38 MAPK and Its Substrates in Neuronal Plasticity and Neurodegenerative Disease. Journal of Signal Transduction, 2012, 649079. doi: 10.1155/2012/649079





Costanzo, M., VanderSluis, B., Koch, E. N., Baryshnikova, A., Pons, C., Tan, G., . . . Boone, C. (2016). A global genetic interaction network maps a wiring diagram of cellular function. Science, 353(6306). doi: 10.1126/science.aaf1420

Coulombe, P., & Meloche, S. (2007). Atypical mitogen-activated protein kinases: structure, regulation and functions. Biochim Biophys Acta, 1773(8), 1376-1387. doi: 10.1016/j.bbamcr.2006.11.001

Coulthard, Lydia R., White, Danielle E., Jones, Dominic L., McDermott, Michael F., & Burchill, Susan A. (2009). p38<sup>MAPK</sup>: stress responses from molecular mechanisms to therapeutics. Trends in Molecular Medicine, 15(8), 369-379. doi: 10.1016/j.molmed.2009.06.005

Cuadrado, A., & Nebreda, A. R. (2010). Mechanisms and functions of p38 MAPK signalling. Biochem J, 429(3), 403-417. doi: 10.1042/bj20100323

Cuenda, A., & Rousseau, S. (2007). p38 MAP-kinases pathway regulation, function and role in human diseases. Biochim Biophys Acta, 1773(8), 1358-1375. doi: 10.1016/j.bbamcr.2007.03.010

Cuevas, B. D., Abell, A. N., & Johnson, G. L. (2007). Role of mitogen-activated protein kinase kinase kinases in signal integration. Oncogene, 26(22), 3159-3171. doi: 10.1038/sj.onc.1210409

Dan, I., Watanabe, N. M., & Kusumi, A. (2001). The Ste20 group kinases as regulators of MAP kinase cascades. Trends Cell Biol, 11(5), 220-230

Davidson, W., Frego, L., Peet, G. W., Kroe, R. R., Labadia, M. E., Lukas, S. M., . . . Werneburg, B. G. (2004). Discovery and characterization of a substrate selective p38alpha inhibitor. Biochemistry, 43(37), 11658-11671. doi: 10.1021/bi0495073

Davidson, Walter, Frego, Lee, Peet, Gregory W., Kroe, Rachel R., Labadia, Mark E., Lukas, Susan M., . . . Werneburg, Brian G. (2004). Discovery and Characterization of a Substrate Selective p38α Inhibitor. Biochemistry, 43(37), 11658-11671. doi: 10.1021/bi0495073

De Nicola, Gian Felice, Martin, Eva Denise, Chaikuad, Apirat, Bassi, Rekha, Clark, James, Martino, Luigi, . . . Marber, Michael S. (2013). Mechanism and consequence of the autoactivation of p38α mitogen-activated protein kinase promoted by TAB1. Nature Structural &Amp; Molecular Biology, 20, 1182. doi: 10.1038/nsmb.2668

del Barco Barrantes, Ivan, Coya, Juan Manuel, Maina, Flavio, Arthur, J. Simon C., & Nebreda, Angel R. (2011). Genetic analysis of specific and redundant roles for p38α and p38β MAPKs during mouse development. Proceedings of the National Academy of Sciences of the United States of America, 108(31), 12764-12769. doi: 10.1073/pnas.1015013108

Deshaies, Raymond J., & Joazeiro, Claudio A. P. (2009). RING Domain E3 Ubiquitin Ligases. Annual Review of Biochemistry, 78(1), 399-434. doi: 10.1146/annurev.biochem.78.101807.093809

Dikic, I. (2017). Proteasomal and Autophagic Degradation Systems. Annu Rev Biochem, 86, 193-224. doi: 10.1146/annurev-biochem-061516-044908

Diskin, R., Askari, N., Capone, R., Engelberg, D., & Livnah, O. (2004). Active mutants of the human p38alpha mitogen-activated protein kinase. J Biol Chem, 279(45), 47040-47049. doi: 10.1074/jbc.M404595200

Diskin, R., Lebendiker, M., Engelberg, D., & Livnah, O. (2007). Structures of p38alpha active mutants reveal conformational changes in L16 loop that induce autophosphorylation and activation. J Mol Biol, 365(1), 66-76. doi: 10.1016/j.jmb.2006.08.043

Diskin, Ron, Engelberg, David, & Livnah, Oded. (2008). A Novel Lipid Binding Site Formed by the MAP Kinase Insert in p38α. Journal of Molecular Biology, 375(1), 70-79. doi: https://doi.org/10.1016/j.jmb.2007.09.002

Duan, G., & Walther, D. (2015). The roles of post-translational modifications in the context of protein interaction networks. PLoS Comput Biol, 11(2), e1004049. doi: 10.1371/journal.pcbi.1004049

Effantin, G., Rosenzweig, R., Glickman, M. H., & Steven, A. C. (2009). Electron microscopic evidence in support of alpha-solenoid models of proteasomal subunits Rpn1 and Rpn2. J Mol Biol, 386(5), 1204-1211. doi: 10.1016/j.jmb.2009.01.039

Engelman, J. A., Lisanti, M. P., & Scherer, P. E. (1998). Specific inhibitors of p38 mitogen-activated protein kinase block 3T3-L1 adipogenesis. J Biol Chem, 273(48), 32111-32120.

Erales, J., & Coffino, P. (2014). Ubiquitin-independent proteasomal degradation. Biochim Biophys Acta, 1843(1), 216-221. doi: 10.1016/j.bbamcr.2013.05.008





Erazo, T., Moreno, A., Ruiz-Babot, G., Rodriguez-Asiain, A., Morrice, N. A., Espadamala, J., . . . Lizcano, J. M. (2013). Canonical and kinase activity-independent mechanisms for extracellular signal-regulated kinase 5 (ERK5) nuclear translocation require dissociation of Hsp90 from the ERK5-Cdc37 complex. Mol Cell Biol, 33(8), 1671-1686. doi: 10.1128/mcb.01246-12

Fan, L., Yang, X., Du, J., Marshall, M., Blanchard, K., & Ye, X. (2005). A novel role of p38 alpha MAPK in mitotic progression independent of its kinase activity. Cell Cycle, 4(11), 1616-1624. doi: 10.4161/cc.4.11.2125

Finley, D. (2009). Recognition and processing of ubiquitin-protein conjugates by the proteasome. Annu Rev Biochem, 78, 477-513. doi: 10.1146/annurev.biochem.78.081507.101607

Finley, Daniel. (2009). Recognition and Processing of Ubiquitin-Protein Conjugates by the Proteasome. Annual Review of Biochemistry, 78(1), 477-513. doi: 10.1146/annurev.biochem.78.081507.101607

Francis, Dana M., Różycki, Bartosz, Koveal, Dorothy, Hummer, Gerhard, Page, Rebecca, & Peti, Wolfgang. (2011). Structural basis of p38α regulation by hematopoietic tyrosine phosphatase. Nature Chemical Biology, 7, 916. doi: 10.1038/nchembio.707

Gaestel, M. (2006). MAPKAP kinases - MKs - two's company, three's a crowd. Nat Rev Mol Cell Biol, 7(2), 120-130. doi: 10.1038/nrm1834

Gaestel, Matthias. (2015). MAPK-Activated Protein Kinases (MKs): Novel Insights and Challenges. Frontiers in Cell and Developmental Biology, 3, 88. doi: 10.3389/fcell.2015.00088

Garai, A., Zeke, A., Gogl, G., Toro, I., Fordos, F., Blankenburg, H., . . . Remenyi, A. (2012). Specificity of linear motifs that bind to a common mitogen-activated protein kinase docking groove. Sci Signal, 5(245), ra74. doi: 10.1126/scisignal.2003004

Garbett, Damien, Bretscher, Anthony, & Kozminski, Keith G. (2014). The surprising dynamics of scaffolding proteins. Molecular Biology of the Cell, 25(16), 2315-2319. doi: 10.1091/mbc.e14-04-0878

Ge, B., Gram, H., Di Padova, F., Huang, B., New, L., Ulevitch, R. J., . . . Han, J. (2002). MAPKK-independent activation of p38alpha mediated by TAB1-dependent autophosphorylation of p38alpha. Science, 295(5558), 1291-1294. doi: 10.1126/science.1067289

Glick, Danielle, Barth, Sandra, & Macleod, Kay F. (2010). Autophagy: cellular and molecular mechanisms. The Journal of pathology, 221(1), 3-12. doi: 10.1002/path.2697

Glotzer, M., Murray, A. W., & Kirschner, M. W. (1991). Cyclin is degraded by the ubiquitin pathway. Nature, 349(6305), 132-138. doi: 10.1038/349132a0

Goloudina, A., Yamaguchi, H., Chervyakova, D. B., Appella, E., Fornace, A. J., Jr., & Bulavin, D. V. (2003). Regulation of human Cdc25A stability by Serine 75 phosphorylation is not sufficient to activate a S phase checkpoint. Cell Cycle, 2(5), 473-478.

Gong, X., Ming, X., Deng, P., & Jiang, Y. (2010). Mechanisms regulating the nuclear translocation of p38 MAP kinase. J Cell Biochem, 110(6), 1420-1429. doi: 10.1002/jcb.22675

González-Rodríguez, Á, Mayoral, R., Agra, N., Valdecantos, M. P., Pardo, V., Miquilena-Colina, M. E., . . . Valverde, Á M. (2014). Impaired autophagic flux is associated with increased endoplasmic reticulum stress during the development of NAFLD. Cell Death &Amp; Disease, 5, e1179. doi: 10.1038/cddis.2014.162

Good, Matthew C., Zalatan, Jesse G., & Lim, Wendell A. (2011). Scaffold Proteins: Hubs for Controlling the Flow of Cellular Information. Science (New York, N.Y.), 332(6030), 680-686. doi: 10.1126/science.1198701

Graves, J. D., & Krebs, E. G. (1999). Protein phosphorylation and signal transduction. Pharmacol Ther, 82(2-3), 111-121

Guay, J., Lambert, H., Gingras-Breton, G., Lavoie, J. N., Huot, J., & Landry, J. (1997). Regulation of actin filament dynamics by p38 map kinase-mediated phosphorylation of heat shock protein 27. J Cell Sci, 110 ( Pt 3), 357-368

Gurgis, F. M. S., Åkerfeldt, M. C., Heng, B., Wong, C., Adams, S., Guillemin, G. J., . . . Munoz, L. (2015). Cytotoxic activity of the MK2 inhibitor CMPD1 in glioblastoma cells is independent of MK2. Cell Death Discovery, 1, 15028. doi: 10.1038/cddiscovery.2015.28

Han, Y. H., Moon, H. J., You, B. R., & Park, W. H. (2009). The effect of MG132, a proteasome inhibitor on HeLa cells in relation to cell growth, reactive oxygen species and GSH. Oncol Rep, 22(1), 215-221





Harmsen, M. M., & De Haard, H. J. (2007). Properties, production, and applications of camelid single-domain antibody fragments. Applied Microbiology and Biotechnology, 77(1), 13-22. doi: 10.1007/s00253-007-1142-2

Hartwell, Leland H., Hopfield, John J., Leibler, Stanislas, & Murray, Andrew W. (1999). From molecular to modular cell biology. Nature, 402, C47. doi: 10.1038/35011540

Haupt, Y., Maya, R., Kazaz, A., & Oren, M. (1997). Mdm2 promotes the rapid degradation of p53. Nature, 387(6630), 296-299. doi: 10.1038/387296a0

Hedges, J. C., Dechert, M. A., Yamboliev, I. A., Martin, J. L., Hickey, E., Weber, L. A., & Gerthoffer, W. T. (1999). A role for p38(MAPK)/HSP27 pathway in smooth muscle cell migration. J Biol Chem, 274(34), 24211-24219.

Hershko, Avram, Ciechanover, Aaron, & Varshavsky, Alexander. (2000). The ubiquitin system. Nature Medicine, 6, 1073. doi: 10.1038/80384

Hitti, E., Iakovleva, T., Brook, M., Deppenmeier, S., Gruber, A. D., Radzioch, D., . . . Gaestel, M. (2006). Mitogen-activated protein kinase-activated protein kinase 2 regulates tumor necrosis factor mRNA stability and translation mainly by altering tristetraprolin expression, stability, and binding to adenine/uridine-rich element. Mol Cell Biol, 26(6), 2399-2407. doi: 10.1128/mcb.26.6.2399-2407.2006

Hochstrasser, M. (1996). Ubiquitin-dependent protein degradation. Annu Rev Genet, 30, 405-439. doi: 10.1146/annurev.genet.30.1.405

Hu, J. H., Chen, T., Zhuang, Z. H., Kong, L., Yu, M. C., Liu, Y., . . . Ge, B. X. (2007). Feedback control of MKP-1 expression by p38. Cell Signal, 19(2), 393-400. doi: 10.1016/j.cellsig.2006.07.010

Hu, Jun-Hao, Chen, Ting, Zhuang, Zi-Heng, Kong, Ling, Yu, Ming-Can, Liu, Yusen, . . . Ge, Bao-Xue. (2007). Feedback control of MKP-1 expression by p38. Cellular Signalling, 19(2), 393-400. doi: https://doi.org/10.1016/j.cellsig.2006.07.010

Hu, S., Xie, Z., Onishi, A., Yu, X., Jiang, L., Lin, J., . . . Zhu, H. (2009). Profiling the human protein-DNA interactome reveals ERK2 as a transcriptional repressor of interferon signaling. Cell, 139(3), 610-622. doi: 10.1016/j.cell.2009.08.037

Huhn, S. C., Liu, J., Ye, C., Lu, H., Jiang, X., Feng, X., . . . Shen, Z. (2017). Regulation of spindle integrity and mitotic fidelity by BCCIP. Oncogene, 36(33), 4750-4766. doi:

10.1038/onc.2017.92

Hui, L., Bakiri, L., Mairhorfer, A., Schweifer, N., Haslinger, C., Kenner, L., . . . Wagner, E. F. (2007). p38alpha suppresses normal and cancer cell proliferation by antagonizing the JNK-c-Jun pathway. Nat Genet, 39(6), 741-749. doi: 10.1038/ng2033

Huse, Morgan, & Kuriyan, John. (2002). The Conformational Plasticity of Protein Kinases. Cell, 109(3), 275-282. doi: 10.1016/S0092-8674(02)00741-9

Hutter, D., Chen, P., Barnes, J., & Liu, Y. (2000). Catalytic activation of mitogen-activated protein (MAP) kinase phosphatase-1 by binding to p38 MAP kinase: critical role of the p38 C-terminal domain in its negative regulation. Biochem J, 352 Pt 1, 155-163.

Huttlin, E. L., Ting, L., Bruckner, R. J., Gebreab, F., Gygi, M. P., Szpyt, J., . . . Gygi, S. P. (2015). The BioPlex Network: A Systematic Exploration of the Human Interactome. Cell, 162(2), 425-440. doi: 10.1016/j.cell.2015.06.043

Hwang, J., & Pallas, D. C. (2014). STRIPAK complexes: structure, biological function, and involvement in human diseases. Int J Biochem Cell Biol, 47, 118-148. doi: 10.1016/j.biocel.2013.11.021

Ichimura, Yoshinobu, Kirisako, Takayoshi, Takao, Toshifumi, Satomi, Yoshinori, Shimonishi, Yasutsugu, Ishihara, Naotada, . . . Ohsumi, Yoshinori. (2000). A ubiquitin-like system mediates protein lipidation. Nature, 408, 488. doi: 10.1038/35044114

Irannejad, Roshanak, & von Zastrow, Mark. (2014). GPCR signaling along the endocytic pathway. Current opinion in cell biology, 27, 109-116. doi: 10.1016/j.ceb.2013.10.003

Jacobs, D., Glossip, D., Xing, H., Muslin, A. J., & Kornfeld, K. (1999). Multiple docking sites on substrate proteins form a modular system that mediates recognition by ERK MAP kinase. Genes Dev, 13(2), 163-175.

Jacobsen, A. V., & Murphy, J. M. (2017). The secret life of kinases: insights into non-catalytic signalling functions from pseudokinases. Biochem Soc Trans, 45(3), 665-681. doi: 10.1042/bst20160331

Kang, Dong Soo, Tian, Xufan, & Benovic, Jeffrey L. (2014). Role of β-arrestins and arrestin domain-containing proteins in G protein-coupled receptor trafficking. Current opinion in cell biology, 0, 63-71. doi: 10.1016/j.ceb.2013.11.005





Karlsson-Rosenthal, C., & Millar, J. B. (2006). Cdc25: mechanisms of checkpoint inhibition and recovery. Trends Cell Biol, 16(6), 285-292. doi: 10.1016/j.tcb.2006.04.002

Keshava Prasad, T. S., Goel, Renu, Kandasamy, Kumaran, Keerthikumar, Shivakumar, Kumar, Sameer, Mathivanan, Suresh, . . . Pandey, Akhilesh. (2009). Human Protein Reference Database—2009 update. Nucleic Acids Research, 37(Database issue), D767-D772. doi: 10.1093/nar/gkn892

Khoury, George A., Baliban, Richard C., & Floudas, Christodoulos A. (2011). Proteome-wide post-translational modification statistics: frequency analysis and curation of the swiss-prot database. Scientific Reports, 1, 90. doi: 10.1038/srep00090

Kim, G. Y., Mercer, S. E., Ewton, D. Z., Yan, Z., Jin, K., & Friedman, E. (2002). The stress-activated protein kinases p38 alpha and JNK1 stabilize p21(Cip1) by phosphorylation. J Biol Chem, 277(33), 29792-29802. doi: 10.1074/jbc.M201299200

Kim, Heon-Ki, Kim, Ryu-Ryun, Oh, Jang-Hyun, Cho, Hanna, Varshavsky, Alexander, & Hwang, Cheol-Sang. (2014). The N-Terminal Methionine of Cellular Proteins as a Degradation Signal. Cell, 156(1), 158-169. doi: 10.1016/j.cell.2013.11.031

Kim, L., Del Rio, L., Butcher, B. A., Mogensen, T. H., Paludan, S. R., Flavell, R. A., & Denkers, E. Y. (2005). p38 MAPK autophosphorylation drives macrophage IL-12 production during intracellular infection. J Immunol, 174(7), 4178-4184.

Kim, M. O., Kim, S. H., Cho, Y. Y., Nadas, J., Jeong, C. H., Yao, K., . . . Dong, Z. (2012). ERK1 and ERK2 regulate embryonic stem cell self-renewal through phosphorylation of Klf4. Nat Struct Mol Biol, 19(3), 283-290. doi: 10.1038/nsmb.2217

Komander, David, & Rape, Michael. (2012). The Ubiquitin Code. Annual Review of Biochemistry, 81(1), 203-229. doi: 10.1146/annurev-biochem-060310-170328

Kon, Maria, & Cuervo, Ana Maria. (2010). Chaperone-mediated Autophagy in Health and Disease. FEBS letters, 584(7), 1399-1404. doi: 10.1016/j.febslet.2009.12.025

Kotlyarov, A., Neininger, A., Schubert, C., Eckert, R., Birchmeier, C., Volk, H. D., & Gaestel, M. (1999). MAPKAP kinase 2 is essential for LPS-induced TNF-alpha biosynthesis. Nat Cell Biol, 1(2), 94-97. doi: 10.1038/10061

Kotlyarov, A., Yannoni, Y., Fritz, S., Laass, K., Telliez, J. B., Pitman, D., . . . Gaestel, M. (2002). Distinct cellular functions of MK2. Mol Cell Biol, 22(13), 4827-4835.

Kotlyarov, Alexey, Neininger, Armin, Schubert, Carola, Eckert, Rolf, Birchmeier, Carmen, Volk, Hans-Dieter, & Gaestel, Matthias. (1999). MAPKAP kinase 2 is essential for LPS-induced TNF-α biosynthesis. Nature Cell Biology, 1, 94. doi: 10.1038/10061

Kotlyarov, Alexey, Yannoni, Yvonne, Fritz, Susann, Laaß, Kathrin, Telliez, Jean-Baptiste, Pitman, Deborah, . . . Gaestel, Matthias. (2002). Distinct Cellular Functions of MK2. Molecular and Cellular Biology, 22(13), 4827-4835. doi: 10.1128/MCB.22.13.4827-4835.2002

Kruse, J. P., & Gu, W. (2009). Modes of p53 regulation. Cell, 137(4), 609-622. doi: 10.1016/j.cell.2009.04.050

Kumar, Sanjay, Boehm, Jeffrey, & Lee, John C. (2003). p38 MAP kinases: key signalling molecules as therapeutic targets for inflammatory diseases. Nature Reviews Drug Discovery, 2, 717. doi: 10.1038/nrd1177

Kung, J. E., & Jura, N. (2016). Structural Basis for the Non-catalytic Functions of Protein Kinases. Structure, 24(1), 7-24. doi: 10.1016/j.str.2015.10.020

Kurokawa, Manabu, Kim, Jiyeon, Geradts, Joseph, Matsuura, Kenkyo, Liu, Liu, Ran, Xu, . . . Kornbluth, Sally. (2013). A Network of Substrates of the E3 Ubiquitin Ligases MDM2 and HUWE1 Control Apoptosis Independently of p53. Science Signaling, 6(274), ra32-ra32. doi: 10.1126/scisignal.2003741

Kusari, A. B., Molina, D. M., Sabbagh, W., Jr., Lau, C. S., & Bardwell, L. (2004). A conserved protein interaction network involving the yeast MAP kinases Fus3 and Kss1. J Cell Biol, 164(2), 267-277. doi: 10.1083/jcb.200310021

Kuzmanic, Antonija, Sutto, Ludovico, Saladino, Giorgio, Nebreda, Angel R., Gervasio, Francesco L., & Orozco, Modesto. (2017). Changes in the free-energy landscape of p38α MAP kinase through its canonical activation and binding events as studied by enhanced molecular dynamics simulations. eLife, 6, e22175. doi: 10.7554/eLife.22175

Kwon, Y. T., & Ciechanover, A. (2017). The Ubiquitin Code in the Ubiquitin-Proteasome System and Autophagy. Trends Biochem Sci, 42(11), 873-886. doi: 10.1016/j.tibs.2017.09.002

Laboratory Stock Solutions and Equipment. (1998). Current Protocols in Cell Biology, 00(1), A.2A.1-A.2A.10. doi: doi:10.1002/0471143030.cba02as00





Lamb, Christopher A., Yoshimori, Tamotsu, & Tooze, Sharon A. (2013). The autophagosome: origins unknown, biogenesis complex. Nature Reviews Molecular Cell Biology, 14, 759. doi: 10.1038/nrm3696

Langeberg, L. K., & Scott, J. D. (2015). Signalling scaffolds and local organization of cellular behaviour. Nat Rev Mol Cell Biol, 16(4), 232-244. doi: 10.1038/nrm3966

Laughlin, John D, Nwachukwu, Jerome C, Figuera-Losada, Mariana, Cherry, Lisa, Nettles, Kendall W, & LoGrasso, Philip V. (2012). Structural Mechanisms of Allostery and Autoinhibition in JNK Family Kinases. Structure, 20(12), 2174-2184. doi: 10.1016/j.str.2012.09.021

Lavoie, J. N., L'Allemain, G., Brunet, A., Muller, R., & Pouyssegur, J. (1996). Cyclin D1 expression is regulated positively by the p42/p44MAPK and negatively by the p38/HOGMAPK pathway. J Biol Chem, 271(34), 20608-20616

Lee, John C., Laydon, Jeffrey T., McDonnell, Peter C., Gallagher, Timothy F., Kumar, Sanjay, Green, David, . . . Young, Peter R. (1994). A protein kinase involved in the regulation of inflammatory cytokine biosynthesis. Nature, 372, 739. doi: 10.1038/372739a0

Leggett, D. S., Hanna, J., Borodovsky, A., Crosas, B., Schmidt, M., Baker, R. T., . . . Finley, D. (2002). Multiple associated proteins regulate proteasome structure and function. Mol Cell, 10(3), 495-507.

Lemmon, Mark A., Freed, Daniel M., Schlessinger, Joseph, & Kiyatkin, Anatoly. (2016). The Dark Side of Cell Signaling: Positive Roles for Negative Regulators. Cell, 164(6), 1172-1184. doi: 10.1016/j.cell.2016.02.047

Levine, Beth, & Kroemer, Guido. (2008). Autophagy in the Pathogenesis of Disease. Cell, 132(1), 27-42. doi: https://doi.org/10.1016/j.cell.2007.12.018

Levine, Beth, Sinha, Sangita C., & Kroemer, Guido. (2008). Bcl-2 family members: Dual regulators of apoptosis and autophagy. Autophagy, 4(5), 600-606. doi: 10.4161/auto.6260

Li, J., Miller, E. J., Ninomiya-Tsuji, J., Russell, R. R., 3rd, & Young, L. H. (2005). AMP-activated protein kinase activates p38 mitogen-activated protein kinase by increasing recruitment of p38 MAPK to TAB1 in the ischemic heart. Circ Res, 97(9), 872-879. doi: 10.1161/01.res.0000187458.77026.10

Li, Q., Zhang, N., Zhang, D., Wang, Y., Lin, T., Wang, Y., . . . Han, J. (2008). Determinants that control the distinct subcellular localization of p38alpha-PRAK and p38beta-PRAK complexes. J Biol Chem, 283(16), 11014-11023. doi: 10.1074/jbc.M709682200

Li, Yang, Xie, Ping, Lu, Liang, Wang, Jian, Diao, Lihong, Liu, Zhongyang, . . . He, Fuchu. (2017). An integrated bioinformatics platform for investigating the human E3 ubiquitin ligase-substrate interaction network. Nature Communications, 8(1), 347. doi: 10.1038/s41467-017-00299-9

Lim, J. H., Park, J. W., Kim, M. S., Park, S. K., Johnson, R. S., & Chun, Y. S. (2006). Bafilomycin induces the p21-mediated growth inhibition of cancer cells under hypoxic conditions by expressing hypoxia-inducible factor-1alpha. Mol Pharmacol, 70(6), 1856-1865. doi: 10.1124/mol.106.028076

Liu, Han, Urbé, Sylvie, & Clague, Michael J. (2012). Selective protein degradation in cell signalling. Seminars in Cell & Developmental Biology, 23(5), 509-514. doi: https://doi.org/10.1016/j.semcdb.2012.01.014

Liu, J., Yuan, Y., Huan, J., & Shen, Z. (2001). Inhibition of breast and brain cancer cell growth by BCCIPalpha, an evolutionarily conserved nuclear protein that interacts with BRCA2. Oncogene, 20(3), 336-345. doi: 10.1038/sj.onc.1204098

Liu, Xin, Zhang, Chen-Song, Lu, Chang, Lin, Sheng-Cai, Wu, Jia-Wei, & Wang, Zhi-Xin. (2016). A conserved motif in JNK/p38-specific MAPK phosphatases as a determinant for JNK1 recognition and inactivation. Nature Communications, 7, 10879. doi: 10.1038/ncomms10879

Lluis, F., Perdiguero, E., Nebreda, A. R., & Munoz-Canoves, P. (2006). Regulation of skeletal muscle gene expression by p38 MAP kinases. Trends Cell Biol, 16(1), 36-44. doi: 10.1016/j.tcb.2005.11.002

Lopez-Aviles, S., Lambea, E., Moldon, A., Grande, M., Fajardo, A., Rodriguez-Gabriel, M. A., . . . Aligue, R. (2008). Activation of Srk1 by the mitogen-activated protein kinase Sty1/Spc1 precedes its dissociation from the kinase and signals its degradation. Mol Biol Cell, 19(4), 1670-1679. doi: 10.1091/mbc.E07-07-0639

López-Avilés, Sandra, Grande, Maribel, González, Marta, Helgesen, Ase-Lill, Alemany, Vicenç, Sanchez-Piris, Maribel, . . . Aligue, Rosa. (2005). Inactivation of the Cdc25 Phosphatase by the Stress-Activated Srk1 Kinase in Fission Yeast. Molecular Cell, 17(1), 49-59. doi: https://doi.org/10.1016/j.molcel.2004.11.043





Lukas, S. M., Kroe, R. R., Wildeson, J., Peet, G. W., Frego, L., Davidson, W., . . . Werneburg, B. G. (2004). Catalysis and function of the p38 alpha.MK2a signaling complex. Biochemistry, 43(31), 9950-9960. doi: 10.1021/bi049508v

Madsen, Chris D., Hooper, Steven, Tozluoglu, Melda, Bruckbauer, Andreas, Fletcher, Georgina, Erler, Janine T., . . . Sahai, Erik. (2014). STRIPAK components determine mode of cancer cell migration and metastasis. Nature Cell Biology, 17, 68. doi: 10.1038/ncb3083

Manasanch, Elisabet E., & Orlowski, Robert Z. (2017). Proteasome inhibitors in cancer therapy. Nature Reviews Clinical Oncology, 14, 417. doi: 10.1038/nrclinonc.2016.206

Manke, I. A., Nguyen, A., Lim, D., Stewart, M. Q., Elia, A. E., & Yaffe, M. B. (2005). MAPKAP kinase-2 is a cell cycle checkpoint kinase that regulates the G2/M transition and S phase progression in response to UV irradiation. Mol Cell, 17(1), 37-48. doi: 10.1016/j.molcel.2004.11.021

Markljung, E., Jiang, L., Jaffe, J. D., Mikkelsen, T. S., Wallerman, O., Larhammar, M., . . . Andersson, L. (2009). ZBED6, a novel transcription factor derived from a domesticated DNA transposon regulates IGF2 expression and muscle growth. PLoS Biol, 7(12), e1000256. doi: 10.1371/journal.pbio.1000256

Marshall, C. J. (1995). Specificity of receptor tyrosine kinase signaling: transient versus sustained extracellular signal-regulated kinase activation. Cell, 80(2), 179-185

Masaaki, Komatsu, & Yoshinobu, Ichimura. (2010). Physiological significance of selective degradation of p62 by autophagy. FEBS Letters, 584(7), 1374-1378. doi: doi:10.1016/j.febslet.2010.02.017

McClendon, Christopher L., Kornev, Alexandr P., Gilson, Michael K., & Taylor, Susan S. (2014). Dynamic architecture of a protein kinase. Proceedings of the National Academy of Sciences, 111(43), E4623-E4631. doi: 10.1073/pnas.1418402111

McClure, K. F., Abramov, Y. A., Laird, E. R., Barberia, J. T., Cai, W., Carty, T. J., . . . Tao, Y. (2005). Theoretical and experimental design of atypical kinase inhibitors: application to p38 MAP kinase. J Med Chem, 48(18), 5728-5737. doi: 10.1021/jm050346q

McDowell, G. S., & Philpott, A. (2013). Non-canonical ubiquitylation: mechanisms and consequences. Int J Biochem Cell Biol, 45(8), 1833-1842. doi: 10.1016/j.biocel.2013.05.026

McKay, M. M., Ritt, D. A., & Morrison, D. K. (2011). RAF inhibitor-induced KSR1/B-RAF binding and its effects on ERK cascade signaling. Curr Biol, 21(7), 563-568. doi: 10.1016/j.cub.2011.02.033

Meister, Melanie, Tomasovic, Ana, Banning, Antje, & Tikkanen, Ritva. (2013). Mitogen-Activated Protein (MAP) Kinase Scaffolding Proteins: A Recount. International Journal of Molecular Sciences, 14(3), 4854-4884. doi: 10.3390/ijms14034854

Menon, Manoj B., Gropengießer, Julia, Fischer, Jessica, Novikova, Lena, Deuretzbacher, Anne, Lafera, Juri, . . . Ruckdeschel, Klaus. (2017). p38MAPK/MK2-dependent phosphorylation controls cytotoxic RIPK1 signalling in inflammation and infection. Nature Cell Biology, 19, 1248. doi: 10.1038/ncb3614

Mikhailov, Alexei, Shinohara, Mio, & Rieder, Conly L. (2004). Topoisomerase II and histone deacetylase inhibitors delay the G2/M transition by triggering the p38 MAPK checkpoint pathway. The Journal of Cell Biology, 166(4), 517-526. doi: 10.1083/jcb.200405167

Mittelstadt, P. R., Yamaguchi, H., Appella, E., & Ashwell, J. D. (2009). T cell receptor-mediated activation of p38{alpha} by mono-phosphorylation of the activation loop results in altered substrate specificity. J Biol Chem, 284(23), 15469-15474. doi: 10.1074/jbc.M901004200

Mizushima, Noboru, Levine, Beth, Cuervo, Ana Maria, & Klionsky, Daniel J. (2008). Autophagy fights disease through cellular self-digestion. Nature, 451(7182), 1069-1075. doi: 10.1038/nature06639

Morreale, F. E., & Walden, H. (2016). Types of Ubiquitin Ligases. Cell, 165(1), 248-248 e241. doi: 10.1016/j.cell.2016.03.003

Mourey, R. J., Burnette, B. L., Brustkern, S. J., Daniels, J. S., Hirsch, J. L., Hood, W. F., . . . Anderson, D. R. (2010). A benzothiophene inhibitor of mitogen-activated protein kinase-activated protein kinase 2 inhibits tumor necrosis factor alpha production and has oral anti-inflammatory efficacy in acute and chronic models of inflammation. J Pharmacol Exp Ther, 333(3), 797-807. doi: 10.1124/jpet.110.166173

Mudgett, John S., Ding, Jixiang, Guh-Siesel, Lucia, Chartrain, Nicole A., Yang, Lu, Gopal, Shobhna, & Shen, Michael M. (2000). Essential role for p38α mitogen-activated protein kinase in placental angiogenesis. Proceedings of the National Academy of Sciences, 97(19), 10454-10459. doi: 10.1073/pnas.180316397





Muñoz, Juan José, Tárrega, Céline, Blanco-Aparicio, Carmen, & Pulido, Rafael. (2003). Differential interaction of the tyrosine phosphatases PTP-SL, STEP and HePTP with the mitogen-activated protein kinases ERK1/2 and p38alpha is determined by a kinase specificity sequence and influenced by reducing agents. Biochemical Journal, 372(1), 193-201. doi: 10.1042/bj20021941

Neininger, A., Kontoyiannis, D., Kotlyarov, A., Winzen, R., Eckert, R., Volk, H. D., . . . Gaestel, M. (2002). MK2 targets AU-rich elements and regulates biosynthesis of tumor necrosis factor and interleukin-6 independently at different post-transcriptional levels. J Biol Chem, 277(5), 3065-3068. doi: 10.1074/jbc.C100685200

Neufeld, Thomas P. (2010). TOR-dependent control of autophagy: biting the hand that feeds. Current Opinion in Cell Biology, 22(2), 157-168. doi: https://doi.org/10.1016/j.ceb.2009.11.005

Noguchi, E., Homma, Y., Kang, X., Netea, M. G., & Ma, X. (2009). A Crohn's disease-associated NOD2 mutation suppresses transcription of human IL10 by inhibiting activity of the nuclear ribonucleoprotein hnRNP-A1. Nat Immunol, 10(5), 471-479. doi: 10.1038/ni.1722

Oh, You-Take, Deng, Liang, Deng, Jiusheng, & Sun, Shi-Yong. (2017). The proteasome deubiquitinase inhibitor b-AP15 enhances DR5 activation-induced apoptosis through stabilizing DR5. Scientific Reports, 7(1), 8027. doi: 10.1038/s41598-017-08424-w

Oksvold, M. P., Pedersen, N. M., Forfang, L., & Smeland, E. B. (2012). Effect of cycloheximide on epidermal growth factor receptor trafficking and signaling. FEBS Lett, 586(20), 3575-3581. doi: 10.1016/j.febslet.2012.08.022

Otto, T., Horn, S., Brockmann, M., Eilers, U., Schuttrumpf, L., Popov, N., . . . Eilers, M. (2009). Stabilization of N-Myc is a critical function of Aurora A in human neuroblastoma. Cancer Cell, 15(1), 67-78. doi: 10.1016/j.ccr.2008.12.005

Pan, Catherine Qiurong, Sudol, Marius, Sheetz, Michael, & Low, Boon Chuan. (2012). Modularity and functional plasticity of scaffold proteins as p(l)acemakers in cell signaling. Cellular Signalling, 24(11), 2143-2165. doi: https://doi.org/10.1016/j.cellsig.2012.06.002

Paramore, Andrew, & Frantz, Simon. (2003). Bortezomib. Nature Reviews Drug Discovery, 2, 611. doi: 10.1038/nrd1159

Parcellier, A., Brunet, M., Schmitt, E., Col, E., Didelot, C., Hammann, A., . . . Garrido, C. (2006). HSP27 favors ubiquitination and proteasomal degradation of p27Kip1 and helps S-phase re-entry in stressed cells. FASEB J, 20(8), 1179-1181. doi: 10.1096/fj.05-4184fje

Parcellier, A., Schmitt, E., Gurbuxani, S., Seigneurin-Berny, D., Pance, A., Chantome, A., . . . Garrido, C. (2003). HSP27 is a ubiquitin-binding protein involved in I-kappaBalpha proteasomal degradation. Mol Cell Biol, 23(16), 5790-5802.

Pargellis, C., Tong, L., Churchill, L., Cirillo, P. F., Gilmore, T., Graham, A. G., . . . Regan, J. (2002). Inhibition of p38 MAP kinase by utilizing a novel allosteric binding site. Nat Struct Biol, 9(4), 268-272. doi: 10.1038/nsb770

Pearson, G., Robinson, F., Beers Gibson, T., Xu, B. E., Karandikar, M., Berman, K., & Cobb, M. H. (2001). Mitogen-activated protein (MAP) kinase pathways: regulation and physiological functions. Endocr Rev, 22(2), 153-183. doi: 10.1210/edrv.22.2.0428

Peitz, M., Pfannkuche, K., Rajewsky, K., & Edenhofer, F. (2002). Ability of the hydrophobic FGF and basic TAT peptides to promote cellular uptake of recombinant Cre recombinase: a tool for efficient genetic engineering of mammalian genomes. Proc Natl Acad Sci U S A, 99(7), 4489-4494. doi: 10.1073/pnas.032068699

Peregrin, S., Jurado-Pueyo, M., Campos, P. M., Sanz-Moreno, V., Ruiz-Gomez, A., Crespo, P., . . . Murga, C. (2006). Phosphorylation of p38 by GRK2 at the docking groove unveils a novel mechanism for inactivating p38MAPK. Curr Biol, 16(20), 2042-2047. doi: 10.1016/j.cub.2006.08.083

Perkins, James R., Diboun, Ilhem, Dessailly, Benoit H., Lees, Jon G., & Orengo, Christine. (2010). Transient Protein-Protein Interactions: Structural, Functional, and Network Properties. Structure, 18(10), 1233-1243. doi: https://doi.org/10.1016/j.str.2010.08.007

Pettersson, Susanne, Kelleher, Michael, Pion, Emmanuelle, Wallace, Maura, & Ball, Kathryn L. (2009). Role of Mdm2 acid domain interactions in recognition and ubiquitination of the transcription factor IRF-2. Biochemical Journal, 418(3), 575-585. doi: 10.1042/bj20082087

Plun-Favreau, H., Klupsch, K., Moisoi, N., Gandhi, S., Kjaer, S., Frith, D., . . . Downward, J. (2007). The mitochondrial protease HtrA2 is regulated by Parkinson's disease-associated kinase PINK1. Nat Cell Biol, 9(11), 1243-1252. doi: 10.1038/ncb1644





Qian, F., Deng, J., Cheng, N., Welch, E. J., Zhang, Y., Malik, A. B., . . . Ye, R. D. (2009). A non-redundant role for MKP5 in limiting ROS production and preventing LPS-induced vascular injury. EMBO J, 28(19), 2896-2907. doi: 10.1038/emboj.2009.234

Qian, Min-Xian, Pang, Ye, Liu, Cui Hua, Haratake, Kousuke, Du, Bo-Yu, Ji, Dan-Yang, . . . Qiu, Xiao-Bo. (2013). Acetylation-Mediated Proteasomal Degradation of Core Histones during DNA Repair and Spermatogenesis. Cell, 153(5), 1012-1024. doi: 10.1016/j.cell.2013.04.032

Qiu, L. Q., Lai, W. S., Bradbury, A., Zeldin, D. C., & Blackshear, P. J. (2015). Tristetraprolin (TTP) coordinately regulates primary and secondary cellular responses to proinflammatory stimuli. J Leukoc Biol, 97(4), 723-736. doi: 10.1189/jlb.3A0214-106R

Qiu, W. R., Xiao, X., Lin, W. Z., & Chou, K. C. (2015). iUbiq-Lys: prediction of lysine ubiquitination sites in proteins by extracting sequence evolution information via a gray system model. J Biomol Struct Dyn, 33(8), 1731-1742. doi: 10.1080/07391102.2014.968875

Raabe, T., & Rapp, U. R. (2002). KSR--a regulator and scaffold protein of the MAPK pathway. Sci STKE, 2002(136), pe28. doi: 10.1126/stke.2002.136.pe28

Raingeaud, J., Gupta, S., Rogers, J. S., Dickens, M., Han, J., Ulevitch, R. J., & Davis, R. J. (1995). Pro-inflammatory cytokines and environmental stress cause p38 mitogen-activated protein kinase activation by dual phosphorylation on tyrosine and threonine. J Biol Chem, 270(13), 7420-7426.

Remy, G., Risco, A. M., Inesta-Vaquera, F. A., Gonzalez-Teran, B., Sabio, G., Davis, R. J., & Cuenda, A. (2010). Differential activation of p38MAPK isoforms by MKK6 and MKK3. Cell Signal, 22(4), 660-667. doi: 10.1016/j.cellsig.2009.11.020

Ridley, S. H., Dean, J. L., Sarsfield, S. J., Brook, M., Clark, A. R., & Saklatvala, J. (1998). A p38 MAP kinase inhibitor regulates stability of interleukin-1-induced cyclooxygenase-2 mRNA. FEBS Lett, 439(1-2), 75-80.

Rogalla, T., Ehrnsperger, M., Preville, X., Kotlyarov, A., Lutsch, G., Ducasse, C., . . . Gaestel, M. (1999). Regulation of Hsp27 oligomerization, chaperone function, and protective activity against oxidative stress/tumor necrosis factor alpha by phosphorylation. J Biol Chem, 274(27), 18947-18956.

Ronai, Ze'ev A. (2016). Monoubiquitination in proteasomal degradation. Proceedings of the National Academy of Sciences, 113(32), 8894-8896. doi: 10.1073/pnas.1610186113

Ronkina, N., Kotlyarov, A., Dittrich-Breiholz, O., Kracht, M., Hitti, E., Milarski, K., . . . Telliez, J. B. (2007). The mitogen-activated protein kinase (MAPK)-activated protein kinases MK2 and MK3 cooperate in stimulation of tumor necrosis factor biosynthesis and stabilization of p38 MAPK. Mol Cell Biol, 27(1), 170-181. doi: 10.1128/mcb.01456-06

Ronkina, N., Kotlyarov, A., & Gaestel, M. (2008). MK2 and MK3--a pair of isoenzymes? Front Biosci, 13, 5511-5521.

Ronkina, N., Menon, M. B., Schwermann, J., Arthur, J. S., Legault, H., Telliez, J. B., . . . Gaestel, M. (2011). Stress induced gene expression: a direct role for MAPKAP kinases in transcriptional activation of immediate early genes. Nucleic Acids Res, 39(7), 2503-2518. doi: 10.1093/nar/gkq1178

Round, J. L., Humphries, L. A., Tomassian, T., Mittelstadt, P., Zhang, M., & Miceli, M. C. (2007). Scaffold protein Dlgh1 coordinates alternative p38 kinase activation, directing T cell receptor signals toward NFAT but not NF-kappaB transcription factors. Nat Immunol, 8(2), 154-161. doi: 10.1038/ni1422

Rouse, J., Cohen, P., Trigon, S., Morange, M., Alonso-Llamazares, A., Zamanillo, D., . . . Nebreda, A. R. (1994). A novel kinase cascade triggered by stress and heat shock that stimulates MAPKAP kinase-2 and phosphorylation of the small heat shock proteins. Cell, 78(6), 1027-1037.

Rousseau, Simon, Morrice, Nick, Peggie, Mark, Campbell, David G., Gaestel, Matthias, & Cohen, Philip. (2002). Inhibition of SAPK2a/p38 prevents hnRNP A0 phosphorylation by MAPKAP-K2 and its interaction with cytokine mRNAs. The EMBO Journal, 21(23), 6505-6514. doi: 10.1093/emboj/cdf639

Roux, P. P., & Blenis, J. (2004). ERK and p38 MAPK-activated protein kinases: a family of protein kinases with diverse biological functions. Microbiol Mol Biol Rev, 68(2), 320-344. doi: 10.1128/mmbr.68.2.320-344.2004

Ruzankina, Y., Pinzon-Guzman, C., Asare, A., Ong, T., Pontano, L., Cotsarelis, G., . . . Brown, E. J. (2007). Deletion of the developmentally essential gene ATR in adult mice leads to age-related phenotypes and stem cell loss. Cell Stem Cell, 1(1), 113-126. doi: 10.1016/j.stem.2007.03.002

Sabio, Guadalupe, Arthur, James Simon Campbell, Kuma, Yvonne, Peggie, Mark, Carr, Julia, Murray-Tait, Vicky, . . . Cuenda, Ana. (2005). p38γ regulates the localisation of SAP97 in the cytoskeleton by modulating its interaction with GKAP. The EMBO Journal, 24(6), 1134-1145. doi: 10.1038/sj.emboj.7600578

Salvador, J. M., Mittelstadt, P. R., Guszczynski, T., Copeland, T. D., Yamaguchi, H., Appella, E., . . . Ashwell, J. D. (2005). Alternative p38 activation pathway mediated by T cell receptor-proximal tyrosine kinases. Nat Immunol, 6(4), 390-395. doi: 10.1038/ni1177

Sandler, H., & Stoecklin, G. (2008). Control of mRNA decay by phosphorylation of tristetraprolin. Biochem Soc Trans, 36(Pt 3), 491-496. doi: 10.1042/bst0360491

Sardon, T., Pache, R. A., Stein, A., Molina, H., Vernos, I., & Aloy, P. (2010). Uncovering new substrates for Aurora A kinase. EMBO Rep, 11(12), 977-984. doi: 10.1038/embor.2010.171

Saxena, M., Williams, S., Brockdorff, J., Gilman, J., & Mustelin, T. (1999). Inhibition of T cell signaling by mitogen-activated protein kinase-targeted hematopoietic tyrosine phosphatase (HePTP). J Biol Chem, 274(17), 11693-11700.

Sczaniecka, M., Gladstone, K., Pettersson, S., McLaren, L., Huart, A. S., & Wallace, M. (2012). MDM2 protein-mediated ubiquitination of numb protein: identification of a second physiological substrate of MDM2 that employs a dual-site docking mechanism. J Biol Chem, 287(17), 14052-14068. doi: 10.1074/jbc.M111.303875

Shah, N. G., Tulapurkar, M. E., Ramarathnam, A., Brophy, A., Martinez, R., 3rd, Hom, K., . . . Hasday, J. D. (2017). Novel Noncatalytic Substrate-Selective p38alpha-Specific MAPK Inhibitors with Endothelial-Stabilizing and Anti-Inflammatory Activity. J Immunol, 198(8), 3296-3306. doi: 10.4049/jimmunol.1602059

Shapiro, P. S., Whalen, A. M., Tolwinski, N. S., Wilsbacher, J., Froelich-Ammon, S. J., Garcia, M., . . . Ahn, N. G. (1999). Extracellular signal-regulated kinase activates topoisomerase IIalpha through a mechanism independent of phosphorylation. Mol Cell Biol, 19(5), 3551-3560.

Sharrocks, A. D., Yang, S. H., & Galanis, A. (2000). Docking domains and substrate-specificity determination for MAP kinases. Trends Biochem Sci, 25(9), 448-453.

Sharrocks, Andrew D., Yang, Shen-His, & Galanis, Alex. (2000). Docking domains and substrate-specificity determination for MAP kinases. Trends in Biochemical Sciences, 25(9), 448-453. doi: https://doi.org/10.1016/S0968-0004(00)01627-3

Shaw, A. S., & Filbert, E. L. (2009). Scaffold proteins and immune-cell signalling. Nat Rev Immunol, 9(1), 47-56. doi: 10.1038/nri2473

Shi, Y., & Gaestel, M. (2002). In the cellular garden of forking paths: how p38 MAPKs signal for downstream assistance. Biol Chem, 383(10), 1519-1536. doi: 10.1515/bc.2002.173

Shi, Yu, & Gaestel, Matthias. (2002). In the Cellular Garden of Forking Paths: How p38 MAPKs Signal for Downstream Assistance (Vol. 383)

Shiryaev, A., & Moens, U. (2010). Mitogen-activated protein kinase p38 and MK2, MK3 and MK5: menage a trois or menage a quatre? Cell Signal, 22(8), 1185-1192. doi: 10.1016/j.cellsig.2010.03.002

Shveygert, M., Kaiser, C., Bradrick, S. S., & Gromeier, M. (2010). Regulation of eukaryotic initiation factor 4E (eIF4E) phosphorylation by mitogen-activated protein kinase occurs through modulation of Mnk1-eIF4G interaction. Mol Cell Biol, 30(21), 5160-5167. doi: 10.1128/mcb.00448-10

Slack, D. N., Seternes, O. M., Gabrielsen, M., & Keyse, S. M. (2001). Distinct binding determinants for ERK2/p38alpha and JNK map kinases mediate catalytic activation and substrate selectivity of map kinase phosphatase-1. J Biol Chem, 276(19), 16491-16500. doi: 10.1074/jbc.M010966200

Soleimani, M., & Nadri, S. (2009). A protocol for isolation and culture of mesenchymal stem cells from mouse bone marrow. Nat Protoc, 4(1), 102-106. doi: 10.1038/nprot.2008.221

Song, Y., Li, S., Ray, A., Das, D. S., Qi, J., Samur, M. K., . . . Anderson, K. C. (2017). Blockade of deubiquitylating enzyme Rpn11 triggers apoptosis in multiple myeloma cells and overcomes bortezomib resistance. Oncogene, 36(40), 5631-5638. doi: 10.1038/onc.2017.172

Stark, C., Breitkreutz, B. J., Chatr-Aryamontri, A., Boucher, L., Oughtred, R., Livstone, M. S., . . . Tyers, M. (2011). The BioGRID Interaction Database: 2011 update. Nucleic Acids Res, 39(Database issue), D698-704. doi: 10.1093/nar/gkq1116

Stein, B., Brady, H., Yang, M. X., Young, D. B., & Barbosa, M. S. (1996). Cloning and characterization of MEK6, a novel member of the mitogen-activated protein kinase kinase cascade. J Biol Chem, 271(19), 11427-11433.





Stelzl, U., Worm, U., Lalowski, M., Haenig, C., Brembeck, F. H., Goehler, H., . . . Wanker, E. E. (2005). A human protein-protein interaction network: a resource for annotating the proteome. Cell, 122(6), 957-968. doi: 10.1016/j.cell.2005.08.029

Stoecklin, G., Stubbs, T., Kedersha, N., Wax, S., Rigby, W. F., Blackwell, T. K., & Anderson, P. (2004). MK2-induced tristetraprolin:14-3-3 complexes prevent stress granule association and ARE-mRNA decay. EMBO J, 23(6), 1313-1324. doi: 10.1038/sj.emboj.7600163

Stommel, J. M., & Wahl, G. M. (2004). Accelerated MDM2 auto-degradation induced by DNA-damage kinases is required for p53 activation. EMBO J, 23(7), 1547-1556. doi: 10.1038/sj.emboj.7600145

Sudo, T., Kawai, K., Matsuzaki, H., & Osada, H. (2005). p38 mitogen-activated protein kinase plays a key role in regulating MAPKAPK2 expression. Biochem Biophys Res Commun, 337(2), 415-421. doi: 10.1016/j.bbrc.2005.09.063

Sudo, T., Yagasaki, Y., Hama, H., Watanabe, N., & Osada, H. (2002). Exip, a new alternative splicing variant of p38 alpha, can induce an earlier onset of apoptosis in HeLa cells. Biochem Biophys Res Commun, 291(4), 838-843. doi: 10.1006/bbrc.2002.6529

Sun, L., Stoecklin, G., Van Way, S., Hinkovska-Galcheva, V., Guo, R. F., Anderson, P., & Shanley, T. P. (2007). Tristetraprolin (TTP)-14-3-3 complex formation protects TTP from dephosphorylation by protein phosphatase 2a and stabilizes tumor necrosis factor-alpha mRNA. J Biol Chem, 282(6), 3766-3777. doi: 10.1074/jbc.M607347200

Sweeney, S. E., & Firestein, G. S. (2006). Mitogen activated protein kinase inhibitors: where are we now and where are we going? Annals of the Rheumatic Diseases, 65(Suppl 3), iii83-iii88. doi: 10.1136/ard.2006.058388

Szklarczyk, Damian, Franceschini, Andrea, Wyder, Stefan, Forslund, Kristoffer, Heller, Davide, Huerta-Cepas, Jaime, . . . von Mering, Christian. (2015). STRING v10: protein–protein interaction networks, integrated over the tree of life. Nucleic Acids Research, 43(Database issue), D447-D452. doi: 10.1093/nar/gku1003

Takaesu, G., Kang, J. S., Bae, G. U., Yi, M. J., Lee, C. M., Reddy, E. P., & Krauss, R. S. (2006). Activation of p38alpha/beta MAPK in myogenesis via binding of the scaffold protein JLP to the cell surface protein Cdo. J Cell Biol, 175(3), 383-388. doi: 10.1083/jcb.200608031

Takekawa, M., Maeda, T., & Saito, H. (1998). Protein phosphatase 2Calpha inhibits the human stress-responsive p38 and JNK MAPK pathways. EMBO J, 17(16), 4744-4752. doi: 10.1093/emboj/17.16.4744

Tanoue, T., Adachi, M., Moriguchi, T., & Nishida, E. (2000). A conserved docking motif in MAP kinases common to substrates, activators and regulators. Nat Cell Biol, 2(2), 110-116. doi: 10.1038/35000065

Tanoue, T., Maeda, R., Adachi, M., & Nishida, E. (2001). Identification of a docking groove on ERK and p38 MAP kinases that regulates the specificity of docking interactions. EMBO J, 20(3), 466-479

Tanoue, T., & Nishida, E. (2002). Docking interactions in the mitogen-activated protein kinase cascades. Pharmacol Ther, 93(2-3), 193-202

Tanoue, T., & Nishida, E. (2003). Molecular recognitions in the MAP kinase cascades. Cell Signal, 15(5), 455-462

Tanoue, T., Yamamoto, T., & Nishida, E. (2002). Modular structure of a docking surface on MAPK phosphatases. J Biol Chem, 277(25), 22942-22949. doi: 10.1074/jbc.M202096200

ter Haar, E., Prabhakar, P., Liu, X., & Lepre, C. (2007). Crystal structure of the p38 alpha-MAPKAP kinase 2 heterodimer. J Biol Chem, 282(13), 9733-9739. doi: 10.1074/jbc.M611165200

The Gene Ontology, Consortium. (2010). The Gene Ontology in 2010: extensions and refinements. Nucleic Acids Research, 38(Database issue), D331-D335. doi: 10.1093/nar/gkp1018

Tobiume, Kei, Matsuzawa, Atsushi, Takahashi, Takumi, Nishitoh, Hideki, Morita, Keiichi, Takeda, Kohsuke, . . . Ichijo, Hidenori. (2001). ASK1 is required for sustained activations of JNK/p38 MAP kinases and apoptosis. EMBO reports, 2(3), 222-228. doi: 10.1093/embo-reports/kve046

Tokunaga, Y., Takeuchi, K., Takahashi, H., & Shimada, I. (2014). Allosteric enhancement of MAP kinase p38alpha's activity and substrate selectivity by docking interactions. Nat Struct Mol Biol, 21(8), 704-711. doi: 10.1038/nsmb.2861





Tokunaga, Yuji, Takeuchi, Koh, Takahashi, Hideo, & Shimada, Ichio. (2014). Allosteric enhancement of MAP kinase p38α's activity and substrate selectivity by docking interactions. Nature Structural &Amp; Molecular Biology, 21, 704. doi: 10.1038/nsmb.2861

Tran, H., Maurer, F., & Nagamine, Y. (2003). Stabilization of urokinase and urokinase receptor mRNAs by HuR is linked to its cytoplasmic accumulation induced by activated mitogen-activated protein kinase-activated protein kinase 2. Mol Cell Biol, 23(20), 7177-7188

Trempolec, Natalia, Dave-Coll, Natalia, & Nebreda, Angel R. (2013). SnapShot: p38 MAPK Substrates. Cell, 152(4), 924-924.e921. doi: 10.1016/j.cell.2013.01.047

Trempolec, Natalia, Muñoz, Juan Pablo, Slobodnyuk, Konstantin, Marin, Silvia, Cascante, Marta, Zorzano, Antonio, & Nebreda, Angel R. (2017). Induction of oxidative metabolism by the p38α/MK2 pathway. Scientific Reports, 7(1), 11367. doi: 10.1038/s41598-017-11309-7

Tzarum, Netanel, Komornik, Nadav, Ben Chetrit, Dorin, Engelberg, David, & Livnah, Oded. (2013). DEF Pocket in p38α Facilitates Substrate Selectivity and Mediates Autophosphorylation. The Journal of Biological Chemistry, 288(27), 19537-19547. doi: 10.1074/jbc.M113.464511

Underwood, K. W., Parris, K. D., Federico, E., Mosyak, L., Czerwinski, R. M., Shane, T., . . . Stahl, M. L. (2003). Catalytically active MAP KAP kinase 2 structures in complex with staurosporine and ADP reveal differences with the autoinhibited enzyme. Structure, 11(6), 627-636

Ventura, Juan José, Tenbaum, Stephan, Perdiguero, Eusebio, Huth, Marion, Guerra, Carmen, Barbacid, Mariano, . . . Nebreda, Angel R. (2007). p38α MAP kinase is essential in lung stem and progenitor cell proliferation and differentiation. Nature Genetics, 39, 750. doi: 10.1038/ng2037

Vilchez, David, Saez, Isabel, & Dillin, Andrew. (2014). The role of protein clearance mechanisms in organismal ageing and age-related diseases. Nature Communications, 5, 5659. doi: 10.1038/ncomms6659

Vousden, Karen H., & Lane, David P. (2007). p53 in health and disease. Nature Reviews Molecular Cell Biology, 8, 275. doi: 10.1038/nrm2147

Wagner, Erwin F., & Nebreda, Ángel R. (2009). Signal integration by JNK and p38 MAPK pathways in cancer development. Nature Reviews Cancer, 9, 537. doi: 10.1038/nrc2694

Wan, P. T., Garnett, M. J., Roe, S. M., Lee, S., Niculescu-Duvaz, D., Good, V. M., . . . Marais, R. (2004). Mechanism of activation of the RAF-ERK signaling pathway by oncogenic mutations of B-RAF. Cell, 116(6), 855-867

Wang, Chun, Hockerman, Susan, Jacobsen, E. Jon, Alippe, Yael, Selness, Shaun R., Hope, Heidi R., . . . Mbalaviele, Gabriel. (2018). Selective inhibition of the p38α MAPK–MK2 axis inhibits inflammatory cues including inflammasome priming signals. The Journal of Experimental Medicine. doi: 10.1084/jem.20172063

Wang, J., Yuan, Y., Zhou, Y., Guo, L., Zhang, L., Kuai, X., . . . He, F. (2008). Protein interaction data set highlighted with human Ras-MAPK/PI3K signaling pathways. J Proteome Res, 7(9), 3879-3889. doi: 10.1021/pr8001645

Wang, X., Stafford, W., Mazurkiewicz, M., Fryknas, M., Brjnic, S., Zhang, X., . . . Linder, S. (2014). The 19S Deubiquitinase inhibitor b-AP15 is enriched in cells and elicits rapid commitment to cell death. Mol Pharmacol, 85(6), 932-945. doi: 10.1124/mol.113.091322

Wang, Yu-Chieh, Peterson, Suzanne E., & Loring, Jeanne F. (2013). Protein post-translational modifications and regulation of pluripotency in human stem cells. Cell Research, 24, 143. doi: 10.1038/cr.2013.151

Weber, H. O., Ludwig, R. L., Morrison, D., Kotlyarov, A., Gaestel, M., & Vousden, K. H. (2005). HDM2 phosphorylation by MAPKAP kinase 2. Oncogene, 24(12), 1965-1972. doi: 10.1038/sj.onc.1208389

Weintz, Gabriele, Olsen, Jesper V., Frühauf, Katja, Niedzielska, Magdalena, Amit, Ido, Jantsch, Jonathan, . . . Lang, Roland. (2010). The phosphoproteome of toll-like receptor-activated macrophages. Molecular Systems Biology, 6, 371-371. doi: 10.1038/msb.2010.29

Welchman, Rebecca L., Gordon, Colin, & Mayer, R. John. (2005). Ubiquitin and ubiquitin-like proteins as multifunctional signals. Nature Reviews Molecular Cell Biology, 6, 599. doi: 10.1038/nrm1700

Wendel, H. G., Silva, R. L., Malina, A., Mills, J. R., Zhu, H., Ueda, T., . . . Lowe, S. W. (2007). Dissecting eIF4E action in tumorigenesis. Genes Dev, 21(24), 3232-3237. doi: 10.1101/gad.1604407

Wenzel, Dawn M., & Klevit, Rachel E. (2012). Following Ariadne's thread: a new perspective on RBR ubiquitin ligases. BMC Biology, 10(1), 24. doi: 10.1186/1741-7007-10-24

Weston, Claire R., Lambright, David G., & Davis, Roger J. (2002). MAP Kinase Signaling Specificity. Science, 296(5577), 2345-2347. doi: 10.1126/science.1073344
White, Andre, Pargellis, Christopher A., Studts, Joey M., Werneburg, Brian G., & Farmer, Bennett T. (2007). Molecular basis of MAPK-activated protein kinase 2:p38 assembly. Proceedings of the National Academy of Sciences, 104(15), 6353-6358. doi: 10.1073/pnas.0701679104

Widmann, C., Gibson, S., Jarpe, M. B., & Johnson, G. L. (1999). Mitogen-activated protein kinase: conservation of a three-kinase module from yeast to human. Physiol Rev, 79(1), 143-180. doi: 10.1152/physrev.1999.79.1.143

Willemen, H. L., Campos, P. M., Lucas, E., Morreale, A., Gil-Redondo, R., Agut, J., . . . Murga, C. (2014). A novel p38 MAPK docking-groove-targeted compound is a potent inhibitor of inflammatory hyperalgesia. Biochem J, 459(3), 427-439. doi: 10.1042/bj20130172

Willemen, Hanneke L. D. M., Campos, Pedro M., Lucas, Elisa, Morreale, Antonio, Gil-Redondo, Rubén, Agut, Juan, . . . Murga, Cristina. (2014). A novel p38 MAPK docking groove-targeted compound is a potent inhibitor of inflammatory hyperalgesia. The Biochemical journal, 459(3), 427-439. doi: 10.1042/BJ20130172

Wiśniewski, Jacek R., Zougman, Alexandre, Nagaraj, Nagarjuna, & Mann, Matthias. (2009). Universal sample preparation method for proteome analysis. Nature Methods, 6, 359. doi: 10.1038/nmeth.1322

Witzel, Franziska, Maddison, Louise, & Blüthgen, Nils. (2012). How scaffolds shape MAPK signaling: what we know and opportunities for systems approaches. Frontiers in Physiology, 3(475). doi: 10.3389/fphys.2012.00475

Xing, Li, Shieh, Huey S., Selness, Shaun R., Devraj, Rajesh V., Walker, John K., Devadas, Balekudru, . . . Monahan, Joseph B. (2009). Structural Bioinformatics-Based Prediction of Exceptional Selectivity of p38 MAP Kinase Inhibitor PH-797804. Biochemistry, 48(27), 6402-6411. doi: 10.1021/bi900655f



Molecular basis of p38α MAPK signaling

Yang, Jing, Carra, Serena, Zhu, Wei-Guo, & Kampinga, Harm. (2013). The Regulation of the Autophagic Network and Its Implications for Human Disease (Vol. 9).

Yasuda, S., Sugiura, H., Tanaka, H., Takigami, S., & Yamagata, K. (2011). p38 MAP kinase inhibitors as potential therapeutic drugs for neural diseases. Cent Nerv Syst Agents Med Chem, 11(1), 45-59

Yoshimori, T., Yamamoto, A., Moriyama, Y., Futai, M., & Tashiro, Y. (1991). Bafilomycin A1, a specific inhibitor of vacuolar-type H(+)-ATPase, inhibits acidification and protein degradation in lysosomes of cultured cells. J Biol Chem, 266(26), 17707-17712

Zeke, A., Bastys, T., Alexa, A., Garai, A., Meszaros, B., Kirsch, K., . . . Remenyi, A. (2015). Systematic discovery of linear binding motifs targeting an ancient protein interaction surface on MAP kinases. Mol Syst Biol, 11(11), 837. doi: 10.15252/msb.20156269

Zeke, A., Misheva, M., Remenyi, A., & Bogoyevitch, M. A. (2016). JNK Signaling: Regulation and Functions Based on Complex Protein-Protein Partnerships. Microbiol Mol Biol Rev, 80(3), 793-835. doi: 10.1128/mmbr.00043-14

Zhang, Jiyan, Shen, Beifen, & Lin, Anning. (2007). Novel strategies for inhibition of the p38 MAPK pathway. Trends in Pharmacological Sciences, 28(6), 286-295. doi: 10.1016/j.tips.2007.04.008

Zhang, Y. Y., Wu, J. W., & Wang, Z. X. (2011). Mitogen-activated protein kinase (MAPK) phosphatase 3-mediated cross-talk between MAPKs ERK2 and p38alpha. J Biol Chem, 286(18), 16150-16162. doi: 10.1074/jbc.M110.203786

Zhang, Yuan-Yuan, Wu, Jia-Wei, & Wang, Zhi-Xin. (2011). A Distinct Interaction Mode Revealed by the Crystal Structure of the Kinase p38α with the MAPK Binding Domain of the Phosphatase MKP5. Science Signaling, 4(204), ra88-ra88. doi: 10.1126/scisignal.2002241

Zheng, N., & Shabek, N. (2017). Ubiquitin Ligases: Structure, Function, and Regulation. Annu Rev Biochem, 86, 129-157. doi: 10.1146/annurev-biochem-060815-014922

Zu, Y. L., Wu, F., Gilchrist, A., Ai, Y., Labadia, M. E., & Huang, C. K. (1994). The primary structure of a human MAP kinase activated protein kinase 2. Biochem Biophys Res Commun, 200(2), 1118-1124